Identification of Biomolecular Pathways Associated With the Central Nervous System Based Symptoms of Gulf War Illness

Thesis

Identification of biomolecular pathways associated with the central nervous system based symptoms of Gulf War Illness

Laila Abdullah

M.Sc. Epidemiology: Principles and Practice

This thesis is being submitted for a degree in Doctor of Philosophy in the discipline of Neuroscience.

Primary supervisors: Drs. Fiona Crawford and Ghania Ait-Ghezala

Additional supervisors: Professor James E. Evans and Professor Michael Stewart

Affiliated Research Center

Roskamp Institute

2040 Whitfield Ave

Sarasota, FL 34234

Submission date: June 28, 2012

DATE of SUBMISSION: 27 JUNE 2012

DATE of AWARD: 1 OCTOBER 2012

ProQuest LLC.
789 East Eisenhower Parkway
P.O. Box 1346
Ann Arbor, MI 48106 – 1346

Acknowledgement:

I would like to express my sincerest thanks and appreciation to my Ph.D. supervisors Drs. Fiona Crawford and Ghania Ait-Ghezala who gave me the opportunity for this research apprenticeship and provided the funding to conduct the experiments detailed in this thesis. This training has equipped me with transferable skills that will be tremendously valuable to my broader career development. I would like to thank Professor James E. Evans for investing time and energy in training me to perform lipidomic experiments. His expertise in mass spectrometry made this learning process fast and efficient and introduced me to a new and exciting area of mass spectrometry and its application in addressing biological questions.

I would also like to thank Dr. Michael Mullan for providing guidance on how to evaluate, interpret and assimilate scientific data with the existing scientific knowledge and to apply critical thinking to problem solving.

My deepest thanks to my Roskamp Institute team members for assisting me with experiments over the years. Thanks to Alex Bishop, Benoit Mouzon, Scott Ferguson, Myles Mullan, Ariel Gonzalez, Christopher Mullan and John Phillips for their assistance with neurobehavioral, neuropathological and lipidomics studies. Many thanks to Gogce Crynen and Jon M. Reed for their assistance on proteomic studies.

A special thank you to Barbara Evans for providing the editorial support. Finally, a thanks to Juliet Mullan, Dennis Tester and Louise Tester and to my family and friends for providing me with encouragement over the years to pursue a career in scientific research.

I would also like to thank Bob and Diane Roskamp for their generosity.

I would like to dedicate this thesis to my mother and father, who have shown me the value of hard work and perseverance.

Preface

Most of the work presented in this thesis was supported by a Department of Defense (DoD) Congressionally Directed Medical Research Program (CDMRP) award (GW080094) to Dr. Fiona Crawford. A small portion of this work was also supported by a DoD CDMRP award (GW100076) to Dr. Ghania Ait-Ghezala.

The main focus of this work was to develop and characterize mouse models of Gulf War Illness (GWI), a multisymptom condition associated with service in the 1990-1991 Persian Gulf War (GW). It is estimated that GWI affects approximately 200,000 of 700,000 U.S. veterans and 6,000 of the 50,000 UK veterans who were deployed to the 1990-1991 Gulf War. This work provides a novel insight into the putative pathological mechanisms that might be associated with GWI. It is anticipated that the work described here will be helpful to future studies aimed at identifying potential therapies for treating GWI and at discovering objective biomarkers for diagnosing GWI.

Collaborators:

Michael Mullan, Jon M. Reed, Gogce Crynen, Alex Bishop, Benoit Mouzon, Scott Ferguson, John Phillips, Myles Mullan, Austin Ferro, Robert Pelot, Ariel Gonzalez, Chris Mullan and Venkatarajan Mathura.

Roskamp Institute

2040 Whitfield Ave

Sarasota, FL, 34234

Peer-reviewed publications:

Abdullah L, Crynen G, Reed J, Bishop A, Phillips J, Ferguson S, Mouzon B, Mullan MA, Mathura V, Mullan M, Ait-Ghezala G, Crawford F. Proteomic CNS profile of delayed cognitive impairment in mice exposed to Gulf War agents. Neuromolecular Med. 2011 Dec;13(4):275-88.

Abdullah L, Evans JE, Bishop A, Reed JM, Crynen G, Phillips J, Pelot R, Mullan MA, Ferro A, Mullan CJ, Mullan MJ, Ait-Ghezala G, Crawford FC (2012). Lipidomic profiling of phosphocholine containing brain lipids in mice with sensorimotor deficits and anxiety-like features after exposure to Gulf War agents. *Neuromolecular Medicine* July 14 [epub ahead of print].

Scientific presentations:

Abdullah L, Bishop A, Phillips J, Mouzon B, Ferguson S, Ganapathi V, Mullan MA, Ait-Ghezala G, Mullan M and Crawford F (2010). Delayed memory impairment in a new mouse model of Gulf War Illness. 40th Annual Meeting of Society for Neuroscience. November, San Diego, California (published).

Abdullah L, Bishop A, Phillips J, Mouzon B, Ferguson S, Ganapathi V, Mullan MA, Ait-Ghezala G, Mullan M and Crawford F (2010). Mice exposed to pyridostigmine bromide and pesticide/insect repellent model CNS symptoms associated with Gulf War Illness. 27th Army Conference Proceedings. December, Orlando, Florida (published).

Abdullah L, Bishop A, Phillips J, Mouzon B, Ferguson S, Ganapathi V, Mullan MA, Ait-Ghezala G, Mullan M and Crawford F (2010). Delayed memory impairment in a new mouse model of Gulf War Illness. 40th Annual Meeting of Society for Neuroscience. November, San Diego, California (published).

Abdullah L, Bishop A, Phillips J, Mouzon B, Ferguson S, Ganapathi V, Mullan MA, Ait-Ghezala G, Mullan M and Crawford F (2011). Proteomic-based identification of a CNS biological profile of delayed cognitive impairment in mice exposed to gulf war agents. 41st Annual Meeting of Society for Neuroscience, November, Washington, D.C (published).

Abdullah L, Bishop A, Crynen G, Reed J, Phillips J, Mouzon B, Ferguson S, Mullan MA, Ait-Ghezala G, Mullan M and Crawford F (2011). Proteomic-based identification of a CNS biological profile of delayed cognitive impairment in mice exposed to gulf war agents. Veterans Administration Research Day. April, Tampa, Florida (published).

Abdullah L, Evans J, Reed J, Crynen G, Bishop A, Phillips J, Mouzon B, Ferguson S, Mullan MA, Pelot R, Moser A, Mullan C, Mathura V, Mullan M, Ait-Ghezala G, Crawford F (2011). Proteomic and lipidomic-based CNS profile of delayed cognitive impairment in mice exposed to Gulf War agents. Bioactive lipid conference meeting. September, Seattle, Washington (published).

Gonzalez A, **Abdullah L**, Bishop A, Crynen G, Reed J, Phillips J, Mouzon B, Ferguson S, Mullan MA, Ait-Ghezala G, Mullan M and Crawford F (2012). Proteomic-based identification of a CNS biological profile of delayed cognitive impairment in mice exposed to gulf war agents. Veterans Administration Research Day. April, Tampa, Florida (published).

Abdullah L, Evans JE, Reed J, Pelot R, Bishop A, Pelot R, Reed J, Evans JE, Bishop A, Crynen G, Mullan MA, Ferro A, Mullan C, Mullan M, Ait-Ghezala G and Crawford F (2012). Lipidomic profiles of motor and anxiety like features of GWI in mice exposed to pyridostigmine bromide, N,N-Diethyl-meta-toluamide, permethrin and stress. The American Society for Mass Spectrometry Meeting, Vancouver, British Columbia (published).

Evans JE, **Abdullah L**, Reed J, Pelot R, Bishop A, Pelot R, Reed J, Evans JE, Bishop A, Crynen G, Mullan MA, Mullan M, Crawford F (2012). Normal phase LCMS with SCID phospholipidomic Analysis of Plasma and Brain from a mouse model of Traumatic Brain Injury. The American Society for Mass Spectrometry Meeting, Vancouver, British Columbia (published).

Abdullah L, Evans JE, Gonzalez A, Bishop A, Reed JM, Crynen G, Mouzon B, Ferguson S, Mullan C, Pelot R, Mullan M, Ait-Ghezala G, Crawford F (2012). Distinct brain phospholipidomic profiles in different mouse models of neurocognitive dysfunction. 42nd Annual Meeting of Society for Neuroscience, New Orleans, Louisiana (published).

List of abbreviations

AA	Arachidonic acid
ACh	Acetylcholine
AChE	Acetylcholinesterase
ACN	Acetonitrile
ACTH	Adrenocorticotropic hormone
2AG	2-arachidonylglycerol
APP	Amyloid Precursor Protein
ANOVA	Analysis of Variance
BACE	β-secretase APP converting enzyme
BBB	Blood brain barrier
CE	Collision energy
CCI	Controlled cortical impact
CHI	Closed head injury
CNS	Central nervous systems
COX	Cyclooxygenase
GFAP	Glial Fibrillary Acid Protein
GH	Growth hormone
DDA	Data-dependent acquisition
DEET	N,N-Diethyl-meta-toluamide
DHA	Docosahexaenoic acid
DHP-CCB	Dihydropyridine calcium channel blocker
2DGE	Two dimensional gel electrophoresis
DoD	Department of Defense
FDR	False discovery rate

FFA	Free fatty acids
GWI	Gulf War Illness
H&E	Hematoxylin and Eosin
ICAT	Isotopic Coded Affinity Tags
IgE	Immunoglobulin E
IFN-γ	Interferon-gamma
IPA	Ingenuity Pathways Analysis
iTRAQ	Isobaric Tagging for Relative and Absolute Quantification
LCFA	Long chain fatty acids
LC/MS	Liquid chromatography with mass spectrometry
LPC	Lysophosphatidylcholine
LOX	Lipooxygenase
mAChR	Muscarinic AChR
MAG	Monoacylglycerol
MAGL	Monoacylglycerol lipase
MeOH	Methanol
MLM	Mixed linear model
MRI	Magnetic Resonance Imaging
MS	Mass spectrometry
mTBI	mild TBI
MUFA	Monounsaturated fatty acids
MWM	Morris Water Maze
nAChR	Nicotinic AChR
NH_4OAc	Ammonium acetate
OFT	Open Field Test
OP	Organophosphate

PA	Phosphatidic acid
PAF	Platelet-activating factor
PB	Pyridostigmine bromide
PC	Phosphatidylcholine
PCA	Principal component analysis
PE	Phosphatidylethanolamine
PER	Permethrin
PG	Phosphatidylglycerol
PI	Phosphatidylinositol
PL	Phospholipids
PLA_2	Phospholipase A2
PNS	Peripheral nervous system
PQD	Pulsed-Q Dissociation
PS	Phosphatidylserine
PUFA	Polyunsaturated fatty acids
PVDF	Polyvinylidene fluoride
rCBF	Regional cerebral blood flow
RPLC/MS	Reverse phase LC /MS
RT	Retention time
TBI	Traumatic Brain Injury
TNF	Tumor necrosis factor
SCID	In-source collision induced dissociation
SFA	Saturated fatty acids
SILAC	Stable Isotope Labeling by Amino Acids in Cell Culture
SILAM	Stable Isotope Labeling by Amino Acids in Mammals
SPECT	Single Photon Emission Computed Tomography

SM	Sphingomyelin
VGSC	Voltage gated sodium channels
VLCFA	Very long chain fatty acids

Abstract:

The clinical profile of GWI is characterized by the presence the central nervous systems (CNS) symptoms which include memory impairment, anxiety, widespread pain and motor problems. Now, even twenty years later, veterans with GWI continue to suffer from these persistent symptoms. Currently, there is no treatment available for treating GWI, which is largely due to the complexity of the clinical presentation of this illness and the heterogeneity of GW exposures. The main goals of this thesis were to develop and characterize GW agent exposure mouse models that recapitulate the CNS symptoms of GWI and to identify the underlying aberrant biological pathways. Three major objectives were undertaken to accomplish these goals: (1) Two mouse models of GW-agent exposure were developed using combination of the anti-nerve gas treatment pyridostigmine bromide (PB), pesticides (permethrin), an insect repellent (N,N-Diethyl-meta-toluamide) and stress. Neurobehavioral studies show that combined exposure to GW agents produced anxiety and sensorimotor deficits in one mouse model and anxiety and cognitive impairment in the other. Neuropathological studies showed a presence of astrogliosis in both models. (2) Exploratory proteomic studies suggested that lipid-metabolism and immune/inflammation were associated with GW-agent exposure. (3) As lipid dysfunction is upstream of the inflammatory pathways, a lipidomics approach was used to identify the GW-agent exposure dependent lipid profiles. Lipid profiles of mouse models of GW-agent exposure were compared with those of other neurological conditions to identify profiles that were unique to GW-agent exposure. Lipid profiles were interrogated to identify lipid-metabolism pathways that may be amenable to therapeutic targeting. Studies described in this thesis provide novel insight into the pathobiology of GWI and suggest that pathways involved in phosphatidylcholine metabolism might be of therapeutic value in treating the CNS symptoms of GWI.

Table of content:

Number of figures 43

Number of tables 4

Number of abbreviations 79

1.0. CHAPTER 1: Introduction to Gulf War Illness

1.1. Background

Gulf War Illness (GWI) represents a significant military health problem that affects approximately 25% of the 700,000 veterans from the 1990-1991 Persian Gulf War (GW). This illness has a complex multisymptom clinical presentation consisting of gastrointestinal problems, pain and neurological symptoms. While a number of other illnesses, such as brain cancer and amyotrophic lateral sclerosis (ALS) afflict GW veterans at a higher rate than veterans from other wars, GWI continues to be the most prevalent disorder among these veterans (Binns et al 2008). Recent longitudinal studies suggest that compared to non-deployed veterans, deployed GW veterans continue to report persistence of this multisymptom illness as well as the new onset of seemingly unrelated chronic diseases, such as hypertension and cardiovascular disease (Li et al 2011a). The severity of GWI ranges from moderate, which does not interfere with a normal daily life, to highly debilitating that disrupts the activities of daily living. To date, there have been only two major federally funded randomized clinical trials for treating symptoms of GWI which include fatigue, pain, distress, cognitive problems and mental health functioning. The doxycycline intervention trial was based on a hypothesis that symptoms of GWI were due to a systemic bacterial infection in these veterans. Another randomized trial using cognitive behavioral therapy was conducted as it had provided relief to patients with fibromyalgia (an illness that has some of the symptoms that overlap with GWI). However, neither trial significantly improved symptoms of veterans with GWI, so thus far GWI remains an untreatable condition (Donta et al 2003; Donta et al 2004).

Over twenty years have now elapsed since the original exposure, and therefore, characterizing the long-term sequelae of this illness is critical to understanding the pathology of GWI. To date, there has been a lack of focused and effective preclinical

research on the CNS symptoms of GWI in well-characterized animal models, an approach which is likely to be extremely valuable in successfully translating therapies for treating GWI. The main objective of this thesis was to develop and characterize mouse models of GWI and to identify the underlying pathobiology of this illness. In these mouse models, neurobehavioral outcomes were examined and were found to be similar to symptoms observed in veterans with GWI. Chronic neuropathological consequences were also examined in the brains, and accompanying biological and molecular changes were identified in the brain and blood of exposed mice compared to controls. It is anticipated that these studies will provide novel avenues for finding therapies against GWI as well as for developing biomarker panels that could aid in providing an objective diagnosis of GWI.

1.2. Central Nervous System component of GWI

Evidence of a CNS component to this illness comes from brain imaging studies, which show a smaller hippocampal volume in deployed and reservist GW veterans compared to healthy civilians, and hypometabolism in the hippocampi of veterans with GWI compared to asymptomatic veterans who served in the GW (Menon et al 2004; Vythilingam et al 2005). In addition, 32% of deployed Gulf War veterans self-reported memory problems compared to 8% of non-Gulf War veterans (Steele 2000). This is supported by neuropsychological studies demonstrating cognitive impairment in deployed GW veterans compared to non-deployed GW military personnel or GW veterans who were deployed elsewhere (David et al 2002; Toomey et al 2009; White et al 2001). Furthermore, even decades later, deployed GW veterans continue to experience deficits in working memory (Toomey et al 2009). Lange and colleagues demonstrated that compared to healthy GW veterans, those with GWI had significant difficulty with information processing and the use of abstract concepts, particularly within the cognitive domains that

require attention and concentration (Lange et al 2001). Among the UK veterans, deployment to the 1990-1991 GW was associated with subjective memory failure and general cognitive and constructional impairment on neuropsychological testing, which remained significant even after adjusting for depression (David et al 2002). While cognitive problems remain one of the top four complaints among veterans with GWI, other neuropsychological problems, such as anxiety, attention deficits and impairment in motor speed are also experienced by these veterans (Toomey et al 2009; Gray et al 1999).

In an attempt to comprehensively evaluate the neurobehavioral symptoms of GWI, an initial survey of 249 members of a naval reserve construction battalion showed that there were six symptom clusters, and, of these, three were categorized as major syndromes (Kurt 1998; Haley et al 1997). All of the participants in this study were noted to have taken the anti-nerve gas treatment pyridostigmine bromide (PB) and therefore exposure to PB was considered to have been associated with all three syndromes. Pesticide application was correlated with Syndrome 1, which was characterized by cognitive impairment. Syndrome 2, consisting of confusion-ataxia, was correlated with the reports of chemical weapons attacks. Syndrome 3 was characterized by an arthro-myo-neuropathy component consisting of symptoms such as muscle pain, fatigue and numbness of hands and feet, which was correlated with a heavy use of the insect repellent N,N-Diethyl-meta-toluamide (DEET) (Kurt 1998; Haley et al 1997). These observations suggest that there are several distinct CNS symptom profiles of GWI, which may be associated with different combinations of chemical exposures. This would be consistent with the complexity of the clinical presentation of this illness, which remains a central challenge in dissecting the CNS pathophysiology of GWI and in identifying appropriate therapeutic approaches for treating this illness.

1.3. Key etiological factors in GWI

In 2008, the Research Advisory Committee on GWI prepared a comprehensive report which concluded that there is now considerable scientific evidence that exposure to pesticides, insect repellents and the use of PB as a pretreatment against neurotoxins, are some of the main contributory factors to GWI (Binns et al 2008). Although a number of other factors (e.g., oil well fires, accidental release of sarin gas) have been identified as potential GW exposures that are also unique to this deployment, epidemiological data are weak and provide limited support for their role as causative factors of GWI. For instance, exposure to Kuwaiti oil well fires was a unique exposure for the deployed service members from the 1990-1991 GW but largely affected only the ground troops stationed in Kuwait. Therefore this exposure does not explain a presence of GWI among veterans stationed elsewhere, such as those in support areas on land and those onboard ships during deployment (Binns et al 2008). Epidemiological studies aimed at determining an association between risk of GWI and oil well fires have provided discrepant results, most showing a lack of such an association (Smith et al 2002; Cowan et al 2002; Lange et al 2002). Similarly, there is a lack of consistent clinical data on a possible association of other GW exposures (e.g., an accidental release of sarin gas, depleted uranium, vaccines) and the risk of GWI (Binns et al 2008). These limitations preclude their further evaluation as potential causative factors of GWI, unless relevant indicative clinical data become available. On the other hand, a recent case-controlled study conducted by Steele and colleagues showed that a nearly 3-fold elevated risk of GWI was associated with PB consumption and about 13-fold increased risk with the use of pesticide treated uniforms as well as pesticide application to the skin (Steele et al 2012). Furthermore, there are considerable clinical data from other sources supporting an individual and a collective role of these chemicals in the manifestation of GWI. These are described in more detail below.

1.3.1 Pyridostigmine bromide exposure

Physostigmine, a pure alkaloid, isolated from Calabar beans by Jobst and Hesse in the 19th century, was later shown to contract pupils and was subsequently shown to have therapeutic properties in treating glaucoma (Pope et al 2005). A series of such compounds are now available and include PB, which was used as a prophylactic agent against organophosphate (OP) nerve agent exposures in the 1990-1991 GW to avoid cholinergic toxicity (Pope et al 2005). Pyridostigmine bromide is a reversible carbamate acetylcholinesterase (AChE) inhibitor, which binds to a serine residue on the active site of AChE and is considered to have an excellent safety profile in treatment of myasthenia gravis (patients generally given 30 mg oral dose every 8 hrs), an autoimmune disorder in which acetylcholine (ACh) receptors are blocked by autoantibodies (Aquilonius et al 1983). Epidemiological studies using retrospective data collection on exposure have consistently reported PB to be associated with GWI (Golomb 2008). In fact, a higher risk of GWI and more severe illness was observed in those veterans who consumed a larger quantity of PB pills (> 22 pills of 30 mg) than those taking fewer pills, which suggests the presence of a biological gradient (Haley 1997; Golomb 2008).

1.3.2. Pesticide exposure

With respect to pesticide exposure among GW personnel, 62% of the ground troops reported using pesticides, and of those, 44% reported using pesticide sprays, which contained permethrin (PER) or other pyrethroids. The Department of Defense (DoD) estimates that the US service members from the 1990-1991 GW may have been exposed to at least 64 different pesticides and insect repellents containing 37 active ingredients, including DEET and pyrethroids, such as PER (Binns et al 2008). A RAND Corporation survey indicated that among GW veterans, overuse of pesticides primarily involved pyrethroids, such as PER and d-phenothrin (Hilborne et al 2005). Veterans with high

pesticide use were at a greater risk of GWI than those with limited use, suggesting a dose-response relationship (Binns et al 2008).

During the GW, military personnel were issued PER imbedded uniforms as well as 0.5% PER containing spray. Surveys conducted by the DoD report that PER was used on average 30 times over a period of one month despite the guidance issued by the military to Army personnel asking that a light-coat of PER should be applied every 4 to 5 days. This is a potential cause of concern since the PER manufacturer's label indication suggested that uniforms should have been sprayed only once every six weeks, or after six launderings. Permethrin is a type I synthetic pyrethroid, which works by prolonging activation of the voltage gated sodium channels (VGSC). Due to its high lipophilicity, once displaced from the binding site, PER can transfer to the adjacent membrane lipids and then rebind to the VGSC (Ray, & Fry 2006).

N,N-diethyl-meta-toluamide, an amide, is used by approximately 30% of both adults and children in the US annually (Boomsma, & Parthasarthy 1990) and generally has a good safety profile in a 10-25% formulation. However, military personnel were issued 33% and 75% formulations of DEET for topical application, much higher concentrations than those used in the civilian population. The primary mode of action for DEET is to modulate the odor-gated ion channels within the insect odor-receptor complex (Pellegrino et al 2011). More recently, DEET was also shown to be a weak AChE inhibitor (Corbel et al 2009). Overexposure to DEET can cause seizures, encephalopathies, tremors and hyperactivity, which are characteristic of cholinergic toxicity (Binns et al 2008). Table 1.1 below provides a summary of pharmacokinetics and adverse effects on human health at high level exposure (Goodyer and Behrens 1998; Baker et al 1978; Vogel et al 2002; Qiu et al 1997).

Table 1.1: Pharmacokinetics and general information on GW agents

GW agent	Mechanism of Action	LD50 dose	Route	Species	Plasma half-life	Side effects in human
Pyridostigmine bromide	AChE inhibitor	4mg/kg	i.p.	mice	1.5- 2hrs❖	Severe allergic reactions, diarrhea, increased production of saliva, small pupils, trouble breathing, vision changes, vomiting and weakness.
Permethrin	Voltage gated sodium channel blocker	429mg/kg	i.p.	mice	24hrs◆	Skin sensations, paraesthesia, numbness, itching and tingling,
N,N-diethyl-m-toluamide	AChE inhibitor	2-4g/kg	oral	rats	3hrs★	Dermititis, encephalopahty, seizures, tremors and hyperactivity.

Note: ❖Based on PB drug insert and pharmacokinetic studies in dogs (Baker et al 1978). ◆Based on studies by Vogel and colleagues (Vogel et al 2002. ★Based on studies on dogs (Goodyer and Behrens 1998, Qiu et al 1997).

1.4. Combined exposure to PB, PER and DEET as a causative factor in GWI

Epidemiological studies have shown a consistent association between GWI and exposure to PB and pesticides and accumulating literature suggests that the combined exposure is one of the key contributory factors to the pathobiology of GWI. For instance, a RAND survey indicated that high exposure to pesticides was associated with high PB use, as nearly one in four GW veterans reported using several pesticides ranging from 51 to 120 times in a month while taking 15-19 PB pills (30 mg each) during the same timeframe (Hilborne et al 2005).

Government sponsored and independent surveys indicate that GW veterans were exposed to a unique mixture of these potentially neurotoxic chemicals which include PB and pesticides/insect repellent. However, very limited information is available on the short or long-term adverse health effects of combined exposure to these neurotoxic chemicals. As a consequence, laboratory animal work has been undertaken to understand the

neurobehavioral and biological effects of combined exposure to these chemicals. Much of the supporting data on combined exposure comes from animal models of GW agent exposure which suggest mediation of adverse effects through the periphery or due to a possible compromise of the blood brain barrier (BBB). Work by Friedman and colleagues showed that at low doses PB alone (0.1-0.5mg/kg) had no effect on brain AChE activity. However, at higher doses (2mg/kg) or when combined with stress, PB was able to inhibit brain AChE activity and induce changes in expression of genes (BDNF, TrkB and CamKIIα) that are involved in learning and memory (Friedman et al 1996; Barbier et al 2009). The authors suggested that, under stress or in high concentration, PB was able to cross the BBB (Friedman et al 1996; Barbier et al 2009). However, accompanying work conducted by Amourette et al, using radiolabeled PB, revealed that even under stress, PB was unable to enter the brain (Amourette et al 2009). Perhaps the neurotoxic effects of PB may be mediated by its interactions with the peripheral system, particularly those that are intimately linked with ACh. Despite this apparent inability of PB to cross the BBB, biochemical analyses continue to show an inhibition of AChE activity in the brain and neurobehavioral tests have shown delayed presentation of cognitive impairment in rats exposed to PB and stress (Barbier et al 2009; Lamproglou et al 2009; Amourette et al 2009).

Studies have shown that combined exposure to PB, DEET, PER and stress (GW agents) for up to 28 days of exposure can disrupt the BBB in several different brain regions which include the cortices and the hippocampi of exposed rats compared to controls (Abdel-Rahman et al 2002). Accompanying work from these studies also showed other neuropathological abnormalities, which included neuronal death and an increase in astrogliosis by nearly 50% in rats at acute post-exposure timepoints after GW agent exposure (Abdel-Rahman et al 2004). Chaney and colleagues demonstrated that immediately after a single combined exposure to high doses of PB and DEET, brain AChE

activity was reduced by 40% in exposed rats compared to controls (Chaney et al 2000). The neurobehavioral consequences of combined exposure to these GW agents include an increase in anxiety and sensorimotor deficits in exposed rodents compared to controls at varying acute post-exposure timepoints (Abou-Donia et al 2004; Hoy et al 2000). Together, these studies provide a compelling argument for an adverse effect of combined exposure to PB, PER, DEET and/or stress on the brain's structural, cellular and molecular integrity, which could be responsible for the symptoms observed in veterans with GWI. These studies support the current contention that combined exposure to PB and pesticides is one of the main causative factors in GWI pathogenesis. These studies also highlight that the heterogeneity of GW agents could further complicate the clinical presentation and that animal modeling work focused on combined exposure to GW agents is likely to produce neurobehavioral features that most closely recapitulate the symptoms observed in veterans with GWI. Development and characterization of such animal models of GW agent exposure will be invaluable in identifying the underlying pathobiological changes associated with GWI.

1.5. Biological mechanism for a role of combined PB, PER and DEET in GWI

Based on the mechanisms of action of these GW agents at acute post-exposure time-points (immediately following the exposure), the biological pathways implicated in GWI may involve both the peripheral and the central cholinergic systems. The literature review below provides biological rationale to assist with dissecting the pathobiology of GWI. Understanding the immediate biological effects of PB, PER, DEET and stress will be useful in conducting further investigation to assess the biological changes several months (chronic) after exposure.

1.5.1. Cholinergic receptor system and GW agents

The studies described in this section provide supporting data for a potential dysfunction of the cholinergic system in GWI, particularly as the chemicals utilized in these studies most likely modulate synaptic ACh levels. Synthesis of ACh occurs in cholinergic neurons by choline acetyltransferase using choline and acetyl coenzyme A as substrates. It is then packaged into synaptic vesicles (Pope et al 2005) and upon terminal depolarization, ACh is transported out of the neurons by the vesicular ACh transporter into the synaptic cleft where it binds to cholinergic receptors and activates a number of intracellular signaling pathways. Under normal conditions, ACh is rapidly hydrolyzed by AChE. However, use of synthetic AChE inhibitors leads to prolonged accumulation of ACh at the synapse and causes an abnormal alteration of the cholinergic receptor-mediated signaling pathways. Studies on combined exposure to a pyrethroid and a carbamate AChE inhibitor have shown to result in a synergistic increase in membrane depolarization accompanied by an increase in ACh release into synapse (Corbel et al 2006). Studies also suggest that excessive synaptic ACh can self-regulate by binding to presynaptic muscarinic AChR (mAChR), promoting negative feedback that inhibits its further release (Zhang et al 2002). It is therefore plausible to suggest that combined exposure to PB, a carbamate AChE inhibitor, and PER, a pyrethroid, may synergistically enhance synaptic ACh levels in the short-term but may result in depletion of synaptic ACh via negative feedback in the long-term (see Figure 1.1).

Additional support for modulation of AChR properties as a consequence of GW agent exposure comes from studies using animal models. For instance, enhanced ligand binding of the muscarinic 2 (M2) AChR subtype in the cortex was observed in a rat model of GWI treated with either PB alone or in combination with PER and DEET (Abou-Donia et al 2004). Combined exposure to these GW agents also increased the ligand binding of

Figure 1.1

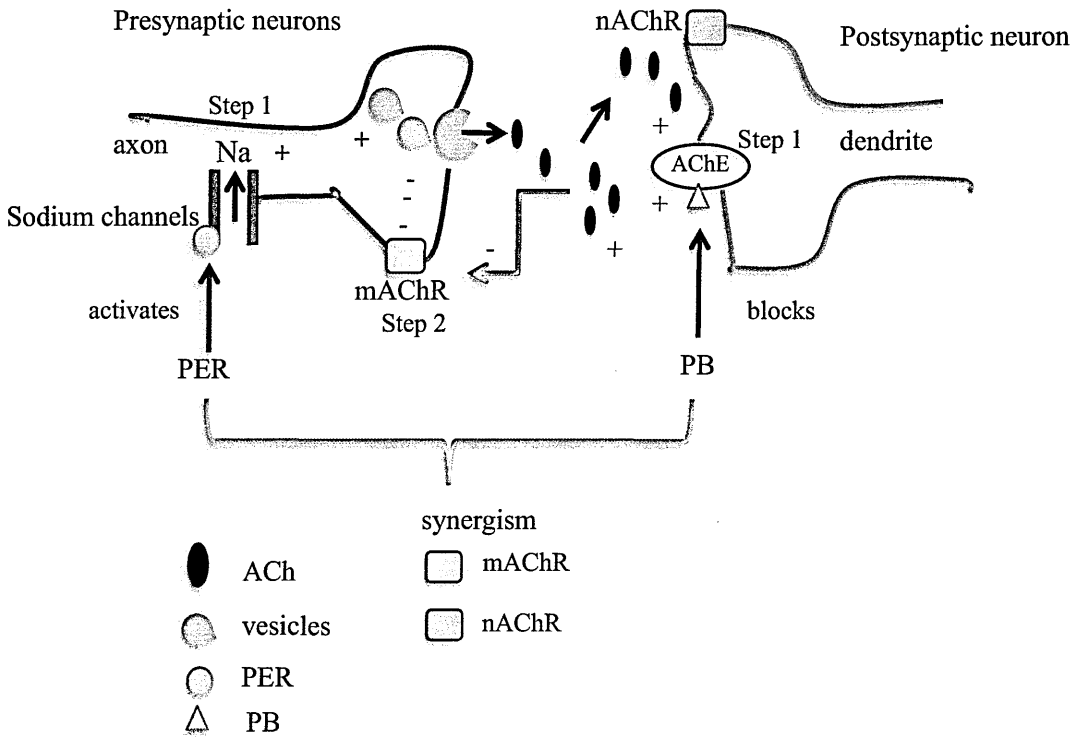

Figure 1.1. Hypothesized synergistic effect of PB and PER on neuronal ACh release: This image, readapted from the original article (Corbel et al 2006), shows that exposure to PB increases synaptic ACh levels (step 1). Binding of PER to VGSC further increases the release of ACh (step 1) within the synaptic cleft (+ sign denotes increase ACh release/ accumulation). The excess of non-hydrolyzed ACh in the synaptic cleft may activate presynaptic mAChR (step 2) involved in the negative feedback mechanism (- sign denotes blocking further ACh release).

nicotinic AChR (nAChR) in the cortex of rodents. However, combined exposure to these chemicals and stress resulted in a decrease in mAChR ligand binding in the midbrain and the cerebellum, although cortical mAChR binding was not examined (Abdel-Rahman et al 2004). A long-term consequence of such an enhanced cholinergic transmission may include a compensatory increase in AChE production which is suggested by studies performed by Bansal and colleagues showing that after 30 days of AChE inhibitor exposure, there is an increase in AChE mRNA levels in the cortex (Bansal et al 2009).

In addition to the animal studies described above, a number of human studies also provide support for a dysfunctional cholinergic system in veterans with GWI. For instance, recent imaging studies have shown an abnormal cholinergic response in veterans

with GWI compared to controls (Liu et al 2011). Using atrial spin labeling Magnetic Resonance Imaging (MRI), Li and colleagues recently demonstrated that upon cholinergic challenge (intravenous infusion with 0.3 mg of physostigmine prior to imaging) veterans with GWI exhibit an abnormal increase of regional cerebral blood flow (rCBF) in the hippocampus compared to control veterans (Li et al 2011b). This work is supported by an earlier study which used Single Photon Emission Computed Tomography (SPECT) to show a similar increase in CBF in response to the cholinergic challenge with physostigmine among veterans with GWI (Haley et al 2009). Although based on a small sample size, these studies do suggest a dysfunctional cholinergic response in veterans with GWI.

1.5.2. Cholinergic system and immune/inflammatory changes in relation to GW agents

In addition to the symptoms described above, the clinical profile associated with GWI also includes gastrointestinal problems, heart rate variability and an increased occurrence of gall bladder disease (Binns et al 2008). These peripheral symptoms, coupled with the CNS symptoms described above, suggest insults to both the CNS and the peripheral nervous system (PNS), possibly mediated through the periphery (Binns et al 2008).

Recently, it was shown that afferent fibers of the vagus nerve provide information to the brain regarding the peripheral inflammatory changes (Tracey 2007). Impaired peripheral immune and inflammatory responses are prominent features of GWI. Studies report a persistent immune imbalance that is accompanied by an increased expression of pro-inflammatory (Interferon-gamma [IFN-γ]) and anti-inflammatory (Interleukin-5 [IL-5]) cytokines in CD4 T-cells from veterans with GWI compared to healthy GW veterans (Skowera et al 2004; Broderick et al 2011).

Studies show that PB and PER can modulate several aspects of both cell-mediated and humoral immunity. For instance, Peden-Adams and colleagues (2004) demonstrated that exposure to PB results in a decreased IgM response to a T-cell dependent antigen, which suggests suppression of the humoral immune response. In this study, exposure to PB resulted in a decrease in both CD4+/CD8+ and CD4-/CD8- cell types (Peden-Adams et al 2004). Studies report that PER can activate the systemic immune responses, which include inhibition of lymphocyte responses and T-cell proliferation (Prater et al 2005; Punareewattana et al 2000). An animal study showed elevation of IL-1β, IFN-γ and IL-10 in PER exposed rats compared to control rats (Vadhana et al 2011). Collectively, these studies support a prominent peripheral immune and inflammatory component to GWI.

The cross-talk between the brain and the immune system is through the "cholinergic anti-inflammatory pathway", which is composed of the afferent and efferent vagus nerve connections, ACh, the α7 nAChR on macrophages in the periphery and the muscarinic receptor subtype 1/subtype 2 (M1/M2) within the CNS. See Figure 1.2 for additional explanation of the cholinergic anti-inflammatory pathway.

Once inflammation is detected in the periphery, information is relayed to the brain through afferent pathways, which consequently leads to stimulation of M1 receptors and a further release of ACh into the periphery via efferent fibers of the vagus nerve. In the periphery, ACh binds to the α7 nAChR on macrophages resulting in activation of cellular cascades that inhibit production of tumor necrosis factor (TNF) and other pro-inflammatory cytokines. Loss of the α7 nAChR on macrophages has been shown to result in increased TNF levels, despite a presence of preserved vagal nerve function. This suggests that the α7 nAChR are a key component of the cholinergic anti-inflammatory pathway (Tracey 2007). As such, a possible explanation of the observed peripheral immune/inflammatory dysfunction in veterans with GWI could include a disruption of the cholinergic anti-inflammatory pathway.

Figure 1.2

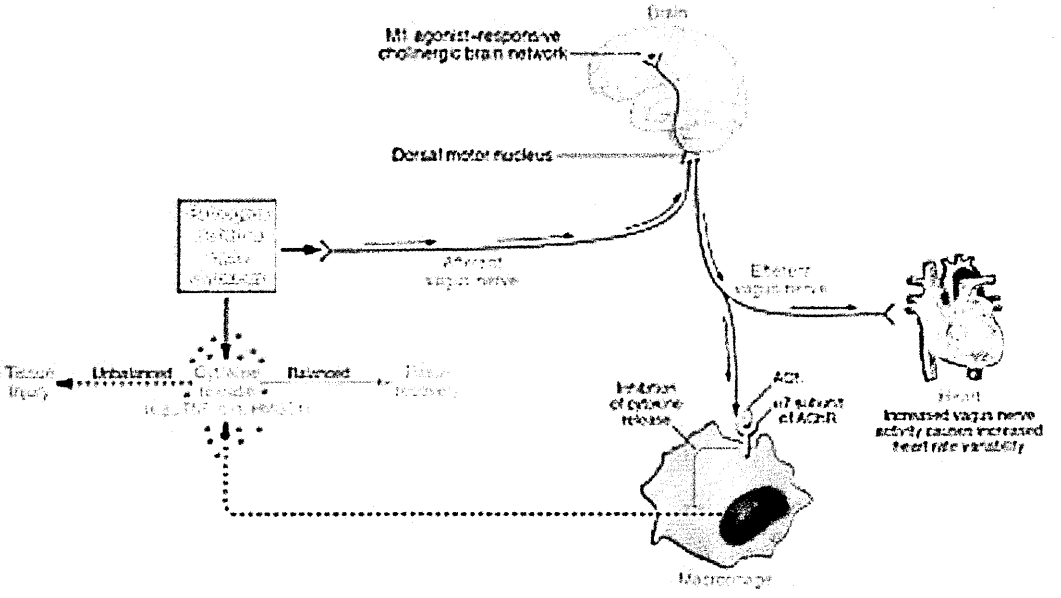

Figure 1.2. ACh anti-inflammatory pathway: Permission to reuse this published image was obtained from Dr. Tracey (Tracey 2007). This image shows that peripheral tissue injury results in cytokine production. However, an imbalance in the cytokine response further exacerbates the injury. Under this abnormal situation, afferent neuronal connections in the vagus nerve send a signal to the brain (involving M1 ACh receptors), which then activates an efferent response to inhibit cytokine release. Efferent signals from the vagus nerve are controlled by brain networks which inhibit cytokine production via ACh pathways that involve the α7 subunit of the AChR on macrophages and other immune cells.

1.5.3. Relevance of lipid metabolism and lipid-mediated pathways to GWI

Although lipid dysfunction has not been examined in veterans with GWI, studies do provide support that exposure to GW agents, such as PER, could affect membrane lipids. For instance, exposure to PER in rats was associated with a decrease in cellular cholesterol and a decrease in membrane fluidity (Vadhana et al 2011). Phospholipids (PLs), particularly those that contain choline, can be metabolized to replenish ACh (Amenta, & Tayebati 2008). Furthermore, PLs and their metabolites are upstream of the inflammatory cascades and contribute to immune and inflammatory balance within the CNS and the periphery. For example, docosahexaenoic acid (DHA) and arachidonic acid (AA) are the most abundant ω-3 and ω-6 polyunsaturated fatty acids (PUFA), respectively, in the brain. Arachidonic acid is a precursor of pro-inflammatory lipid mediators, such as

prostaglandins and leukotrienes and DHA is a precursor of the anti-inflammatory mediators, neuroprotectins and resolvins (Serhan et al 2008; Fredman, & Serhan 2011). A number of other lipid metabolites, such as lysophosphatidylcholine (LPC) and platelet-activating factor (PAF) also have important roles in regulating immune/inflammatory changes (Hasegawa et al 2011). These studies suggest that examination of PL and their metabolites may be useful in providing novel insight into the pathobiology of GWI.

1.6. Hypothesis

Long-term outcomes of GW agent exposure may include chronic ACh depletion, and consequently activation of the biological pathways which break down PLs in cell membranes to replenish synaptic ACh to normal levels (Amenta, & Tayebati 2008). Acetylcholine receptors can modulate cascades of lipid-mediated intracellular biological events that are implicated in a number of neurocognitive disorders (Isacson et al 2002; Gallegos et al 2008). As described above, ligand binding of both mAChR and nAChR is increased in several different brain regions of rodents exposed to GW agents. It can then be assumed that combined exposure to GW agents may produce cumulative adverse effects on the cholinergic signaling pathways given their ability to affect the ACh turnover and ACh receptor activation that are described above. Hence, the central hypothesis of this thesis is that exposure to GW agents disrupt biological pathways that are downstream of ACh receptors which include inflammation related lipid metabolism pathways.

1.7. Objectives of this thesis

1. The first objective was to develop mouse models that recapitulate CNS symptoms of GWI. Neurobehavioral studies were conducted to characterize changes at a range of timepoints (both acute and chronic). Neuropathological studies were conducted at chronic post-exposure timepoints.

2. Exploratory studies using targeted protein and proteomics analyses were conducted at chronic post-exposure timepoints to identify biomolecular pathways using brain and plasma samples from the two mouse models of GW agent exposure.
3. As proteomic findings suggested an involvement of lipid metabolism related pathways, lipidomic profiling was performed on brain and plasma samples from these mouse models of GW agent exposure.
4. Lipidomic profiles of GWI mouse models were compared with mouse models of other neurological illnesses in order to identify lipid profiles that were unique to GW agent exposure in mice.
5. Lipidomic profiles were interrogated to identify potential biological pathways which may be implicated GWI.

1.8. A summary of the upcoming Chapters

The chapters below provide a detailed account of the development of two mouse models of GW agent exposure and characterization of the neurobehavioral and neuropathological consequences of GW agent exposure over time (Objective 1). This is followed by a summary of exploratory studies that are aimed at identifying the biological pathways perturbed in response to GW agent exposure (Objective 2). The fourth chapter will highlight lipidomic studies performed using plasma and brain samples from GWI mouse models as well as other mouse models of neurodegenerative illnesses (Objectives 3 and 4) in order to determine lipidomic changes that are specific to GW agent exposure in these mouse models (Objective 5).

2.0. Chapter 2: Development of mouse models that recapitulate CNS symptoms of GWI

This chapter details the neurobehavioral and neuropathological work performed for the development of mouse models of GW agent exposure. Mouse model A was based on previously published work by Abdel-Rahman and colleagues, which at the time of development of this model was the only combined GW agent exposure that included PB in combination with pesticide/insect repellent. The main goal was to translate this GW agent exposure paradigm from rats to mice. Mouse model B was subsequently developed using high doses of PB and PER and the main goal was to examine if there is an adverse cognitive outcome associated with this exposure.

2.1. *GW agent exposure model consisting of PB, PER, DEET and stress - model A*

2.1.1. Introduction

To date, the most well-characterized GW agent exposure paradigm consists of combined exposure to PB, PER, and DEET with or without stress in rats and was previously employed by Abou-Donia et al (Abou-Donia et al 2001) and Abdel-Rahman and colleagues (Abdel-Rahman et al 2004). GW agent exposure consisting of PB, PER, and DEET was shown to produce sensorimotor deficits in exposed rats compared to controls (Abou-Donia et al 2001). An increased anxiety in rats exposed to PER and DEET compared to unexposed rats has been previously reported (Hoy et al 2000). However, effects of combined exposure to PB, PER, DEET and stress on anxiety-related outcomes have not been examined. Furthermore, there are no published reports suggesting that exposure to this particular GW agent combination results in cognitive impairment. In rats exposed to this particular GW agent combination, Abdel-Rahman and colleagues

characterized neuronal loss using Hematoxylin and Eosin (H&E) staining. However, there have been some concerns over whether neuronal death characterized as a presence of dark neurons (basophilic and having a dark blue color of the perikaryal and dendritic cytoplasm detected using H&E staining) in studies by Abdel-Rahman and colleagues may have been an histopathological artifact (Jortner 2006). Jortner suggested that these findings are possibly a consequence of inadequate brain perfusion–fixation during tissue extraction (Jortner 2006). Other neuropathological findings included an observed increase of astrogliosis using Glial Fibrillary Acid Protein (GFAP) in exposed rats compared to controls but microglia activation was not evaluated (Abdel-Rahman et al 2004). Generally, microglia activation is considered to precede neuronal loss, and thus it might be an important marker of the CNS immune/inflammation status. Despite some limitations of this GW agent exposure paradigm, an extensive neuropathological characterization and some neurobehavioral studies presented by the original investigators provided a good starting point for development of a mouse model of GW agent exposure. Therefore, PB, PER, DEET and stress were utilized to develop mouse model A, which would help address the limitations described above and fill current gaps in knowledge regarding the cognitive consequences with this particular combination of GW agent exposures.

2.1.2. Materials and methods

2.1.2.1 Chemicals

Pyridostigmine bromide was purchased from Fisher Scientific (USA), PER (an analytical standard containing a mixture of 26.4% cis and 71.7% trans isomers) and DEET (97% purity) were both purchased from Sigma Aldrich (USA). In the absence of information on the cis/trans ratio of PER used in the 1990-1991 Gulf War, the above ratio was chosen since it was similar to that recommended by the World Health Organization (25% cis and 75% trans).

2.1.2.2 Animals

Animal experiments described here were approved by the Roskamp Institute's Institutional Animal Care and Use Committee (IACUC) and conducted in accordance with the Office of Laboratory Animal Welfare and the Association for the Assessment and Accreditation of Laboratory Animal Care guidelines. Each mouse was individually caged in a controlled environment (regulated 14 hr day/10 hr night cycle) and maintained on a standard diet. Mice were randomized to either the exposure or the control group using an Excel-based random number generator.

This exposure paradigm was administered as previously utilized by Abdel-Rahman and colleagues in rats (Abdel-Rahman et al 2004). Twenty C57BL6 mice (age 15-17 weeks, and mean weight 23.5 g ± 3.01 SD) were randomized within each gender to either the exposure or the control group using an Excel-based random number generator (n = 10; 6F, 4M in exposed and n = 10, 6F, 4M in control). The exposure consisted of 1.3mg/kg PB orally in water, 0.13mg/kg PER and 40mg/kg DEET in 50µl of 70% ethanol, both as dermal applications on an approximately 2 cm^2 pre-clipped area (at the back of the neck), and 5 minutes (min) of restraint stress in a plexiglass rodent restrainer. The authors had suggested that these doses represented the low level chronic exposure to which GW veterans were exposed (Abdel-Rahman et al 2004) (Abou-Donia et al 2001). The exposure was administered daily over a period of 28 days. The control group was given water and topical application of 70% ethanol throughout the same time-period.

2.1.2.3. Neurobehavioral testing

All behavior testing was performed during the light phase of the circadian cycle with operators blinded to the exposure assignment. The rotarod, open field test (OFT) and Morris water maze (MWM) tests were performed as briefly described below (see Figure 2.1 for a timeline of behavior experiments).

Figure 2.1

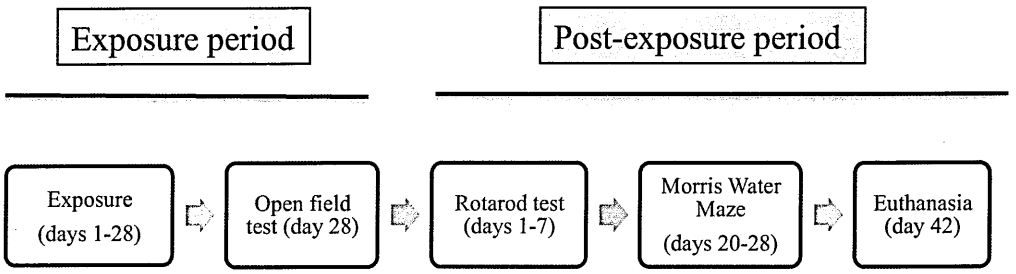

Figure 2.1. Timeline of neurobehavioral experiments for mouse model A of GW agent exposure. Only the open field test was performed during the exposure period. All other tests were performed on post-exposure days.

2.1.2.3.1. The open field test

The OFT was conducted using a 1m diameter arena on the last day of the exposure and a single trial lasting 15 min was conducted for each mouse. The test was conducted in a brightly lit room. The total distance traveled by each mouse within the arena was recorded to determine motor function and the amount of time spent in the periphery (perimeter activity) was used to quantify anxiety-related behavior. This measure has consistently been shown to reflect the anxiolytic state in animals (Blanchard et al 2001; Stanford 2007). The Ethovision tracking software (Noldus) was used for recording these experiments.

2.1.2.3.2. Rotarod

Baseline performance for each mouse was determined prior to the exposure period. Mice were allowed to acclimate to the experimental paradigm using 1 trial at 5 rpm fixed speed over 5 min. The baseline was established using 3 trials of 5 min each, conducted daily for 3 consecutive days (prior to initiating the exposure paradigm), during which the speed was accelerated from 5 to 60 rpm within each trial (with a 3 minute inter-trial interval). The average value for latency to fall on all 3 trials of the last day was used as

baseline. Main testing occurred every other day from post-exposure days 1 to 7 using the same speed as above. The latency to fall on each day was averaged from three consecutive trials and the percent change from baseline was calculated to determine the exposure effect.

2.1.2.3.3. Morris Water Maze

The MWM test was conducted using a 2.5m^2 diameter pool filled with cloudy water (addition of white non-toxic powdered paint), situated in a room with visual cues on the wall and on the pool edge above the water level. The acquisition trials were conducted on post-exposure days 20-28. Four acquisition trials were administered daily with an inter-trial interval of approximately 30 min. For the acquisition trials, a platform was placed 1.5 cm below the water surface in the North East (NE) quadrant of the pool. Mice that failed to find the hidden platform within 90 seconds (sec) were guided to the platform and required to remain there for 30 sec before being returned to the cage. A probe trial was conducted 24 hrs after the acquisition trial on post-exposure day 28, for which the platform was removed. During this trial, the latency to reach the location where the target platform was previously located and the time spent in the original target quadrant were recorded using the Ethovision software.

2.1.2.3. Statistical analyses for the neurobehavioral studies

Post-hoc power calculations were performed using the G-power software (Faul, & Erdfelder 2007) and a power of 80% was detected for the rotarod test, 65% for the OFT and 31% for the MWM (based on the differences for the probe trial) at alpha 0.05 for the sample size using the described statistical analyses. A mixed linear model (MLM) regression was employed to examine the independent effects of exposure, time and any potential interactions between them, on the neurobehavioral outcomes. The MLM-based regression analysis approach is generally considered superior to other ANOVA methods

due to its flexibility to accommodate both fixed and random effects of the independent variables (Katz 2011). For OFT, distance travelled and perimeter activity within the arena were used as the outcome measures where exposure and time (three 5 min-intervals over 15 min) were used as fixed factors with each mouse as a random factor. For the rotarod test, latency to fall (sec) was examined as an outcome variable, each mouse as a random factor, and exposure and time (days) as fixed factors. Similarly, for the MWM, escape latency (sec) and amount of time spent in the target quadrant were considered outcome measures while time (days) and exposure were considered fixed factors and mouse as a random factor. All analyses were performed with SPSS 13.0 (IBM Corp. Armonk, NY) and the statistical significance was set at an alpha 0.05 level.

2.1.2.4. Histopathological analyses

Animals (n = 5 [3F, 2M] per exposure/control) were euthanized on post-exposure day 42 for the neuropathological study. All animals were transcardially perfused with PBS followed by an overnight fixation of brain samples in 4% paraformaldehyde and paraffin embedding. Six μm thick coronal sections were rehydrated in a gradient of ethanol before the immunohistochemical procedure. Nissl substance was stained with 0.25% Cresyl Violet to assess neuronal loss, described elsewhere (Bondolfi et al 2002). Antibodies for GFAP (1:10,000, Dako, Carpinteria, CA) and CD45 (1:50 Serotec, Raleigh, NC) were used to stain astrocytes and microglia, respectively. All primary antibodies were localized using Vectastain ABC kits (Vector Laboratories, Burlingame, CA). Both microscopy and quantification were performed with the operator blinded to the exposure assignment. Three stained sections from each mouse brain were visualized with an Olympus (BX60) light microscope and 2D images were acquired using an Olympus MagnaFire SP camera and analyzed using Image-Pro Plus software (Bethesda, MD). The dentate gyrus of the hippocampus and the cerebral cortex were examined. Within the cerebral cortex, 3 different locations were used for quantification and the same locations were examined

from each mouse. For statistical analyses, the total area occupied by the stained material (consisting of both processes and cell bodies that were present in the field of view) was analyzed and compared using the Student's t-test.

2.1.3. Results

2.1.3.1. Neurobehavioral testing

Mice were tested for anxiety and related behavior using the OFT. The time spent at the perimeter and the overall distance traveled within the arena were used as the outcome measures (Figure 2.2). For the time spent at the perimeter, there was a significant main effect of exposure ($F_{(1, 50)} = 4.15$, $p = 0.047$) and a confounding effect of gender ($F_{(1, 50)} = 13.22$, $p = 0.001$). Figure 2.2A shows that female exposed mice spent more time at the

Figure 2.2A **The open field test**

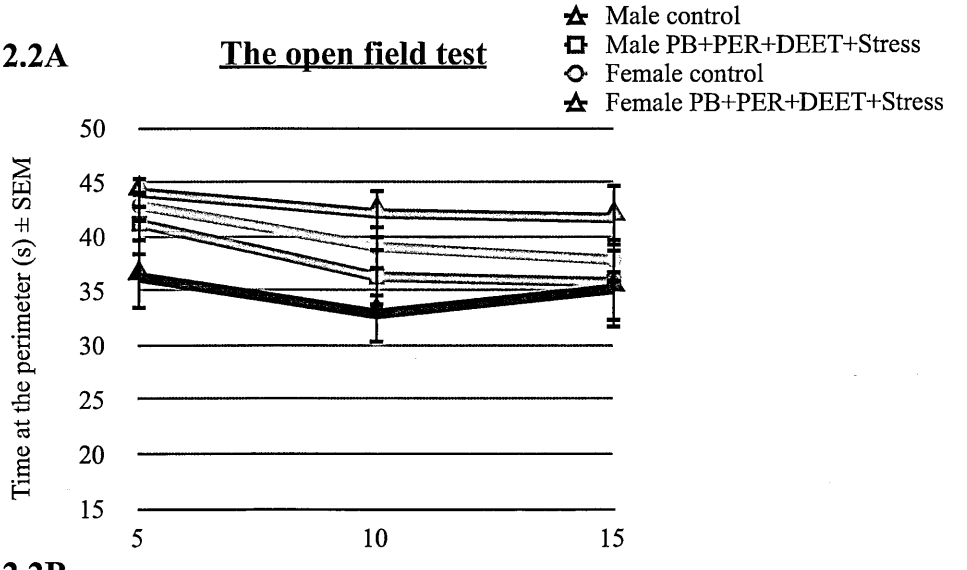

Figure 2.2B

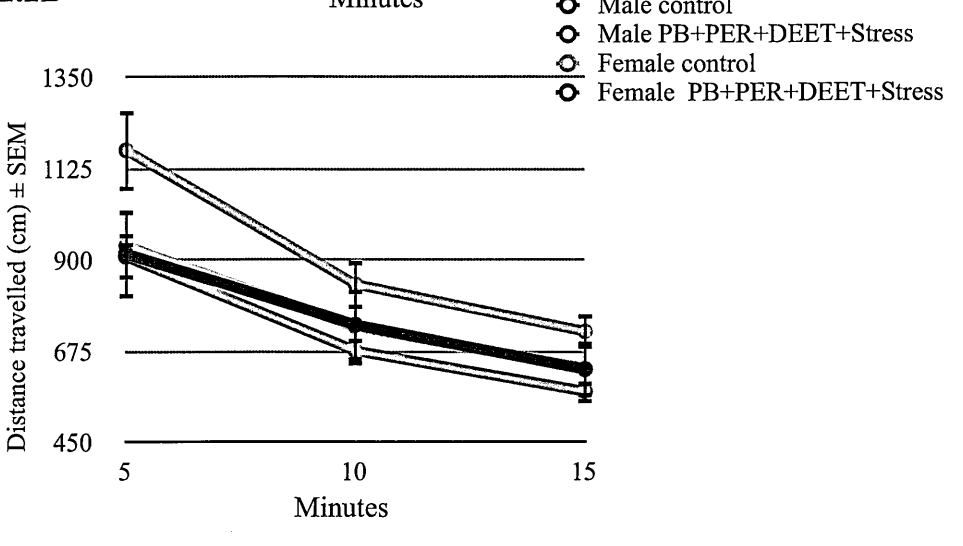

Figure 2.2. The open field test: Mean ± SEM, n = 10 in each of the exposed and control groups. (A) An increase in perimeter activity was noted in exposed mice compared to controls on the OFT conducted on last exposure day (day 28) and a significant confounding effect of gender was also observed, $p < 0.05$ (based on MLM regression, a main effect was observed irrespective of time, which was also a fixed main factor in the regression model). Exposed female mice spent more time (s) at the perimeter than control female mice. Male exposed mice spent more time at the perimeter than control male mice, but only during the first 10 minutes. Female mice spent more time at the perimeter than male mice. (B) There was no main effect of exposure, $p > 0.05$ nor an interaction between time and exposure, $p > 0.05$. An interaction was observed between exposure and gender on the locomotor activity in the arena, $p < 0.05$, (based on MLM regression as described in A above) indicated by a larger distance (cm) traveled by male exposed mice than control male mice. Female exposed mice traveled less distance within the arena than control female mice. *Note: A version of this figure is published (Abdullah et al 2012).*

Figure 2.3

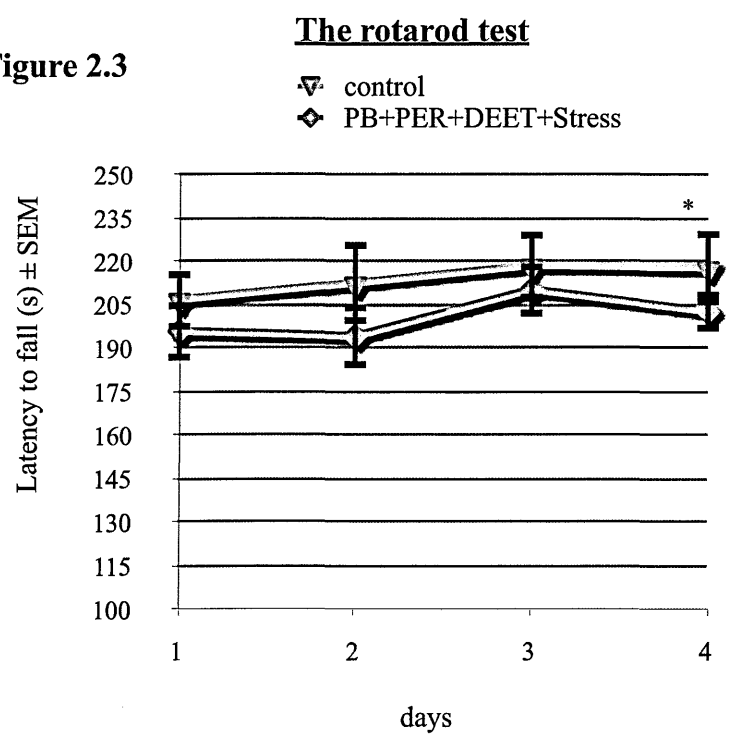

Figure 2.3. The rotarod test: Mean ± SEM, n = 10 in each of the exposed and the control group. Exposed animals had a shorter latency to fall compared to controls, * denotes $p < 0.05$ for a main exposure effect (based on MLM regression where days and exposure were fixed main independent factors). This test was conducted on every alternate day during post-exposure days 1 to 7. *Note: A version of this figure is published (Abdullah et al 2012).*

perimeter than female control mice. Similarly, exposed male mice spent more time at the perimeter than control male mice. Overall, female mice spent more time at the perimeter than male mice. For the distance travelled, there was no main effect of exposure ($F_{(1, 47)} = 1.092$, $p = 0.17$), but an interaction between exposure and gender ($F_{(1, 44)} = 7.42$, $p < 0.01$) as well as a confounding effect of time ($F_{(2, 39)} = 30.57$, $p = < 0.01$) was observed on this

outcome. Figure 2.2B shows that compared to female control mice, exposed female mice travelled less distance over the three timepoints. Conversely, male exposed mice traveled more distance within the arena than control male mice.

Differences in sensorimotor coordination between exposed and control animals were assessed based on their ability to stay on an accelerating rotating rod. A shorter mean latency to fall was observed in the exposure group than the control group ($F_{(1, 70)} = 8.20$, $p = 0.006$). Figure 2.3 shows that compared to their baseline values, exposed animals had approximately 13% lower latency to fall on day 1, 15% on day 3, 10% on day 5 and 11% on day 7, while control mice performed within 8% of their baseline performance, indicating a significant motor impairment in the exposed animals. There was a marginal confounding effect of gender ($F_{(1, 70)} = 3.17$, $p = 0.08$) on this sensorimotor performance measure.

During post-exposure days 20-28, mice were evaluated on the spatial memory task using MWM. Throughout the acquisition trials (days 20-28), there was an effect of training days on the escape latencies ($F_{(8, 30)} = 2.63$, $p = 0.03$), but there was no difference between exposed and control mice on this outcome ($F_{(8, 150)} = 0.48$, $p = 0.49$, Figure 2.4a). There was a main exposure effect on the distance travelled ($F_{(1, 151)} = 10.88$, $p < 0.01$, Figure 2.4B), and a confounding effect of both gender ($F_{(1, 151)} = 6.99$, $p < 0.01$) and of training days ($F_{(1, 147)} = 5.10$, $p < 0.01$) on the relationship between GW exposure and this outcome. There was also a significant exposure effect on the swim speed ($F_{(1, 145)} = 4.18$, $p = 0.04$, Figure 2.4C) and a confounding effect of gender on this relationship ($F_{(1, 145)} = 4.75$, $p = 0.03$, figure 2.4D). On the final day 28, a single probe-test was conducted 24 hours post-acquisition to evaluate long-term memory. Both the control and exposed groups displayed similar average escape latency ($t\text{-test}_{(18)} = 0.94$, $p = 0.36$, figure 2.4D) and duration of time spent in the quadrant which previously contained the platform ($t\text{-test}_{(18)} = -0.23$, $p = 0.82$, figure 2.4E).

The Morris water maze tests
Acquisition

Figure 2.4A

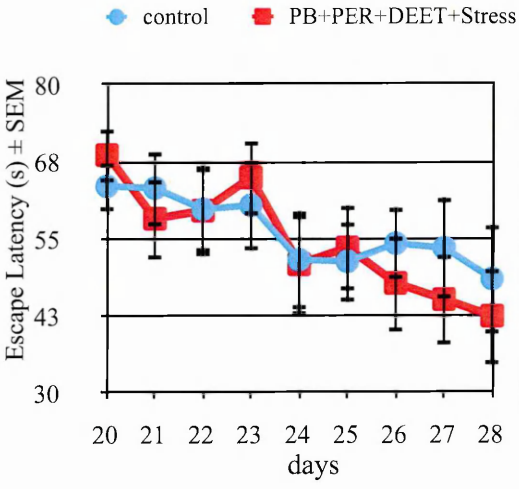

Figure 2.4B

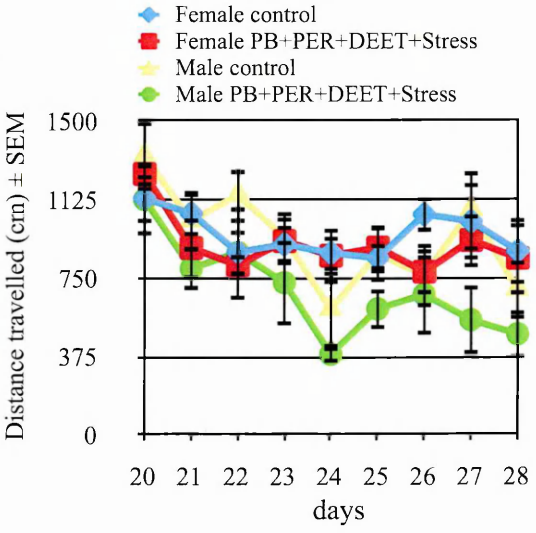

Figure 2.4C

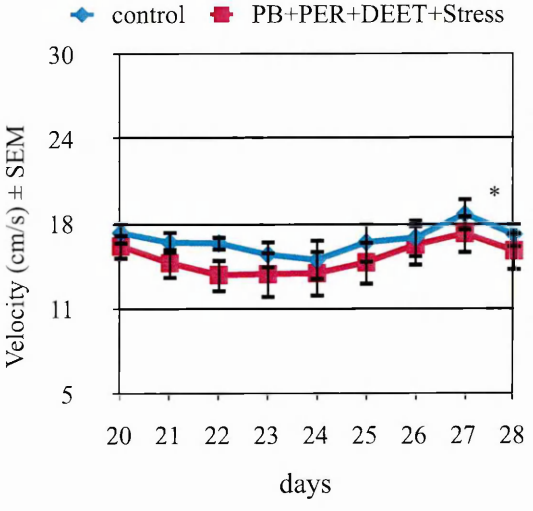

Figure 2.4D

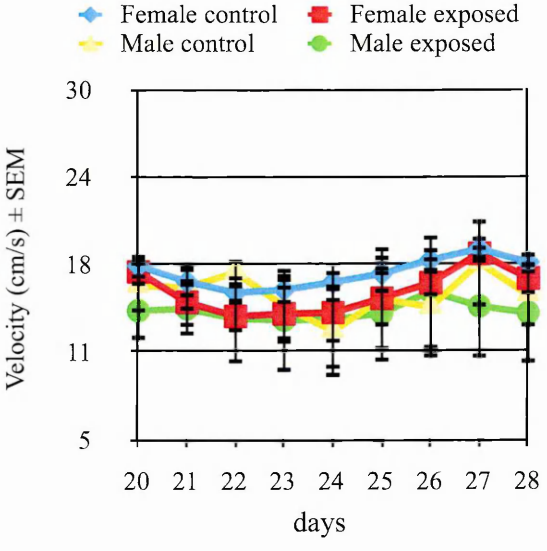

The Morris water maze tests
Probe trial

Figure 2.4E

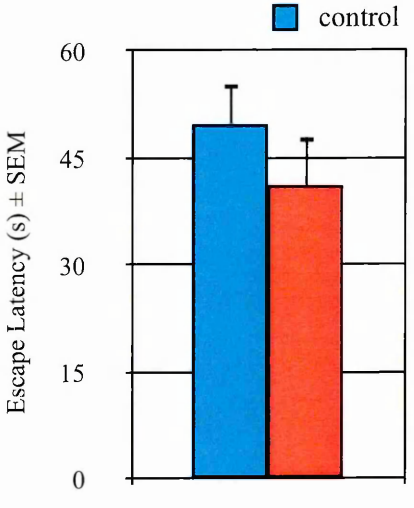

Figure 2.4F

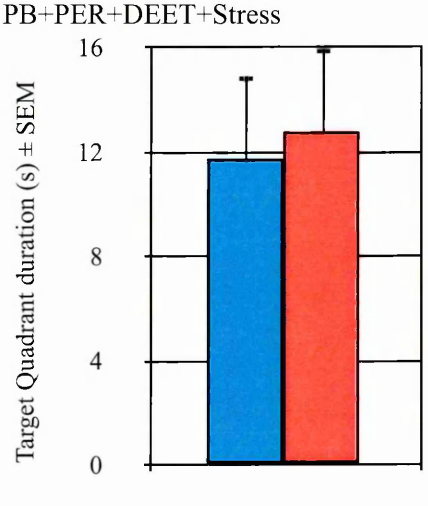

Figure 2.4. The Morris water maze test: Mean ± SEM, n = 10 in each of the exposed and the control group. (A) There were no differences between the two groups on escape latency during the acquisition trials (post-exposure days 20-28), $p > 0.05$. (B) Significant differences on total distance travelled in the maze were observed between the two groups and a confounding effect of gender was noted, $p < 0.05$ (based on MLM regression where training days, gender and exposure were all fixed main independent factors). Within each gender, exposed mice performed worse than control mice. (C) For the swim velocity, there was a significant difference between the two groups and a main exposure effect was observed, *$p < 0.05$ denotes a main exposure effect (based on MLM regression as described for B above). (D) Figure depicting a confounding effect of gender on the relationship between exposure and swim velocity, $p < 0.05$ (based on MLM regression as described above). Female exposed had lower swim velocity that control female mice. Male exposed mice also had lower swim velocity than male control mice but only on last two days of the acquisition trials. (E-F) During the probe trials conducted on day 28, there were no differences between the two groups on either the (E) latency to escape or the (F) duration of time in the target quadrant, $p > 0.05$ (based on the Student's t-test) . *Note: A version of this figure is published (Abdullah et al 2012).*

GFAP staining

Figure 2.5A

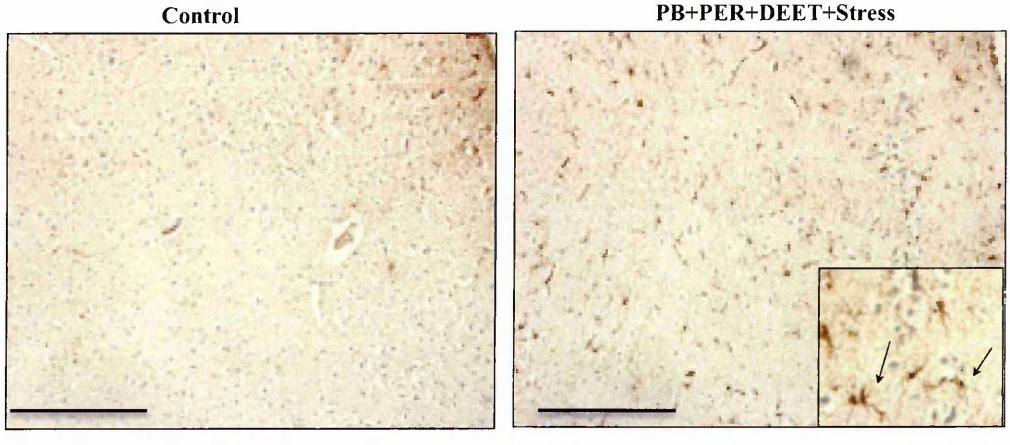

GFAP quantification

Figure 2.5B

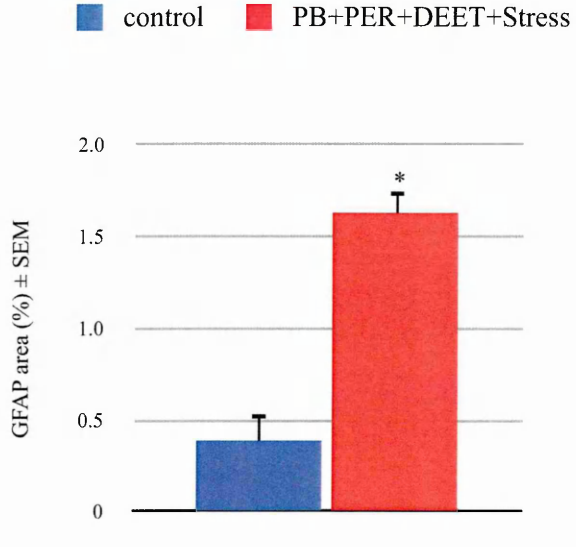

Figure 2.5. GFAP staining: Mean ± SEM, n = 5 in each of the exposed and the control group. (A) Representative images of cerebral cortices after GFAP staining from mice exposed to GW agent and control mice, taken with a 20x objective providing a 200x magnification. The insert is an image of exposed mice taken with a 60x objective showing 600 x magnification. Arrows point to reactive astrocytes in the cerebral cortex of exposed mice. *Note: A version of this figure is published (Abdullah et al 2012).* (B) Quantification depicting a nearly four-fold increase in GFAP reactivity in response to exposure. This increase was statistically significant based on the Student's t-test, *p < 0.001.

Nissl staining

Figure 2.6

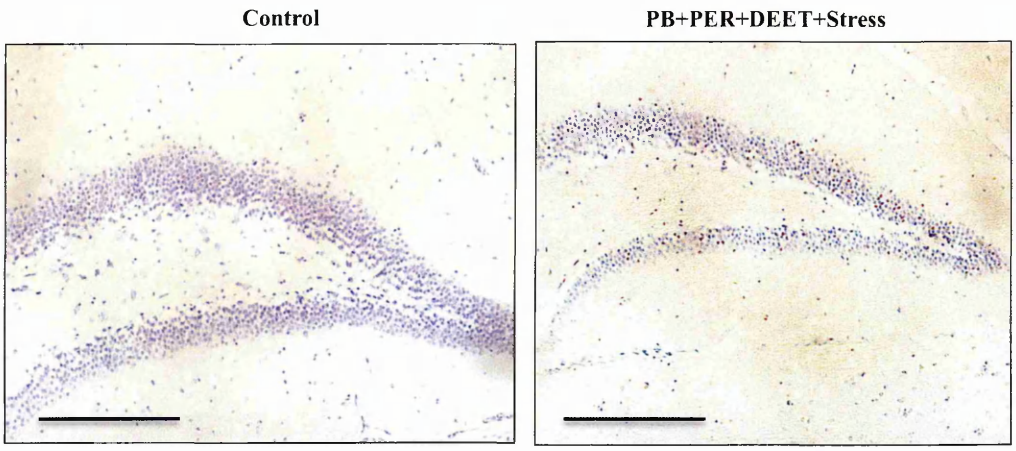

Figure 2.6 Nissl staining Mean ± SEM, n = 5 in each of the exposed and the control group. Representative images of Dentate Gyrus after Nissl staining from mice exposed to GW agent and control mice, taken with a 20x objective providing a 200x magnification. Visual inspection did not reveal any differences between the two groups. The scale bar represents 50μm in each image.

2.1.3.2 Histopathological analyses

Astrogliosis was quantified using GFAP staining which showed a robust presence of reactive astrocytes in the cerebral cortex of exposed animals as compared to controls (t-test = -6.43 (df = 8), $p < 0.01$, Figure 2.5a and 2.5b). No differences were observed in the hippocampus between the two groups. The results from Nissl staining do not show any differential neuronal loss between the two groups in either the cortex or the hippocampus (Figure 2.6). Microgliosis was measured using CD45 staining but no staining was detected in neither controls nor exposed mice (data not shown).

2.1.4. Discussion

These studies indicate that the sensorimotor deficits and astrogliosis observed in rats exposed to PB, PER, and DEET with or without stress were also present in mice

exposed to PB, PER, DEET and stress. In addition, these studies also provide novel data with respect to the evidence of anxiety-related behavior in mice administered this particular GW agent combination as compared to controls. The OFT has been in use for several decades to assess motor function, exploration and anxiety over a short-time period (Blanchard et al 2001; Aguilar et al 2002). Using this apparatus, anxiety-like features were observed in mice exposed to PB, PER, DEET and stress, as indicated by an increase in time spent at the periphery of the OFT arena. Several studies using rodents show altered OFT behavior in response to PB and PER, or to PER and DEET (Abdullah et al 2011; Hoy et al 1999).

Interestingly, gender differences were observed in this anxiety measure within the OFT arena, where female mice generally appeared more anxious than male mice. Cross-sectional analyses using a sample from UK Armed Forces showed much higher rates of psychological distress and chronic fatigue in women deployed to the 1990-1991 GW than men (Rona et al 2007). These studies support a potential influence of GW agents in producing the anxiety symptoms which may be different between male and female veterans with GWI and warrant further investigation.

Previous studies conducted by Abou-Donia and colleagues showed a presence of sensorimotor impairment in rats exposed to PB, PER and DEET (Abou-Donia et al 2001). Sensorimotor deficits were observed in mice exposed to PB, PER, DEET and stress compared to control mice in mouse model A. To date, there are only two reports showing cognitive impairment in animals exposed to combinations of PB and PER or PB and stress, in particular both showing a presence of delayed learning and/or cognitive impairment (Abdullah et al 2011; Lamproglou et al 2009). However, the GW exposure paradigm utilized in the current study produced considerable sensorimotor impairment, evident in the rotarod studies and MWM swim velocity. This confounded the cognitive testing

performed using the MWM. A recent study by Patil and colleagues demonstrated that the mouse strain of C57BL6 utilized in the current study is prone to anxiety which affects performance on the MWM (Patil et al 2009). Perhaps an alternative cognitive testing method, such as novel object recognition test, which is less physically demanding for the animals, might be ideal under these circumstances.

Having demonstrated neurobehavioral outcomes, the next goal was to determine if some of the pathological features examined in the original rat model are also present in this mouse model. The observed presence of an increase in reactive astroglia is consistent with findings from Abdel-Rahman and colleagues (Abdel-Rahman et al 2004). A particular characteristic of reactive astrogliosis is an increase in GFAP (a member of the intermediate filament family), as observed here, which is thought to be an early marker of CNS injury (Zhang et al 2010). The literature suggests that microglial activation precedes astrogliosis and microglia can revert to its resting state if homeostasis is restored (Lue et al 2010). However, there was no presence of reactive microglia in neither exposed nor control mice. Given that a long time had elapsed between exposure and neuropathological examination (42 days), it is possible that reactive microglia were present at an earlier timepoint. It is also suggested by a recent astroglial imaging study that astrocytosis may be an early event in a neurodegenerative condition, which could explain why neuronal loss was not observed at this stage (Carter et al 2012).

In summary, translation of this GW agent combination from rats produced previously reported sensorimotor deficits and astrogliosis (Abdel-Rahman et al 2004; Abou-Donia et al 2001). However, cognitive impairment was not detected in model A due to the confounding effects of sensorimotor deficits, which is reported to be one of the top four complaints among veterans with GWI. Therefore, additional work (i.e. examination of a different exposure paradigm) was required to determine if a different combination of

GW agents may produce cognitive impairment in a mouse model. The next section will describe work that was particularly focused on characterizing cognition after combined exposure to another GW agent combination.

2.2. GW agent exposure model consisting of high dose PB and PER - model B

2.2.1. Introduction

At the time this work was undertaken, only one rat model of GW-agent exposure (stress and PB) had conclusively demonstrated significant memory impairment (Lamproglou et al 2009) while most other rat models had only reported sensorimotor deficits in response to PB, DEET and PER alone or in combination with each other (Abou-Donia et al 2001). In model A above, the presence of motor impairment confounded the MWM experiments and, as a consequence, cognitive data were uninterpretable. As one of the main goals of this thesis was to develop mouse models of GW-agent-induced phenotypes, particularly one that includes cognitive dysfunction, a combination of high dose PB and PER was administered and post-exposure neurobehavioral characterization was performed over an extended time period in order to maximize the likelihood of obtaining a cognitive outcome. The combined exposure of PB and PER was chosen based on earlier genomic work conducted at the Roskamp Institute, which showed a greater disruption of neuronal gene expression with PER exposure than with DEET (Kayihan et al 2010). In addition, a recent case-control study conducted by Steele and colleagues demonstrated much higher risk of GWI among veterans who were exposed to PB and wore pesticide imbedded uniforms, which largely contained PER (Steele et al 2012).

For these studies, high doses of PB and PER were chosen in an attempt to mimic a high-level exposure likely to be experienced by GW veterans. For instance, daily

consumption of 120 mg of PB (equivalent to 4 PB pills containing 30 mg each) for an average weight of 75kg per individual would approximate 1.6 mg/kg; 2 mg/kg PB exposure is shown to inhibit AChE and activate pathways involved in the formation of long-term memory (Friedman et al 1996). Permethrin was provided to the enlisted personnel as a 0.5% spray and according to the RAND survey, the PER spray use may have been as high as 360 times per month (Binns et al 2008). This PER usage far exceeded that stated on the PER label, which recommended that uniforms should have been sprayed only once every six weeks or after six launderings (Binns et al 2008). Given the paucity of information on doses and routes (e.g., inhaled, skin absorption) of PER delivery, there is no accurate way of estimating the exact dose of PER exposure to GW veterans. Thus, 200 mg/kg of PER was administered to mimic a high-level exposure. Although maximum permitted intake in human is 3.75 mg for a 75 kg person, the dose of 200 mg/kg was chosen since it was used in mice by previous studies showing adverse behavioral or pathological outcomes (Dodd, & Klein 2009; Pittman et al 2003; permethrin information sheet). The doses for PB and PER used in this study are approximately half of the LD_{50} dose in rodents for each chemical (4mg/kg for PB and 429mg/kg for PER via i.p. in mice, see Table 1.1 for more details), respectively (Chaney et al 2002). These studies will characterize some of the key neurobehavioral and neuropathological features associated with GWI and provide a mouse model of GW-agent exposure for further biochemical studies aimed at identifying biological pathways involved in GWI.

2.2.2. Materials and Methods

2.2.2.1. Chemicals

Reagents were obtained through Fisher scientific and Sigma Aldrich as described above.

2.2.2.2. Animals

Study animals were housed, maintained on standard diet and randomized using IACUC approved procedures described above. Pilot studies were performed to determine the upper limits of doses, survival and the maximum tolerated dose for PB and PER using apolipoprotein E (APOE) knockout mice which were available in our vivarium at that time. Death was observed at 4 mg/kg (as previously reported (Grauer et al 2001) for PB and 300 mg/kg of PER also suggested lethality. Therefore, doses of PB and PER were further reduced to 2 mg/kg PB and 200 mg/kg PER for the following study with CD1 mice, an out-bred strain derived from in-bred swiss albino mice. Thirty-two CD1 mice (male, age 10 weeks, weight 40.76 g ± 2.38 SD) were purchased (Harlan Animal Research Laboratories, FL) and allowed to acclimate for one week to the new environment at the Roskamp Institute in accordance with the American Association for Laboratory Animal Science guidelines. Mice were co-administered 2 mg/kg PB and 200mg/kg of PER in a single i.p. injection volume of 50µl of 100% dimethyl sulfoxide (DMSO) or the same volume of DMSO alone (vehicle control) daily for 10 consecutive days. This timepoint was chosen based on previous reports of minimal time of GW agent exposure experience by veterans. The choice of i.p. injection was chosen since PB has poor oral bioavailability (see Mestinon® drug insert for details) and PER has low solubility in certain aqueous solutions (Ray, & Fry 2006), which can potentially impact overall results by introducing variability due to inconsistent delivery.

2.2.2.3. Neurobehavioral testing

Neurobehavioral testing was performed during the light phase of the circadian cycle by two investigators who were blinded to the exposure assignment. A timeline of these studies is provided in Figure 2.7.

Motor coordination was assessed using the rotarod test during the exposure period (days 5, 7 and 9) and on post-exposure days 1, 3, 5 and 7. On the first day of testing, mice

Figure 2.7

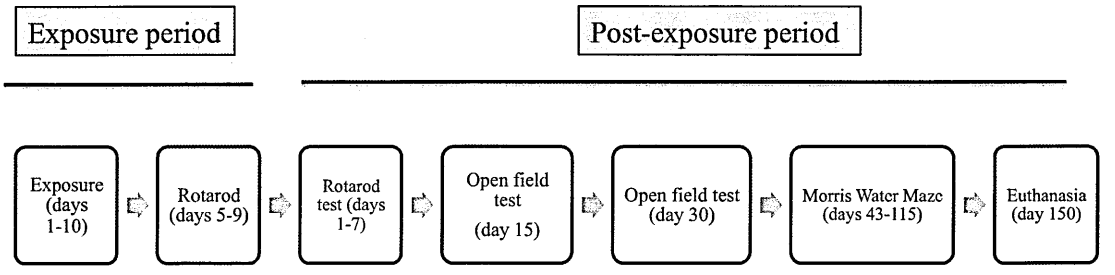

Figure 2.7. Timeline of neurobehavioral experiments for mouse model B of GW agent exposure: Rotarod experiments were performed during both the exposure period and the post-exposure period. All other tests were performed on post-exposure days.

were allowed to acclimate to the experimental paradigm using 3 trials at 5 rpm fixed speed over 5 minutes per trial with 3-minute inter-trial rest intervals on the first testing day. Subsequently, 3 trials of 5 minutes each were conducted per day, during which the speed was accelerated from 5 to 50 rpm (with the same inter-trial interval) within each trial. The latency to fall was evaluated as the outcome measure. The OFT was performed using a 1m arena on post-exposure days 15 and 30 and a single trial lasting 15 minutes was conducted as described above for model A. Total distance travelled in the arena and perimeter activity were used as outcome measures.

The MWM test was conducted using a 2.5m^2 pool filled with cloudy water, situated in a room with visual cues on the wall and on the pool above the water level. The acquisition trials were conducted on post-exposure days 43-51. Briefly, 4 acquisition trials were administered (each for 90 seconds) with an inter-trial interval of approximately 30 minutes. Each probe trial was for 60 seconds. All procedures for acquisition trials and probe trials were conducted as described above for model A with the exception that after the first probe trial on post-exposure day 51, additional probe tests were performed (without repeating the acquisition trials) at approximately 30-day intervals (post-exposure days 86 and 115) to determine long-term memory retention (Lamproglou et al. 2009). The experimental conditions and the arena settings were kept consistent for each probe test

with the aid of the Ethovision software. If a mouse did not reach the target platform location at the end of the session, each mouse was guided to the general location where the platform was originally placed and then retrieved from the pool. All OFT and MWM trials were recorded and analyzed with the Ethovision tracking system.

2.2.2.4. Statistical analyses for neurobehavioral studies

Post-hoc power calculations were performed using the G-power software (Faul, & Erdfelder 2007) to determine the adequacy of the study sample. For the sample size and the statistical analyses utilized in each neurobehavioral test, a power of 99% was detected for the rotarod test, 67% for the OFT and 100% for the MWM at alpha 0.05. All statistical analyses for the OFT, the rotarod and the MWM were performed as described above for model A. For the MWM test, one of the exposed mice developed a tumor growth on its ear and was therefore excluded from the studies. All analyses were performed with SPSS 13.0 (IBM corp. Armonk, NY) and the statistical significance was set at the alpha 0.05 level.

2.2.2.5. Histopathological studies

A subset of animals were euthanized (n = 5 GW agent/control) on post-exposure day 8 (an acute post-exposure timepoint) after the rotarod test. The remaining mice were allowed to live up to post-exposure day 150 (a chronic post-exposure timepoint) and were then euthanized for neuropathological studies. All histopathological studies were performed as described above for model A with the exception that for post-exposure acute studies, a 1:1000 fold dilution of the GFAP antibody was used. For acute studies, presence of reactive microglia was also examined using ionized calcium binding adaptor molecule 1 (Iba1) at a 1:1000 fold dilution and visualized as described above for neuropathology work on model A. For chronic 150 post-exposure timepoint, an Alzheimer's disease (AD) mouse model (PSAPPswe mouse, see chapter 4 for more information on these mice) was used as a positive control.

2.2.3. Results

2.2.3.1. Neurobehavioral studies

On post-exposure day 15, there were no differences between the GW agent exposed mice and control mice for psychomotor function, as measured by the distance traveled within the OFT arena (Figure 2.8A). For this outcome, a significant effect of time was observed ($F_{(2, 36)} = 6.32$, $p = 0.004$) but no significant interaction between time and exposure ($F_{(2, 36)} = 0.10$, $p = 0.9$) was seen. A decrease in the time spent at the perimeter

The open field test 15 days

Figure 2.8A

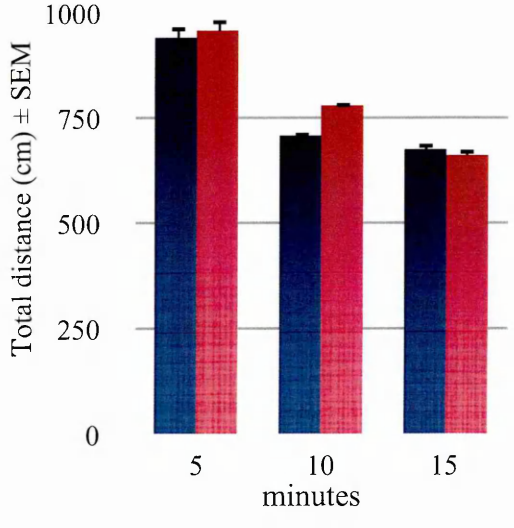

Figure 2.8B

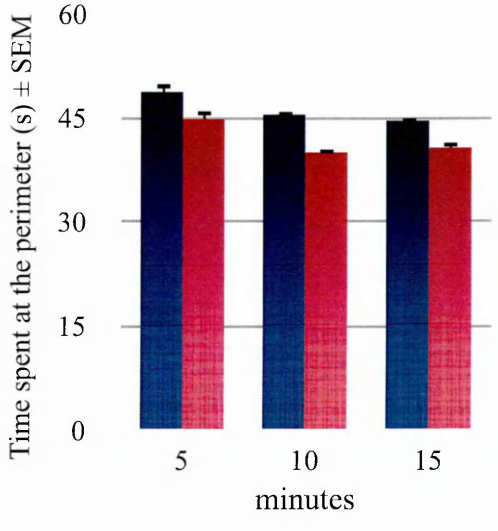

The open field test 30 days

Figure 2.8C

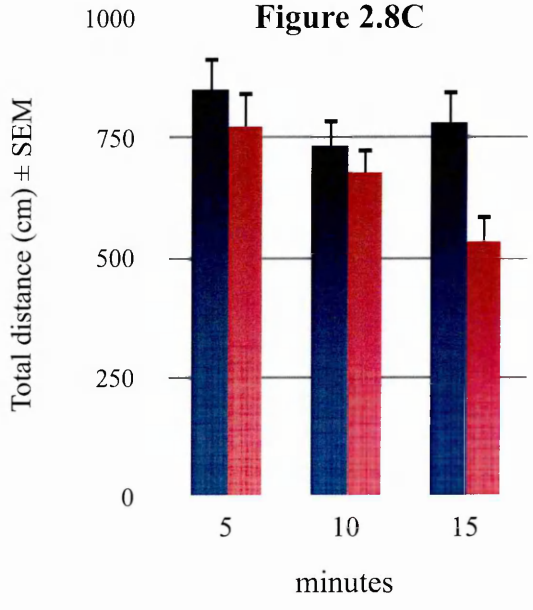

Figure 2.8D

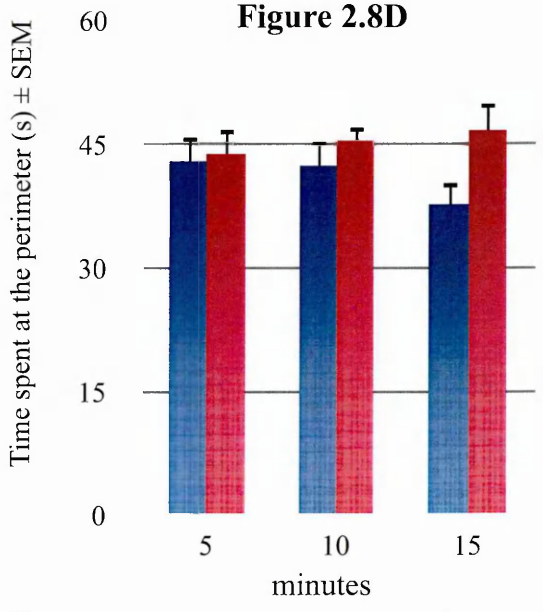

Figure 2.8. The Open Field Test: Mean ± SEM, n = 10 in each of the exposed and the control group. (A) On post-exposure day 15, distance (cm) ± SEM traveled within the arena did not differ between GW agent exposed and control mice, $p > 0.05$. (B) On post-exposure day 15, duration of time (s) spent at the perimeter was shorter for exposed mice compared to control mice over 15 minutes displayed by 5 minute interval (average of 0-5 minute = 5, average of 6-10 minutes = 10 and average of 11-15 minutes = 15), $p < 0.01$, (based on MLM regression where time and exposure were fixed factors). (C) On post-exposure day 30, distance (cm) traveled in the OFT was significantly lower for GW agent exposed animals compared to controls over the 15 minutes testing period, $p < 0.05$ (based on MLM regression as described for B above). (D) On post-exposure day 30, mean time spent at the perimeter for exposed mice, as compared to control mice, was numerically higher during the last 11-15 minute interval for exposed animals compared to controls, $p > 0.05$. *Note: A version of these figures is previously published (Abdullah et al 2011).*

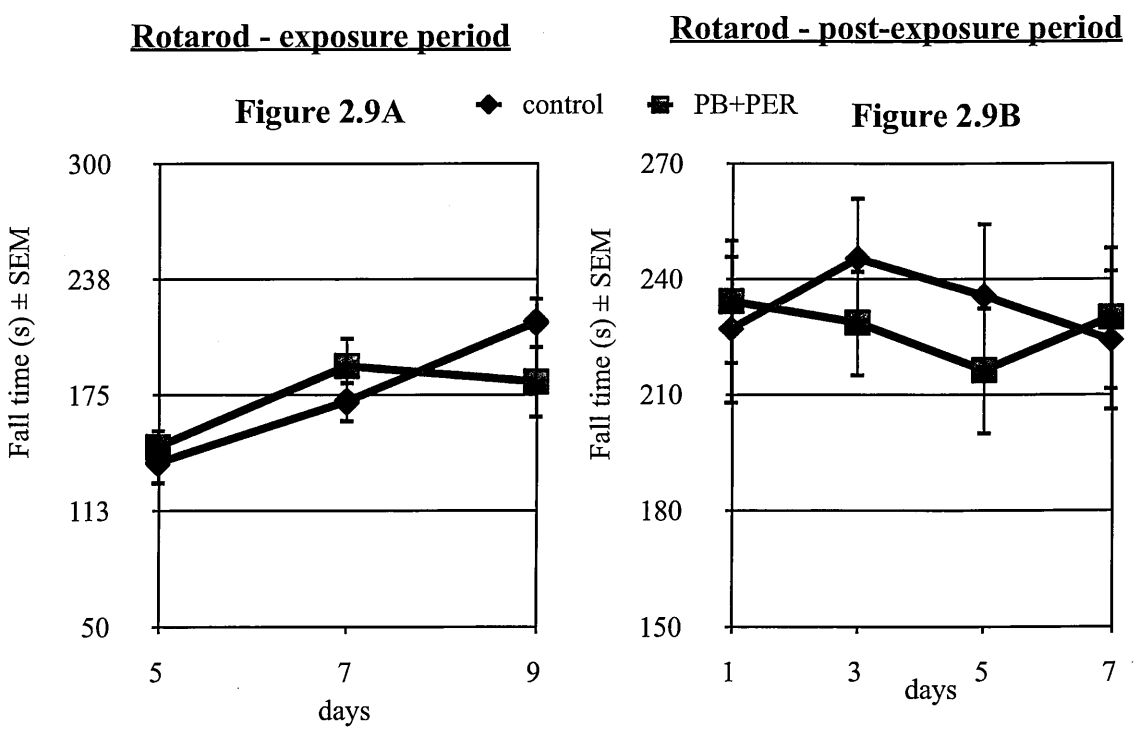

Figure 2.9. The Rotarod Test: Mean ± SEM, n = 16 in each of the exposed and the control group (A) Mean ± SEM latency to fall (s) of exposed to PB and PER and control mice was similar during days 5 to 9 of the exposure period, $p > 0.05$. (B) Rotarod experiments were performed during the post-exposure period covering days 1-7, although mean was shorter in exposed mice on days 3 and 5 but there was no statistically significant difference between mice, $p > 0.05$ (based on MLM regression with post-exposure days and exposure were main fixed factors). *Note: A version of figure 2.8 is published (Abdullah et al 2011).*

was observed in exposed mice compared to controls ($F_{(1, 54)} = 18.19$, $p < 0.001$, Figure 2.8B). On post-exposure day 30, GW agent exposed mice traveled less distance than control mice ($F_{(1, 52)} = 5.92$, $p = 0.018$, Figure 2.8C) and there was no confounding effect of the testing-period ($F_{(2,37)} = 3.07$, $p = 0.06$) nor an interaction ($F_{(2, 37)} = 1.46$, $p > 0.05$. At this timepoint, GW agent exposed mice spent more time at the perimeter compared to

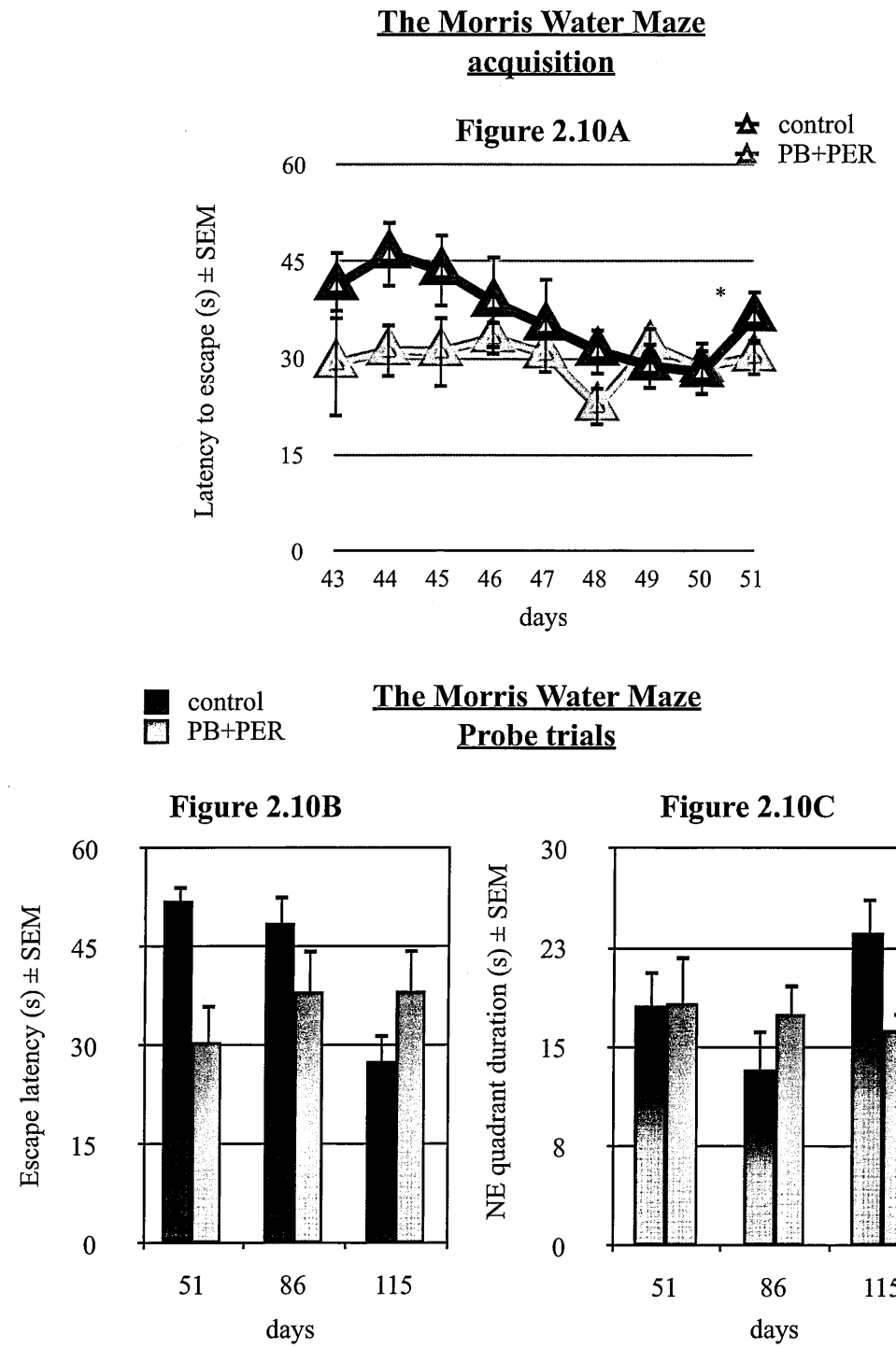

Figure 2.10. The Morris Water Maze test: Mean ± SEM, n = 10 within the exposed group and n = 11 within the control group. (A) GW agents exposed mice showed a significantly lower latency to escape than control mice throughout the acquisition period (post-exposure days 43 to 51), *denotes $p < 0.05$ for a main exposure effect (based on MLM with both training days and exposure were fixed main factors). (B) During probe trials, for escape latency, on post-exposure days 51 and 86, exposed mice performed better than control mice but performed worse on day 115 and an interaction between post-exposure days and exposure itself was significant, $p < 0.05$ (based on MLM with exposure and post-exposure days as fixed main factors). (C) For the duration of time spent in the North East (NE) quadrant of the MWM, exposed mice performed similar to control mice on days 51 and 86. However, numerical value for control mice was larger than exposed mice on day 115, $p > 0.05$ (based on MLM regression as described above for B). *Note, a black and white version of these figures are published (Abdullah et al 2011).*

control mice during the 11-15 minute interval ($F_{(1, 52)} = 3.31$, $p = 0.07$, Figure 2.8D). There was no confounding effect of time ($F_{(1, 35)} = 0.19$, $p > 0.05$) nor an interaction ($F_{(2, 35)} = 0.92$, $p > 0.05$) between time and exposure on this outcome measure.

On the rotarod test, there were no differences between the two groups on sensorimotor function during the exposure period (Figure 2.9A) and, although exposed mice had a shorter numerical value for latency to fall than control mice on post-exposure days 3 and 5, there were no statistically significant differences between the two groups ($F_{(1, 118)} = 0.21$, $p > 0.05$, Figure 2.9B).

For the MWM acquisition trials conducted on post-exposure days 43-51, a significant difference between control and exposed mice was observed for the latency to reach the escape platform ($F_{(1, 141)} = 7.97$, $p = 0.005$, Figure 2.10A). Figure 2.10B-C illustrates that for the probe trials, exposed mice had shorter escape latency than control mice on post-exposure days 51 and 86 but control mice performed better than exposed on post-exposure day 115. For these probe trials, a significant interaction between GW agent exposure and post-exposure days (on which the probe trials were conducted) was observed ($F_{(2, 37)} = 5.58$, $p = 0.008$, Figure 2.9B). There was no independent effect of exposure ($F_{(1, 55)} = 3.00$, $p = 0.09$) or post-exposure days ($F_{(2, 37)} = 2.2$, $p = 0.12$) for this outcome measure. Gulf War agent exposed mice spent a similar time searching the target quadrant as control mice on post-exposure days 51 and 86 but spent less time searching the target quadrant on post-exposure day 115. There was no effect of exposure ($F_{(1, 53)} = 0.19$, $p > 0.05$) nor of post-exposure days ($F_{(2, 43)} = 1.66$, $p > 0.05$) and no interaction between exposure and post-exposure days ($F_{(2, 43)} = 3.84$, $p = 0.07$, Figure 2.10C) was observed. There were no significant differences between the two groups on swim speed, as demonstrated by a lack of main exposure effect on the swim velocity ($F_{(1, 57)} = 1.74$, $p > 0.05$) and a lack of interaction between post-exposure day and GW agent exposure ($F_{(1, 38)} = 0.90$, $p > 0.05$).

GFAP staining 8-days post exposure

Figure 2.11A

Control **PB+PER**

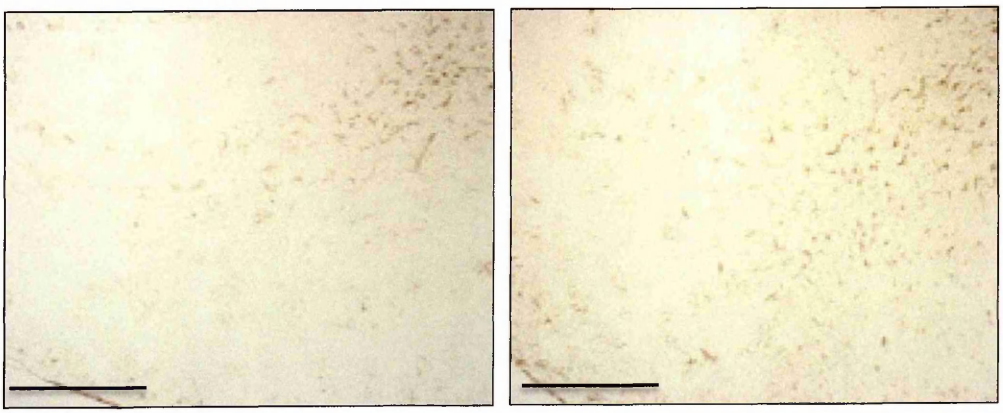

Figure 2.11B

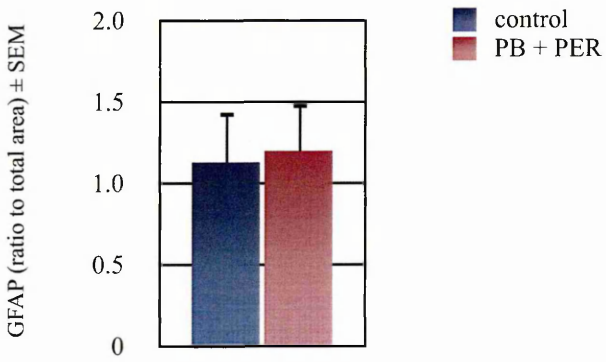

GFAP staining 150 days post-exposure

Figure 2.11C

Control **PB+PER**

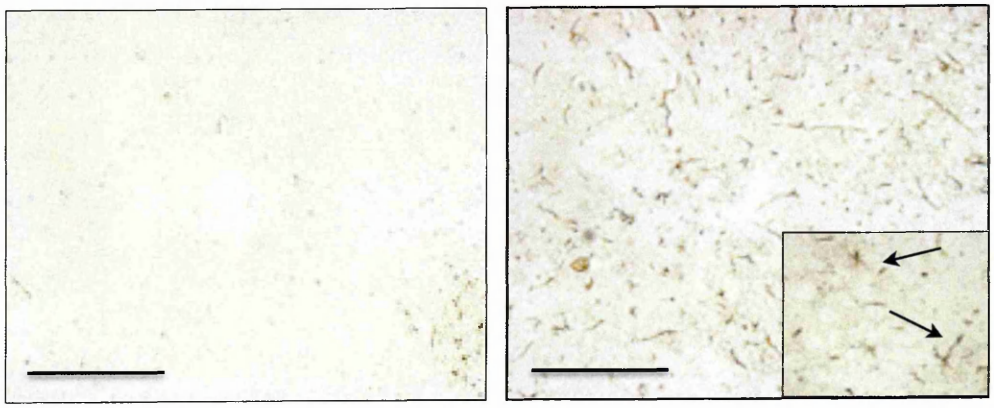

Figure 2.11D

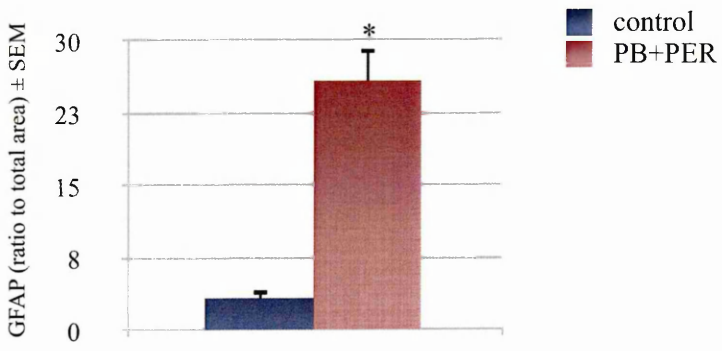

Figure 2.11 GFAP staining: Mean ± SEM, n = 5 within each of the exposed group and the control group. Representative images of the cerebral cortex of a PB+PER exposed mouse and a control mouse, euthanized on post-exposure day 8. Images acquired with a 20x objective providing 200 x magnification. (B) Quantification shows no differences between the two groups.(C) Representative images of PB+PER exposed and control mice at 150 days post-exposure (n = 5 per group). The insert is an image of GW agent exposed mice taken with a 60x objective showing 600 x magnification. Arrows point to reactive astrocytes in the cortex of GW agent exposed mice. The scale bar represents 50μm. (D) Quantification shows a 350% increase in GFAP reactive astrocytes (at 150 days) in the cerebral cortex of GW agents exposed mice relative to control mice, $p < 0.05$ based on the Student's t-test (Abdullah et al 2011).

Nissl staining 8 days post-exposure

Figure 2.12A

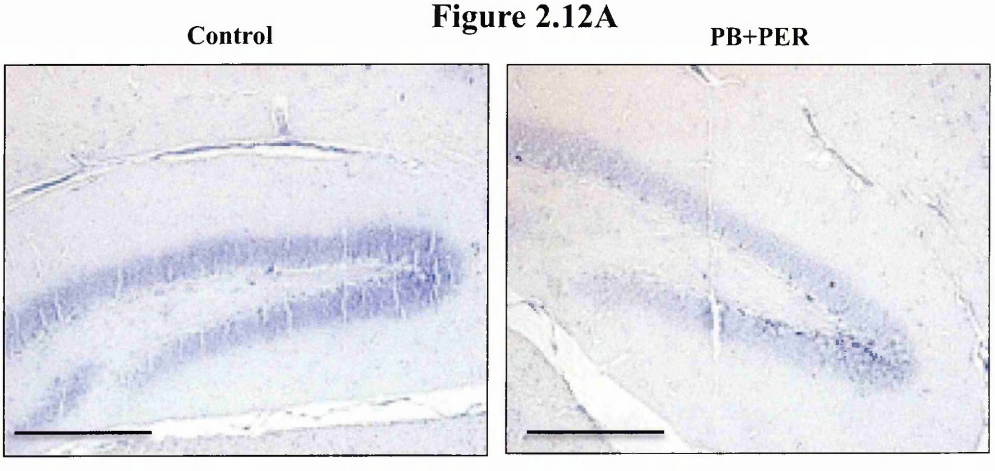

Nissl staining 150 days post-exposure

Figure 2.12B

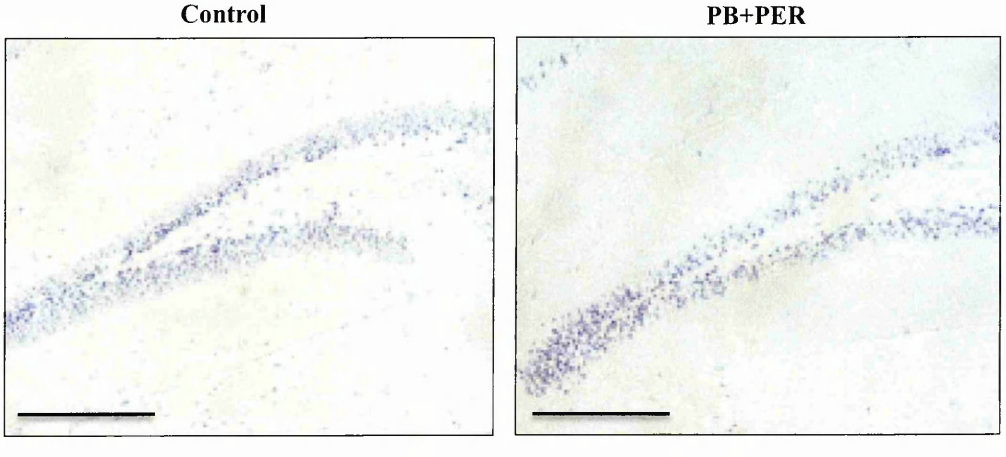

Figure 2.12. Nissl staining: Mean ± SEM, n = 5 within each of the exposed group and the control group. Representative images of the dentate gyrus of a PB+PER exposed mouse. (A) Exposed and control mice euthanized on post-exposure day 8 and (B) at post-exposure 150 days (n = 5 per group) showing no differences between the two groups. The scale bar represents 50μm.

Iba1 staining 8 days post-exposure

Figure 2.13

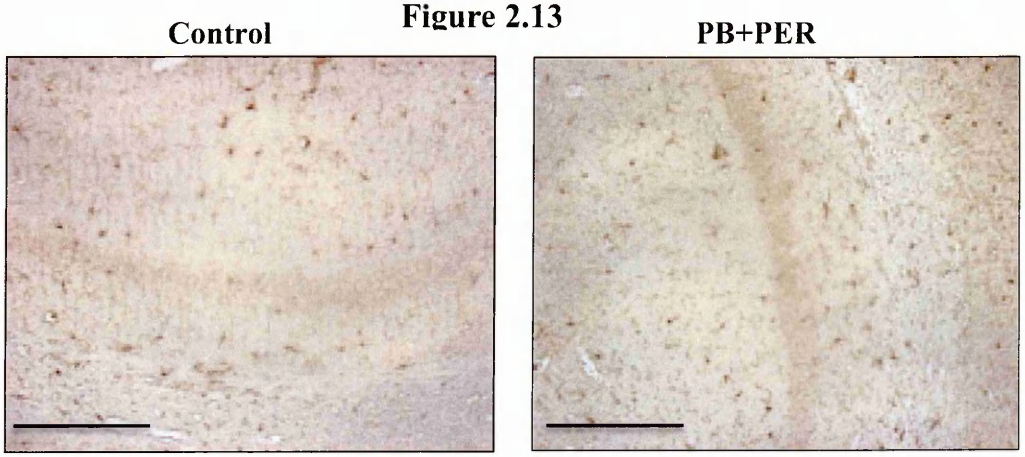

Figure 2.13. Iba1 staining: Mean ± SEM, n = 5 within each of the exposed and the control group. An image acquired with a 20x objective from Iba1 stained CA1 hippocampal regions on post-exposure day 8. Microglia staining was detected but there were no differences between the two groups. The scale bar represents 50μm.

CD45 staining 150 days post-exposure

Figure 2.14

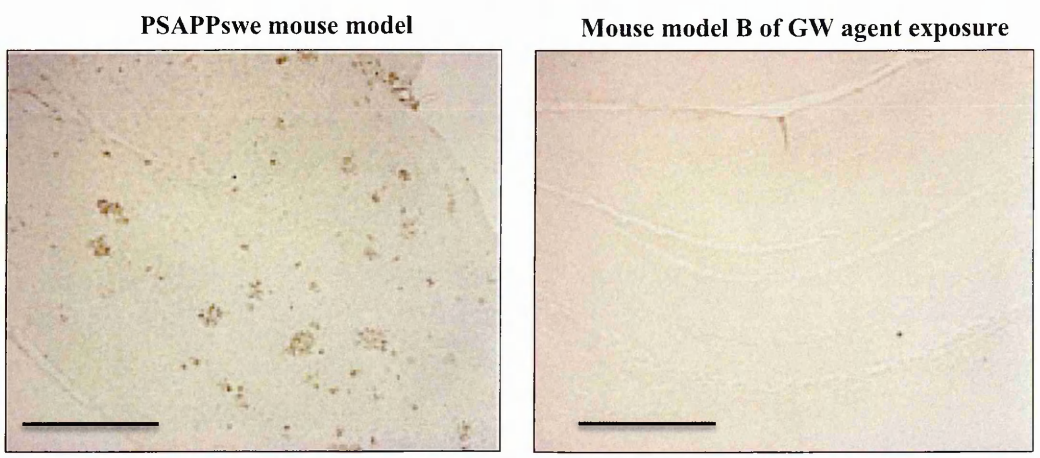

Figure 2.14 CD45 staining: A representative image (taken with a 10× objective providing a 100× magnification), which depicts the presence of extensive microgliosis (quantified using CD45) in the hippocampal region of the AD mouse model (left image) but a complete lack of it in the mice exposed to PB+PER in the GWI mouse model (right image). The scale bar represents 50μm.

2.2.3.2. Histopathological studies

At an early timepoint (post-exposure day 8), within both the cortex and the hippocampus, there were no differences between the groups in astrogliosis ($t = -0.15$, $df = 7$, $p > 0.05$, Figure 2.11A-B). Interestingly, at the later timepoint of 150 days post-exposure, a significant increase in astrogliosis was observed in the cortex of exposed mice

compared to control mice (t-test = -6.10, df = 8, p = 0.04, Figure 2.11C-D), but there were no differences in the hippocampus between the two groups. There was no evidence of neuronal loss in response to GW agent exposure in either the cortex or the hippocampus at either early or late timepoints (Figures 2.12A and 2.12B). As we were unable to visualize any microglia with CD45 staining in model A, Iba1 staining was used to detect total microglia. Figure 2.13 shows presence of microglia but there was no evidence of reactive microglia (as quantified using Iba1 staining) at the early timepoint, as microglia appeared to be ramified in both the exposed and unexposed animals. CD45 staining was used to visualize reactive microglia on post-exposure day 150 but there was no evidence of microgliosis at this later timepoint, evident by a lack of CD45 staining compared to an image from the brain of an AD mouse (positive control) that shows significant microgliosis (Figure 2.14)

2.2.4. Discussion

To date, a study by Lamproglou et al. 2009 is the only one showing memory impairment, but the exposure paradigm in this study included stress, which is an inherent feature of most military combat, including the Persian GW (Lamproglou et al 2009). As a goal of studies described in this thesis was to focus on memory impairment associated with exposures that were directly relevant to the 1990-1991 GW conflict, combined exposure to PB and PER was used since this particular combination is shown to cause neuropathological changes that could potentially give rise to cognitive impairment (Abdel-Rahman et al 2004).

This is the first report showing delayed cognitive impairment after combined exposure to PB and PER in mice. GW agent exposed mice consistently performed better than unexposed mice over the 9 days of the MWM acquisition trials. The data from escape latency during the probe trials conducted on post-exposure days 51 and 86 show that

exposed mice performed better than control mice, but on post-exposure day 115, control mice performed better than exposed mice. These data suggest that earlier on, exposed mice had better spatial memory than control mice for reaching the exact location where the escape platform was previously located, and this was subsequently impaired in exposed mice. Data from time spent in the target quadrant (a less precise measure of spatial memory than escape latency) suggest that there were no differences between the two groups in the earlier two probe trials, but the probe trial on post-exposure day 115 suggests that exposed mice spent less time in the target quadrant than control mice. Hence, data from 115 days post-exposure provide additional support for the escape latency data. As mice were retrieved from the previous location of the hidden target platform, data from 115 post-exposure day suggest that additional learning had occurred in control mice but not in exposed mice. This may also suggest that delayed memory problems in exposed mice might be a consequence of impaired learning. However, this outcome is somewhat ambiguous as the difference between the two groups is largely driven by continual learning in controls and a lack thereof in exposed mice. As such, additional work, which may include examination of cognitive outcome after PB and PER exposure in a different strain of mice, is required to validate cognitive impairment in mice exposed to PB and PER.

Although the biochemical mechanism of this delayed cognitive impairment in response to PB and PER exposure is unknown, the mechanism may be similar to that proposed for exposure to other AChE inhibitors (Terry et al 2011). It is suggested that there might be a compensatory increase in AChE after prolonged exposure to AChE inhibitors, as observed in studies showing that after 30 days of AChE inhibitor exposure, there is an increase in AChE mRNA levels in the cortex (Bansal et al 2009). An electrophysiology study of insect larvae showed that combined exposure to PER and Propoxur (another carbamate AChE inhibitor), at a maximum tolerable concentration,

resulted in a synergistic increase in membrane depolarization, which was evidenced by a reduction in the amplitude of the excitatory post-synaptic potential (EPSP) and is indicative of an increase in synaptic ACh (Corbel et al 2006). Studies also suggest that excessive synaptic ACh can self-regulate by binding to presynaptic muscarinic receptors (mAChR) subtypes 2 and 4, which activate negative feedback that inhibits further ACh release (Zhang et al 2002). Hence, these studies suggest that some of the effects of GW agents on memory may be impacted by ACh availability, but further investigation is required.

In response to PB exposure in rats, a dose-dependent increase in anxiety at 30 minutes post-exposure has been reported (Hoy et al 1999). Habituation was reported in rats 24 hours after exposure to PB and PER (Hoy et al 2000). Habituation was observed on post-exposure day 15 in exposed mice. However, on post-exposure day 30, a weak association was observed between anxiety parameter and GW agent exposure where exposed mice spent more time at the perimeter than control mice, during the last 11-15 minute timepoint. Increased mood and anxiety dysfunction were observed in deployed GW veterans compared to non-deployed veterans, which has persisted decades after the GW conflict (Toomey et al 2009; Gray et al 1999). Thus, the animal studies discussed above provide some support for an association of anxiety disorder with GWI, and warrants further investigation.

A decrease in motor function (distance traveled) in the OFT was observed on post-exposure day 30 in the exposed mice compared to controls, but there was no evidence of motor coordination problems in the rotarod test. Sensorimotor deficits using beam-walk (balance) and grip strength tests have been observed in response to combined PB and PER exposure (Abou-Donia et al 2004). Examination of motor function in clinical studies suggested that veterans with GWI do not show any overt muscle damage or peripheral nerve pathology. However, studies did show a dose-response for psychomotor impairment

where veterans with the highest exposure to both pesticides and PB had worse performance in psychomotor tasks than those with low-level exposure (Binns et al 2008). These data support a psychomotor-related dysfunction rather than fine motor coordination problems, observations that are similar to that reported for another organophosphate (OP) AChE inhibitor pesticide, diisopropyl-fluorophosphate (Terry et al 2011). It is also possible that GW-agent induced neurobehavioral changes may be a consequence of circadian abnormalities, often reported by veterans with GWI (Haley et al 2004), and thus are likely to be a consequence of GW agent exposure. The observed delayed presentation of neurobehavioral symptoms in GW agent exposed mice is consistent with the observation of delayed manifestation of GWI in veterans, where 60% of GWI symptoms developed once veterans returned from the war and 40% of the symptoms emerged years later (Kroenke et al 1998). These neurobehavioral studies show delayed emergence of anxiety and cognitive impairment in mice exposed to PB and PER compared to control mice.

A significant increase in astrogliosis was detected in exposed mice compared to controls after a timepoint at which cognitive impairment was evident. This observed increase in astrogliosis is consistent with the observed modulation of immune/ inflammatory response and with a report showing increased astrocyte reactivity in response to PER exposure alone and PB and PER with DEET in rodent brain (Abdel-Rahman et al 2004). At this acute timepoint, there was no difference between the two groups with respect to GFAP immunohistochemistry. As CD45 staining was undetectable in model A, Iba1 stain was used since it can detect both the reactive and ramified microglia through morphological analyses. There were no differences in Iba1 staining between the exposed and control animals, in both the hippocampi and the cortices. The morphology of Iba1 stained microglia (ramified) appeared similar in both exposed and control mice. Since CD45 staining is considered to be more specific to reactive microglia, this stain was chosen for the post-exposure day 150 timepoint. A positive control was also used (brain

section from an 18-month old PSAPPswe mouse model of AD) which showed a presence of extensive microgliosis. As in mouse model A, there were no reactive microglia present in either the control or the exposed mice. Thus it can be presumed that after exposure to GW agents, there is no microgliosis. Similarly, there were no differences between exposed and control mice on measures of neuronal loss, assessed using Nissl staining.

Observations of astrogliosis at only the chronic timepoint suggests an association between GW-agent induced astrogliosis and behavioral changes, since these changes succeeded the emergence of the cognitive impairment phenotype. However, the presence of such pronounced astrogliosis in response to GW agent exposure merits further examination to determine a possible causal relationship between astrogliosis and behavioral outcomes after GW-agent exposure. Collectively, these studies demonstrate that exposure to GW agents used in mouse model B may produce neurobehavioral features that are similar to those suffered by veterans with GWI.

2.3. Validation of cognitive studies for mouse model B of GW agent exposure

2.3.1. Introduction

It is anticipated that the future work at the Roskamp Institute will involve the C57BL6 strain, which is the most commonly used strain in laboratory research, particularly for research requiring genetic manipulations. Additional work for a DoD CDMRP award (PI: Ait-Ghezala) will require examination of cognitive dysfunction in response to GW agent exposure and to determine if cognitive dysfunction could be ameliorated by targeting inflammatory/immune pathways. Thus a main focus of GWI work at the Roskamp Institute will be to evaluate the cognitive component associated with GW agent exposure in genetically manipulated mice (i.e., CD40L deficient mice on C57BL6 background). Therefore, studies were performed to validate cognitive outcomes in C57BL6 mice.

2.3.2. Material and Methods

2.3.2.1. Animals

For validation studies of cognitive neurobehavioral findings, the C57BL6 in-bred strain was used. Initial pilot studies were performed to ensure that doses of PB and PER administered to CD1 mice were suitable for this C57BL6 strain. However, a 2 mg/kg dose of PB was found to be lethal, which can be explained by the fact that C57BL6 is genetically predisposed to cholinergic deficiencies (Schwab 1990; Bentivoglio 1994). Subsequent pilot studies were performed to reduce PB dose through a serial dose reduction process. A dose of 0.7 mg/kg of PB was found to be tolerable in these mice and this dose was used to ensure survival in this strain over the experimental time-period. The dose of PER was kept constant at 200mg/kg. This combination was administered to mice daily for 10 days, as described previously in section 2.2.above for the development of mouse model B. Animal work was performed in accordance with the animal welfare guidelines described above.

2.3.2.2. Barnes Maze

During the experiments conducted using the C57BL6 strain in mouse model A, it was observed that these mice performed poorly in the MWM. Patil and colleagues performed a comparison of CD1 mice and C57BL6 mice using the Barnes Maze (BM) and MWM (Patil et al 2009). These studies demonstrated that while CD1 mice performed better in the MWM than C57BL6 mice, C57BL6 mice performed much better than CD1 mice in the BM. Therefore this test was chosen for cognitive validation studies in C57BL6 mice. The BM protocol was based on work described elsewhere (Berta et al 2007). Briefly, each mouse was adapted to the maze and the escape hole on the first day of the acquisition trial, during which each mouse was separately placed in the middle of the maze and then guided to the escape hole where it remained for 2 min. Following that,

acquisition trials were conducted over 4 days (days 10-13) for 180 seconds per trial and 4 trials were administered per mouse with an inter-trial interval of 15 min. Each mouse was placed in the middle of the maze and the trial ended when the mouse entered the escape hole or after 180 seconds had elapsed. A rotating fan was on during the trials but was turned off when a mouse entered the target hole and escape into the escape box, where it was allowed to stay for 1 min. If the mouse did not reach the escape hole within 3 minutes, the experimenter guided the mouse gently to the escape hole and left the mouse inside for 1 min. A probe trial was conducted on post-exposure day 14, 24 h after the last training day. The escape hole was removed for the probe trials. Each mouse was placed in the middle of the maze and allowed to explore the maze for a fixed interval of 90 seconds. The number of pokes in each hole and the latency and distance travelled to reach the virtual target hole were measured as outcome factors. To assess long-term retention, additional probe trials were administered approximately 30 days on post-exposure days 47 and 77.

2.3.2.3. Statistical analyses:

For Barnes Maze, statistical analyses were conducted using a generalized linear model (GzLM) to accommodate non-normally distributed dependent variables. All analyses were performed with SPSS 13.0 (IBM corp. Armonk, NY) and the statistical significance was set at the alpha 0.05 level.

2.3.4. Results

For these validation studies, acquisition trials were conducted daily on post-exposure days 10-13 to train mice to locate and enter the escape hole. Figure 2.15A shows that exposed mice learned this task better than control mice, as evidenced by a shorter duration of time spent in the arena over the 4 day training period (Wald = 12.08, $p < 0.01$). For probe trials, on post-exposure day 14, exposed mice more frequently visited the escape

hole location than control mice. On post-exposure day 47, there were no differences between the two groups. However, on post-exposure day 77, exposed mice less frequently visited the escape hole than control mice and these differences were statistically significant (Wald = 5.93, p = 0.05, Figure 2.15B). Examination of primary errors (represented by a comparison of percentage frequency of nose-poke in escape hole vs. other holes - not including two holes adjacent to the target hole) provided supporting data that on post-exposure day 77, exposed mice had less accuracy than control mice in identifying the escape hole (Wald = 3.03, p = 0.08, Figure 2.15C).

Barnes Maze

Figure 2.15A

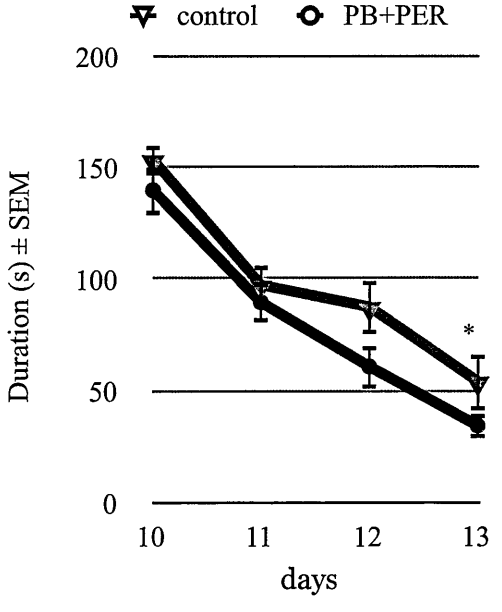

Figure 2.15B

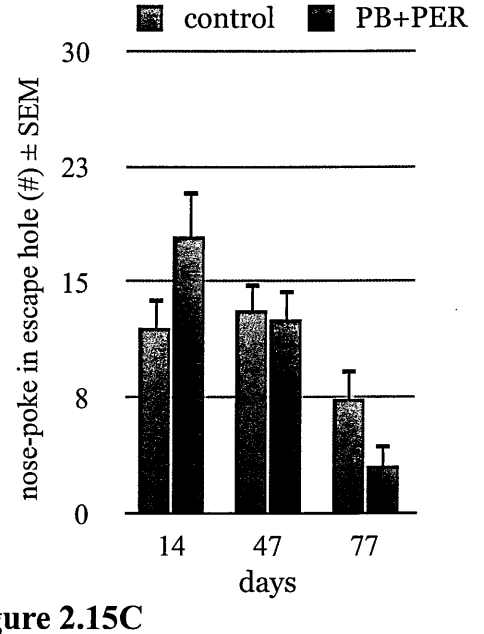

Figure 2.15C

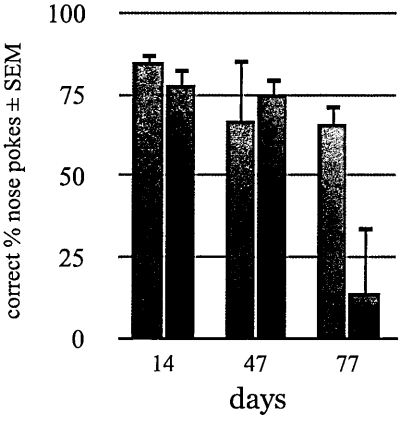

Figure 2.15. Barnes Maze: Mean ± SEM, n = 10 within each of the exposed group and the control group. (A) For the acquisition trials, duration of time in arena was lower for PB +PER exposed mice than controls and a significant interaction between training days and exposure was observed, *denotes $p < 0.01$ for a main exposure effect (based on GzLM where training days and exposure were incorporated as fixed main factors). (B) Data on the frequency of nose-pokes in the escape hole during the probe trials showed a significant interaction between exposure and post-exposure days on this outcome, where exposed mice performed better than control mice on day 14, but this pattern reversed on day 77, $p < 0.05$ (based on GzLM with days and exposure were incorporated as fixed main factors). (C) Examination of primary error % (as measured by % frequency of correct nose-poke vs. those in other holes outside of target zone) showed that the error rate was numerically increased in PB+PER exposed mice compared to control mice on post-exposure day 77, $p > 0.05$.

2.3.4. Discussion

As described above, C57BL6 mice have cholinergic deficiencies; thus a much lower dose of PB was utilized in this strain. In addition, studies also show that these mice experience an elevated level of stress in the MWM and perform better in the BM (Patil et al 2009) and therefore the BM was utilized for cognitive validation studies of mouse model B of GW agent exposure. These data show that during the acquisition trials, all mice learned how to escape into the target box, where exposed mice learned the task more quickly than control mice during post-exposures days 10-13. During probe trials, the same pattern was evident on post-exposure day 14 as nose pokes in the target hole were higher in exposed vs. control mice. There were no differences between the two groups on post-exposure day 47. On the contrary, by post-exposure day 77, a reverse pattern was seen where exposed mice performed worse than control mice, which is similar to the observations on post-exposure day 115 in CD1 mice experiments. These data clearly demonstrate that the cognitive impairment observed in this BM study is not an artifact of changes in control mice, as both exposed and control mice had lowered frequency of nose pokes in the escape hole and a concomitant increase in the frequency of incorrect nose-pokes when comparing post-exposure days 14 vs. 77.

2.5. Summary of animal modeling of GW agent exposure

The animal modeling work described in this chapter suggests that different combinations and doses of GW agents may produce different neurobehavioral profiles, albeit with neuropathologically similar outcomes. For instance, GW agents administered to mouse model A included DEET and stress, along with PB and PER. In mouse model B, PB and PER were also utilized, although doses of PB and PER were much higher and administration time was different from that in mouse model A. Neurobehavioral studies in mouse model A suggest a significant motor impairment component along with anxiety. However, cognitive capabilities could not be ascertained due to marked motor problems in exposed mice, further complicated by the fact that the C57BL6 inbred strain is shown to perform poorly in the MWM due to its predisposition to anxiety (Patil et al 2009). Interestingly, earlier work conducted by Haley and colleagues aimed at sub-classification of veterans with GWI showed that Syndrome 3, which was associated with DEET exposure had a significant arthro-myo-neuropathy component consisting of symptoms such as pain, fatigue and numbness of extremities. One can then speculate that perhaps overexposure to DEET in combination with other GW agents may precipitate symptoms resembling those in veterans that were classified under Syndrome 3. On the other hand, while cognitive impairment was observed in mouse model B along with anxiety, there was no motor impairment, except perhaps psychomotor problems. This particular neurobehavioral profile may be similar to Syndrome 1 which also has a prominent cognitive component. Despite these clear differences in neurobehavioral presentations of the two mouse models of GW agent exposure, neuropathological findings were virtually identical where profound astrogliosis was noted in the cortex but not in the hippocampus. Similarly, in both mouse models of GW agent exposure, there was no neuronal loss or microgliosis in either the hippocampus or the cortex. Hence, GWI mouse modeling work

based on the combinations of GW agents utilized in these studies may be extremely valuable in capturing different phenotypes of GWI symptomatology. It is anticipated that these mouse models of GW-agent exposure will be useful in molecular biology studies aimed at characterizing the underlying dysfunctional biomolecular pathways.

The next chapter describes molecular biology and proteomic studies performed on brain tissue and blood from these mouse models for identification of possible biological mechanisms associated with GW agent exposure.

3.0. Chapter 3 Exploratory studies of brain and blood samples from mouse models of GW agent exposure

This Chapter presents exploratory work conducted on two mouse models of GW agent exposure characterized in Chapter 2 above. The western blot studies performed on the brain tissue from mouse model A of GW agent exposure (PB, PER, DEET and stress) to explore biological links with neurodegeneration, which was suggested to be an outcome from neuropathological studies conducted by Abdel-Rahman and colleagues (Abdel-Rahman et al 2004). Mouse model B of GW agent exposure used a combination of high doses of PB and PER. Unlike for mouse model A, there was no information available from the literature about potential biological mechanisms that might be affected in response this particular GW agent exposure. Consistent with the literature, genomic work performed at the Roskamp Institute using an *in vitro* model of GW agent exposure suggested that several different biological pathways are affected in response to a combined PB and PER exposure. Therefore, for mouse model B, proteomic studies were performed on the brain and blood samples in order to obtain information on several biological pathways in a single experiment.

3.1. Exploratory biochemical studies of mouse model A of GW agent exposure

3.1.1. Introduction

As described in Chapter 1, the presence of memory impairment and reduced hippocampal volume observed in veterans with GWI suggests that hippocampal dysfunction may be associated with this illness (Menon et al 2004; Vythilingam et al 2005). Memory problems, along with hippocampal volume loss, are generally characteristic of Alzheimer's disease (AD), a neurodegenerative disorder. Abdel-Rahman and colleagues observed degenerating neurons in several brain regions, including the hippocampi, of rats

exposed to PB, PER, DEET and stress (Abdel-Rahman et al 2004). It was therefore hypothesized that biological pathways affected in response to GW agent exposure might overlap with those for AD. Support for this comes from studies showing modulation of mAChR activity after GW agent exposure. Downstream signaling pathways that are linked with mAChR activation include metabolism of the Amyloid Precursor Protein (APP), a key protein implicated in AD pathogenesis.

There is considerable support for modulation of mAChR activity after exposure to GW agents (Abdel-Rahman et al 2004; Mauck et al 2010). For example, an increase in mAChR subtype 2 (M2 AChR) ligand binding within the cortex was observed in rats exposed to PB, PER, and DEET (Abou-Donia et al 2001), although no findings have been reported for PB, PER and DEET in combination with stress for this particular brain region. It was also noted that the activity of M2 AChR was decreased after exposure to PB, PER, DEET and stress in the forebrain, midbrain and cerebellum (Abdel-Rahman et al 2004). Mauck and colleagues demonstrated that densities of M3 AChRs were decreased in the cortex after exposure to PB in rats (Mauck et al 2010). These studies suggest brain-region specific modulation of the cholinergic system in response to GW agents, particularly for the combination that was administered in mouse model A.

Muscarinic AChRs are widely known for their role in maintaining and regulating synaptic ACh levels and differential activation of these receptors can also modulate cascades of intracellular biological events that are implicated in AD pathogenesis (Isacson et al 2002). The Amyloid Precursor Protein is a type I transmembrane protein, which is processed via α-secretase (precluding the formation of the β-amyloid peptide and thus termed non-amyloidogenic processing) or by β- and γ-secretases (amyloidogenic). The latter pathway generates pathologic Aβ fragments and is considered to play a key role in AD pathobiology (Tandon et al 2000). Activation of M2 AChR is shown to lower expression of the β-secretase APP converting enzyme (BACE) via adenylyl cyclase-

coupled pathways (Züchner et al 2004). Activation of the M1 AChR has consistently been shown to result in increased sAPPα release via protein kinase C (PKC) dependent pathways (Jones et al 2008; Slack et al 1995). Recent studies have shown that M1 AChR activation can reduce BACE expression and consequently Aβ levels (Fisher 2012). In two different transgenic mouse models of AD, M1 AChR deletion resulted in an increase of amyloid plaque burden and tangle formation (Medeiros et al 2011). However, stimulation of the M1 or M3 subtype with its agonists has also been shown to increase BACE expression by two-fold, also through PKC (Isacson et al 2002; Züchner et al 2004). Although these are conflicting reports with respect to mAChR and BACE activation, they nevertheless suggest modulation of APP processing upon activation of mAChR signaling pathways.

Since evaluation of the present literature suggested that mAChR signaling pathways are modulated in response to the GW agent exposure utilized in mouse model A and may impact APP processing in neurodegenerative conditions, it can then be postulated that GW agent exposure might also affect APP levels. Therefore, studies were performed to evaluate APP levels for mouse model A. In addition, western blot studies were also performed to validate the histopathological findings of increased astrogliosis observed in mouse model A of GW agent exposure.

3.1.2. Materials and methods

Mice examined in model A were euthanized on post-exposure day 42 (after 28 days of PB, PER, DEET and stress exposure) via cardiac puncture followed by perfusion as described in Chapter 2 above. Extracted brains were homogenized in 1.5 ml of Mammalian Protein Extraction Buffer (MPER, Pierce) using a dounce homogenizer, followed by centrifugation at 21,000 x g for 15 minutes. Next, 150 μg of brain homogenate was combined with about 6μl of laemmli buffer (containing beta-mercaptoethanol) and this

sample was loaded onto a Tris-HCL gel for electrophoresis. Proteins were transferred to a polyvinylidene fluoride (PVDF) membrane using a Biorad transblot apparatus overnight at 90 mA. The membrane was blocked for 1 hour in 5% blocking milk (Biorad), then incubated with mouse primary antibody for full length APP, clone 22c11 (Millipore) at 1:1000 dilution for 2hrs followed by incubation with anti-mouse secondary antibody for 1hr and then visualized using West-Femto substrate (Pierce). A band of 110 kd was detected, no other bands were detectable. Membrane was then stripped with Restore stripping buffer (Pierce) and re-probed with mouse primary GFAP antibody (Dako) at 1:1000. The same procedure was followed for actin (Pierce) using conditions described above. Subsequently, PVDF membrane was stained with Coomassie blue stain to visualize transferred proteins and to ensure that the transfer in each well was consistent. All statistical analyses were performed using the Student's t-test and $p < 0.05$ was considered statistically significant.

3.1.3. Results

There was a 1.25 fold increase in full length APP levels in exposed mice compared to controls but this difference did not reach statistical significance ($t = -0.91$, $df = 8$, $p > 0.05$). Western blot analysis using the GFAP antibody validated the neuropathological findings of increased astrogliosis. Figure 3.1A shows the images for APP, GFAP and actin western blots. Total proteins are visualized on the blot using Coomassie stained PVDF, (Figure 3.1B). Quantification is presented in Figure 3.1C and supports a limited increase in expression of APP and considerable increase of GFAP. Consistent with neuropathology findings, a statistically significant increase of 1.5 fold was observed for GFAP levels in exposed mice compared to control mice ($t = -2.50$, $df = 8$, $p = 0.04$).

APP and GFAP western blot analyses

Figure 3.1A

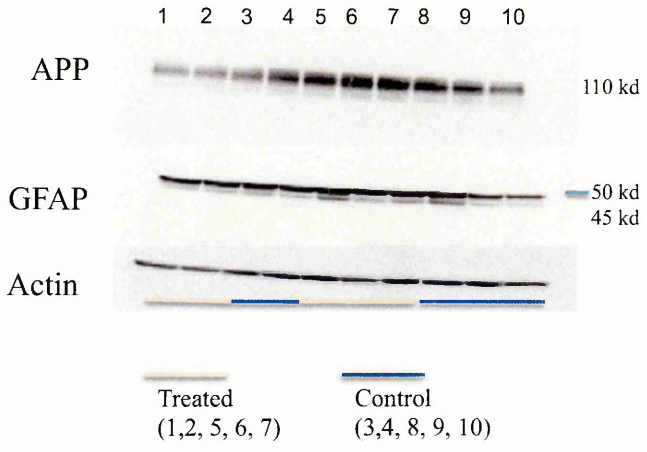

Figure 3.1B

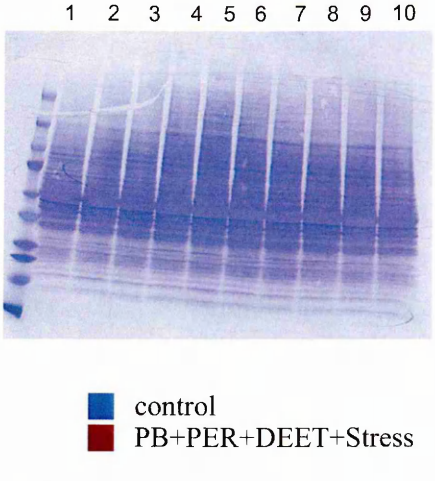

Figure 3.1C

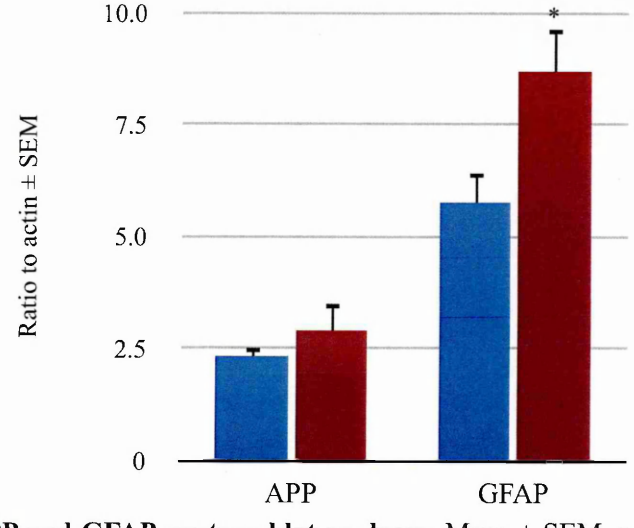

Figure 3.1. APP and GFAP western blot analyses: Mean ± SEM, n = 5 within each of the exposed group and the control group. (A) Western blot images of APP (110kd), GFAP (50kd) and actin (42kd). (B) Membrane was stained with Coomassie blue which shows similar gel loading per well. (C) APP and GFAP densitometry values were normalized against actin for quantification. A 1.25 fold increase in APP expression was noted in exposed mice compared to control mice using western blot analyses but these differences did not reach statistical significance, $p > 0.05$. For GFAP, about 1.5 fold increase was noted and this difference was significant, *denotes $p < 0.05$ based on the Student's t-test.

3.1.4. Discussion

The work conducted by Abdel-Rahman and colleagues suggested neuronal degeneration (characterized by dying neurons detected using H&E staining) in response to the GW agent exposure paradigm that was used in mouse model A. However, as described in Chapter 2 above, this work remains controversial since the method of detecting degenerative neurons by Abdel-Rahman and colleagues was considered to be an artifact of

sample handling (Jortner 2006) and has not yet been validated using another neuropathology technique.

The amyloid precursor protein

The limited exploratory biochemical studies of APP conducted here, along with the histopathological work presented in Chapter 2, do not indicate the presence of a neurodegenerative component in response to GW agent exposure. An examination of full-length APP alone is not fully informative of APP processing and more conclusive evidence would likely come from examination of fragments of APP, such as Aβ40 and Aβ42. However, other experiments conducted at the Roskamp Institute using Enzyme-Linked Immunosorbent Assay (ELISA) for endogenous mouse Aβ40 quantification did not accurately detect Aβ levels in wild type mice as the endogenous levels of this peptide were very close to the lower detection limit of the ELISA. Hence, due to these limitations, additional work aimed at examining fragments of APP (i.e. Aβ) was not pursued further for this thesis. Future examination of tau and phosphotau levels may be useful for determining a possible presence of neurodegenerative response to GW agent exposure. Findings of an increase in GFAP stained astrocytes in exposed mice compared to controls in model A are similar to the findings originally reported by Abdel-Rahman and colleagues.

The Glial Fibrillary Acidic Protein

The neuropathological findings of astrogliosis in model A are confirmed by GFAP western blot studies. As described in Chapter 2 above, astroglia play a prominent role in modulating inflammatory responses in the CNS. Therefore, it appears that exposure to GW agents may have an inflammatory component, which is supported by observations of altered immune and inflammation profiles in veterans with GWI. As such, examination of inflammation related changes might be helpful in understanding the pathobiology of GWI.

3.2. Exploratory biochemical studies of mouse model B of GW agent exposure

3.2.1. Introduction

The molecular biological work on model A described above, combined with the complicated clinical presentation in veterans with GWI, suggests that despite having a cognitive deficit component, veterans with GWI may not have a prominent neurodegenerative pathology at this stage of the illness. Current research on GWI pathology also suggests that several biological processes and functions are likely to be perturbed (Binns et al 2008). For example, clinical studies showed an abnormal suppression of adrenocorticotropic hormone (ACTH) levels in response to metyrapone challenge in symptomatic veterans who were deployed to GW compared to non-deployed asymptomatic GW veterans (Golier et al 2009). This suggests an impairment of the endocrine system in veterans with GWI. Similarly, several studies also suggest an increase in the production of inflammatory cytokine by lymphocytes obtained from veterans with GWI compared to asymptomatic GW veterans (Skowera et al 2004; Broderick et al 2011). Because of the indicated involvement of several biological systems, a comparative approach that can profile a large number of biological pathways in any given experiment may be useful in order to understand the biological dysfunction associated with GWI.

Over the last two decades, technological advances have allowed global examination of components of cellular networks and their interactions using Omics technology, which is coupled with similarly powerful computational tools (bioinformatics) that aid in the calculation and further interpretation of large datasets. Such an approach is now termed systems-biology, which encompasses genomics, proteomics, lipidomics and metabolomics techniques that quantify thousands of genes, proteins, lipids and metabolites, respectively, in a single experiment. These systems-biology approaches can potentially play an

important role in identifying disease mechanisms in complex disorders (Filiou et al 2012; Bayes, & Grant 2009).

Advances in mass spectrometry (MS) have greatly facilitated protein identification and characterization. In the recent past, two dimensional gel electrophoresis (2DGE) was the primary tool used to visualize the proteome of a given biological sample and identify its components. However, this proteomic technique suffered from a limited range, as not all proteins (i.e., membrane proteins and proteins with extreme molecular weights and pH) were detectable using this gel-based system. Over the last decade, use of liquid chromatography with mass spectrometry (LC/MS) technique has gained widespread popularity due to its ability to identify and quantify a wider range of proteins than that visualized with 2DGE methods. As a consequence, numerous LC/MS-based quantitative techniques have emerged allowing accurate quantitation of proteins from a large variety of biological samples. For example, Isotopic Coded Affinity Tags (ICAT) uses chemical labeling strategies which allows addition of isotope-coded affinity tags that react with the cysteine residues on the proteins in a biological sample. Samples are then combined and analyzed using LC with tandem mass spectrometry (LC/MS/MS). However, this approach can be biased against proteins that do not contain this residue.

Another quantitative proteomic approach that enables accurate quantitation of proteins is called Stable Isotope Labeling by Amino Acids in Cell Culture (SILAC), which allows direct *in vitro* metabolic labeling of proteins and peptides with isotope labels (i.e., ^{18}O, ^{13}C, ^{15}N). Recently, SILAC methodology has been modified to accommodate *in vivo* labeling of mammals (SILAM), such as mice and rats. However, these experiments are extremely costly and time consuming as they require metabolic labeling of cells/mammals and may introduce biologic or phenotypic changes due to unexpected and unpredictable biological responses to the isotopes (Ong 2012; Xie et al 2011; Filiou et al 2012; Zieske 2006).

While each technique listed above has provided a unique contribution to the proteomic field, there remained a need for a cost-effective technology that could examine proteins from samples where metabolic labeling is not feasible, label all peptides and allow simultaneous quantitation of proteins in multiple samples. These prerequisites have been addressed by the recently developed Isobaric Tagging for Relative and Absolute Quantification (iTRAQ)-based proteomic approach, which has gained widespread popularity due to its ability to simultaneously identify and quantify proteins from up to 8 samples in a single experimental run (Zieske 2006). This technique allows incorporation of isobaric tags that maintain an overall atomic mass of 144, but upon fragmentation with MS/MS, give peptide peaks with unique reporter ions (i.e., m/z 114, 115). This allows for better quantitation by providing a strong ion signal. Furthermore, these tags react with all primary amines, and as such provide better peptide coverage than ICAT.

Hence, proteomic techniques (including iTRAQ), because of their ability to identify and quantify several thousand proteins in a given experiment, are well suited for examining complex illnesses, such as GWI. Furthermore, when proteomic technology is used in conjunction with a bioinformatics platform, it can provide a comprehensive view of disease-related changes (Bayes, & Grant 2009). Therefore, iTRAQ-based proteomics coupled with bioinformatic tools was applied to generate a proteomic dataset in order to characterize biomolecular pathways that were affected in GW exposed mice compared to control mice from model B. Given the paucity of reliable biomarkers of GWI, iTRAQ experiments were also performed on plasma samples from mouse model B to determine if such an approach can be used to discover objective biomarkers of chronic CNS changes associated GW agent exposure in this mouse model.

3.2.2. Material and methods

3.2.2.1. Brain sample processing

Following exsanguination, animals were perfused with PBS. Whole brains were extracted, immediately frozen in liquid nitrogen and transferred to a -80°C freezer until further use. Four biological replicates were used for each group (n = 4 for each control and exposed) and each sample was individually prepared and processed. Using a dounce homogenizer, brains were homogenized in chilled lysis buffer (Membrane Protein Extraction Reagents, Pierce, Rockford, IL) containing protease (Roche, Indianapolis IN) and phosphatase inhibitor (Pierce) cocktails and centrifuged at 20,000 x g for 15 min at 4°C. The supernatant was collected and quantified using the bicinchoninic acid assay ([BCA], Pierce), and examined by SDS-PAGE. Aliquots equivalent to about 100µg protein for each sample were precipitated in 4 volumes of acetone and pelleted by centrifugation. The pellets were reduced, alkylated and digested according to Masuda and colleagues with trypsin at a 1:200 enzyme to substrate ratio (Masuda et al 2008).

3.2.2.2. Plasma sample processing

Plasma samples from the same mice (on whom the brain samples were analyzed for iTRAQ) were prepared for iTRAQ experiments, as described elsewhere (Crawford et al 2012) and briefly outlined here. Following exsanguination via cardiac puncture using a 18 gauge wide-bore needle to prevent hemolysis of red blood cells (RBC) during blood collection. Blood samples were collected into a 1.5ml Eppendorf tube containing 10U of heparin and a protease inhibitor cocktail (PIC) (Roche) to a final concentration of 1X. Samples were immediately centrifuged at 3,000 x g for 5 minutes and plasma was transferred to a new 1.5mL Eppendorf tube and snap frozen in liquid nitrogen. Plasma samples were subjected to a delipidation procedure using a non-denaturing biphasic solvent system according to previously published methods (Wong, & Ladisch 1983).

Briefly, plasma was mixed with an equal volume of diisopropyl ether-butanol (3:2, v/v) and vortexed for 10 minutes at 4°C, followed by centrifugation at 15,000 x g for 5 minutes at 4°C to accomplish phase separation The lower phase was then transferred to a new tube and further diluted (5x) in chilled 1X PBS (supplemented with protease inhibitor cocktails). Albumin was depleted using a solvent-based system (Fu et al 2005) where chilled ethanol was added to a final concentration of 42%. The samples were incubated for 60 minutes at 4°C on an end-over shaker. The samples were again subjected to centrifugation at 15,000 x g for 5 minutes at 4°C. The albumin-depleted protein precipitate was quantified using the BCA assay and verified by SDS-PAGE. The pellet was reduced/ alkylated in 8M urea, then diluted 8-fold with 20mM HEPES, pH 8.0 to 20µl. Aliquots equivalent to about 100µg protein for each sample were subjected to tryptic digestion for iTRAQ studies described below.

3.2.2.3. Isobaric Tagging for Relative and Absolute Quantitation (iTRAQ) labeling

Following the sample processing and protein standardization steps above, as per manufacturer's instructions, tryptic peptides in each sample were individually labeled with iTRAQ reagents (4-plex labeling system from Applied Biosystems) at room temperature for 4 hours. Samples were pooled at this stage of the iTRAQ experiments (50µg of each) to allow simultaneous quantification. Each 4-plex group contained two control samples (114 and 116 mass tags) and two exposed samples (115 and 117 mass tags), for a total of 8 samples divided into two 4-plex groups. For brain samples, an additional step was included following labeling and pooling to remove sodium deoxycholate was depleted as described elsewhere (Masuda et al 2008).

3.2.2.4. LC/MS/MS experiments

The peptide containing aqueous phase was transferred to a new tube, dried using vacuum centrifugation and re-suspended in 20mM ammonium formate, pH10. Samples were fractionated using offline high-pH reversed phase chromatography using C18 spin

columns (Pierce) and eluted stepwise in an increasing concentration of acetonitrile (ACN) in 20mM ammonium formate, pH10. This generated five fractions (flow-through, 10, 20, 30, and 40%ACN fractions), which were dried in a vacuum centrifuge and then re-suspended in mobile phase A (99.9% water, 0.1% FA) for LC-MS/MS analysis.

Samples were applied to a 100mm by 0.1mm C18 (3μm, 300Å) column and infused into an LTQ-Orbitrap (Thermo Scientific) via an ADVANCE ion source (Michrom) over a 2.5 hr linear gradient of increasing amounts of mobile phase B (0.1% formic acid, 99.9% acetonitrile) from 2-45% at a 300 nl/min flow rate using an Eksigent nano-2DLC system. Xcalibur 2.4 software (Thermo Scientific) was used to control MS instrument settings. Mass spectrometry data was collected in automated fashion in data-dependent acquisition (DDA) mode. Full scan MS spectra were acquired in Fourier transform mode, at resolution = 60,000 FWHM, between 300 and 1,200 m/z. Peptides were fragmented using pulsed-Q dissociation (PQD) in ion trap (IT) mode, at a relative collision energy (CE) setting of 31. Q (rf) settings and activation times were 0.55 and 0.4ms, respectively, with the number of ions for an MS/MS spectrum set at 40,000 and the maximum injection time at 200ms, with 2 microscans in MS/MS mode and repeat counts of 2. These settings were adapted from work by the Kuster group (Bantscheff et al 2008).

3.2.2.5. Proteomic data analysis

LC-MS/MS data files (*.raw) were transferred to Bioworks 3.3.1 (Thermo Scientific) to identify peptides using the SEQUEST search algorithm. The spectra were searched against the IPI.MOUSE.v3.59 database using the following search criteria: maximum allowed missed cleavages for trypsin, 2; fixed modifications of +57.02146 for iodoacetamide-modified cysteine residues; variable modifications of +144Da for iTRAQ-labeled peptide N-termini and lysine side chains; and fixed modifications of +15.99491 for oxidized methionine. The resulting Bioworks. SRF files were converted to .OUT and .DTA files to import the results into the Trans Proteomic Pipeline (TPP) v 4.2 software

where peptides (and their corresponding proteins) were quantified using the Libra feature of the TPP software and reference ions were set as 114.1, 115.1, 116.1, and 117.1. The PeptideProphet feature of the TPP software was used to calculate a probability value for each peptide and these probabilities were used to set a false discovery rate (FDR) of 0.05. Peptides with a probability value equal to or lower than this cutoff value were exported to Excel. The Excel files were imported to JMP (SAS) 8.0.2 for data cleaning and statistical analysis as described below.

For data cleaning, reporter ion counts below 20 were assigned a value of zero; peptides that did not yield any ion count for any of the iTRAQ labels were deleted. Proteins identified with 2 or more peptides were used for the quantitative analysis and those identified by a single peptide were only included in the analysis if the same peptide was identified in multiple biological replications. All reporter ion peak intensities were ln transformed to make intensity data additive, and the loading bias was removed by mean normalization on each replication and label. MS data were analyzed by Analysis of Variance (ANOVA) using models adapted from Hill and colleagues (Hill et al 2008) that were crafted specifically for iTRAQ experiments. Briefly, a linear mixed model was used where mouse was treated as a random variable, whereas exposure was treated as a fixed variable. ANOVA of the quantitative dataset identified proteins for which the variable "exposure" was significant. All proteins that showed statistically significant ($p < 0.05$) response to exposure to the GW agents were analyzed using the Ingenuity Pathways Analysis (IPA, Ingenuity® Systems, www.ingenuity.com) software. These analyses were conducted as described elsewhere (Abdullah et al 2011). Briefly, the Ingenuity knowledgebase comprises a repository of proteins/genes that are grouped based on biological interactions and functional relationships. Once a dataset is uploaded to IPA (e.g., brain proteins demonstrating expression changes in response to GW agent exposure), the proteins are mapped onto biological functions and pathways in IPA from which the

biological relevance of the response can be inferred. Assignment of each uploaded protein to particular biofunctions and pathways is determined by the IPA using published literature and scientific databases. The IPA uses a right-tailed Fisher's exact test to calculate a p-value to determine the probability of whether each biofunction and/or disease assigned to that dataset is due to chance alone.

3.2.3. Results

3.2.3.1. Quantitative proteomic studies of brain samples from GW agent exposure model B

Proteomic studies conducted using iTRAQ LC/MS analyses at post-exposure day 150 identified and quantified 1,089 proteins from 114,767 spectra. Figure 3.2 shows an example of MS data from an iTRAQ labeled peptide from a mouse brain lysate. Subsequent ANOVA showed that 31 proteins were differentially expressed in response to exposure, of which 8 were upregulated and 23 were downregulated (see

Images of MS spectra

Figure 3.2

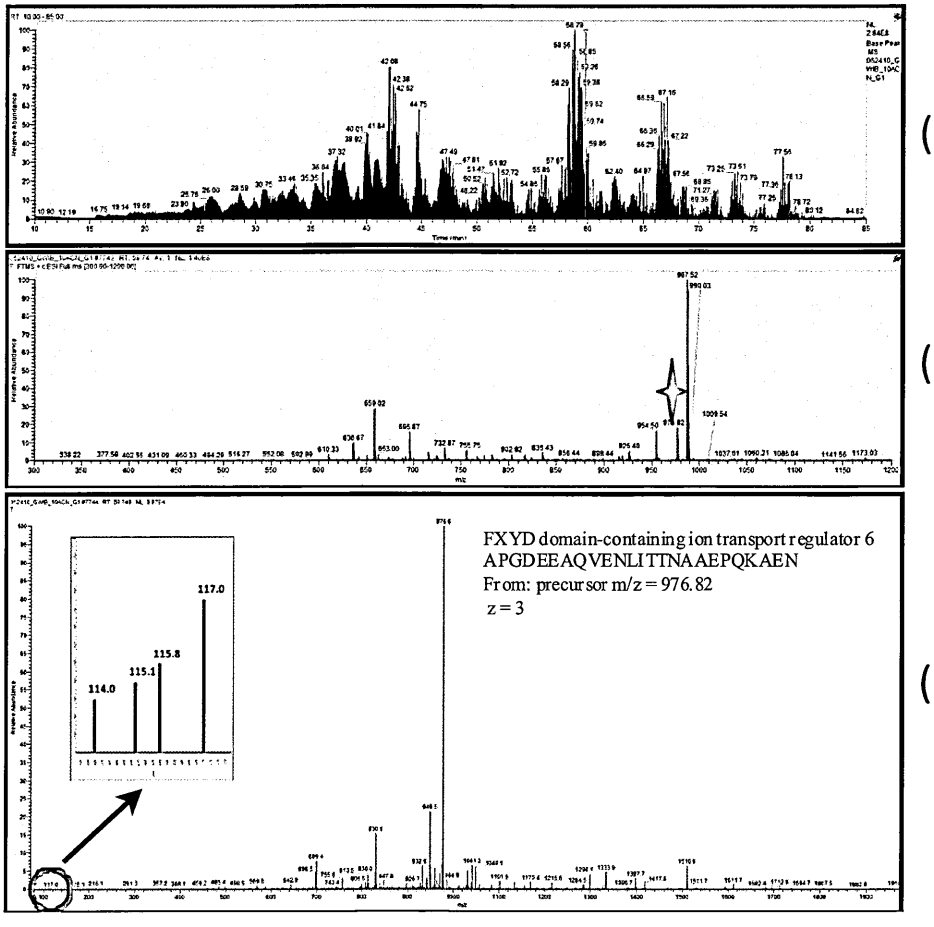

Figure 3.2. Example of MS data from iTRAQ labeled peptide from mouse brain lysate reveals differential expression of FXYD protein. Pictured are (A) base peak LC/MS chromatogram, (B) full-scan MS spectrum in high resolution (Fourier Transform) mode and (C) the PQD MS/MS spectrum from the 976.82 m/z precursor ion (indicated by a red diamond). Expanded from the MS/MS spectrum are the iTRAQ reporter ion peaks (circled region and blown-up insert) from which the quantitative measurements were made, while the 200 – 2000 m/z range of the spectrum contains the amino acid sequence-informative fragment ions. *Note:* though the relative intensity of the reporter ions on the MS/MS spectrum is low (~1%) relative to those observed using beam-type fragmentation, these are typical for 2D trap fragmentation of iTRAQ labeled peptides. To ensure statistically-relevant ion counts of the reporter fragments for quantification and to account for the insufficient fragmentation efficiency observed in PQD MS/MS spectra, 40,000 precursor peptide ions were accumulated in the trap prior to fragmentation. *Note, image already published (Abdullah et al 2011).*

Table 3.1). Based on fold-change, the top five upregulated molecules were histidine triad nucleotide binding protein 2, vinculin, nucleophosmin, UBX domain protein 6 and propionyl CoA carboxylase. The top five downregulated molecules included isoleucyl-tRNA synthetase, growth hormone 1 (GH), proteasome subunit alpha type 2 and adaptor-related protein complex 1 sigma 1 subunit. Two of the 31 proteins were unnamed proteins and were not mapped in IPA; the remaining differentially-expressed named proteins (n = 29) with a protein/gene ID were further examined using IPA. The biofunctions identified by IPA to be significantly associated with these molecules are presented in Figure 3.3. *Lipid metabolism*, *molecular transport*, *the endocrine system* and *the nervous system* were among the top five biofunctions.

3.2.3.2. Quantitative proteomic studies of plasma samples from GW agent exposure model B

Plasma samples were also analyzed from the mice euthanized at 150 days post-exposure. A total of 198 proteins were identified from 18,034 spectra. Of these, 23 proteins (Table 3.2) were significantly different between GW agent exposed mice compared to controls. A total of 9 proteins were downregulated and 14 were upregulated. Ingenuity Pathways Analysis software was used to examine the functional relevance of differentially expressed proteins. The top five molecules included CAS1 domain containing 1 (CASD1), apolipoprotein A (APOA1), immunoglobulin heavy constant μ (IGHM), Carboxylesterase 1G (Ces1g) and Igh-1a Igh protein (Ighg2a). The proteins that were significantly

Table 3.1. GW-agent induced differentially expressed proteins in the brain

IPI Accession No.	Entrez Gene Name	p-value	Fold change	Type(s)
IPI00133034.3	Histidine triad nucleotide binding protein 2	0.00	2.21	Other
IPI00405227.3	Vinculin	0.04	1.97	Enzyme
IPI00127415.1	Nucleophosmin 1	0.03	1.82	Transcription regulator
IPI00121151.1	UBX domain protein 6	0.04	1.71	Other
IPI00330523.1	Propionyl Coenzyme A carboxylase, α polypeptide	0.04	1.71	Enzyme
IPI00133224.1	FXYD domain containing ion transport regulator 6	0.02	1.77	Ion channel
IPI00831256.1	Unc-13 homolog C	0.04	1.93	Other
IPI00415908.4	Protein phosphatase methylesterase 1	0.01	1.64	Enzyme
IPI00115085.1	Inositol(myo)-1(or 4)-monophosphatase 1	0.02	-1.03	Phosphatase
IPI00329927.4	Neurofascin homolog	0.04	-1.04	Other
IPI00230124.5	Fatty acid binding protein 3, muscle and heart	0.05	-1.04	Transporter
IPI00321919.1	G protein-coupled receptor 56	0.05	-1.04	GPCR
IPI00338094.6	Bone morphogenetic protein receptor, type II (serine/threonine kinase)	0.02	-1.05	Kinase
IPI00857233.1	Glia maturation factor, beta	0.04	-1.05	Growth factor
IPI00331066.6	Calbindin 1, 28kDa	0.03	-1.05	Other
IPI00134191.3	Solute carrier family 2 (facilitated glucose transporter), member 3	0.01	-1.05	Transporter
IPI00284505.1	Cadherin, EGF LAG seven-pass G-type receptor 3	0.03	-1.06	GPCR
IPI00471348.3	Not available	0.02	-1.06	Other
IPI00319406.6	EF-hand domain (C-terminal) containing 1	0.05	-1.06	Other
IPI00762293.2	Chromobox homolog 7	0.00	-1.06	Other
IPI00123223.2	Murinoglobulin 1	0.01	-1.07	Transporter
IPI00755154.7	Leiomodin 3 (fetal)	0.00	-1.07	Other
IPI00221615.5	ADP-ribosylation factor 5	0.05	-1.08	Transporter
IPI00114416.1	Dodecenoyl-Coenzyme A delta isomerase	0.04	-1.08	Enzyme
IPI00314054.3	Solute carrier family 6, member 6	0.03	-1.09	Transporter
IPI00127930.1	Guanine nucleotide binding protein, beta 5	0.01	-1.11	Enzyme
IPI00118026.1	Adaptor-related protein complex 1, sigma 1 subunit	0.03	-1.11	Transporter
IPI00890001.1	Proteasome subunit, alpha type, 2	0.02	-1.16	Peptidase
IPI00129161.1	Growth hormone 1	0.01	-1.08	Hormone
IPI00271869.1	Glyceraldehyde-3-phosphate dehydrogenase pseudogene	0.03	-1.03	Other
IPI00225201.5	Isoleucyl-tRNA synthetase	0.03	-1.89	Enzyme

Note: A list consisting of IPI accession numbers, names, types and p-values for proteins shown to be differentially expressed in response to GW agent exposure. A ratio of ln-transformed value for each protein was calculated for GW agent exposure/control and the corresponding fold change is indicated using color, where red indicates up-regulation and blue indicates down-regulation.

modulated at 150 days post-exposure to PB+PER compared to control were associated with biofunctions (see Figure 3.4) that regulate immune parameters, such as *immune cell trafficking, inflammatory responses, immunological disease, humoral immune response*

Ingenuity analyses based biofunctions

Figure 3.3

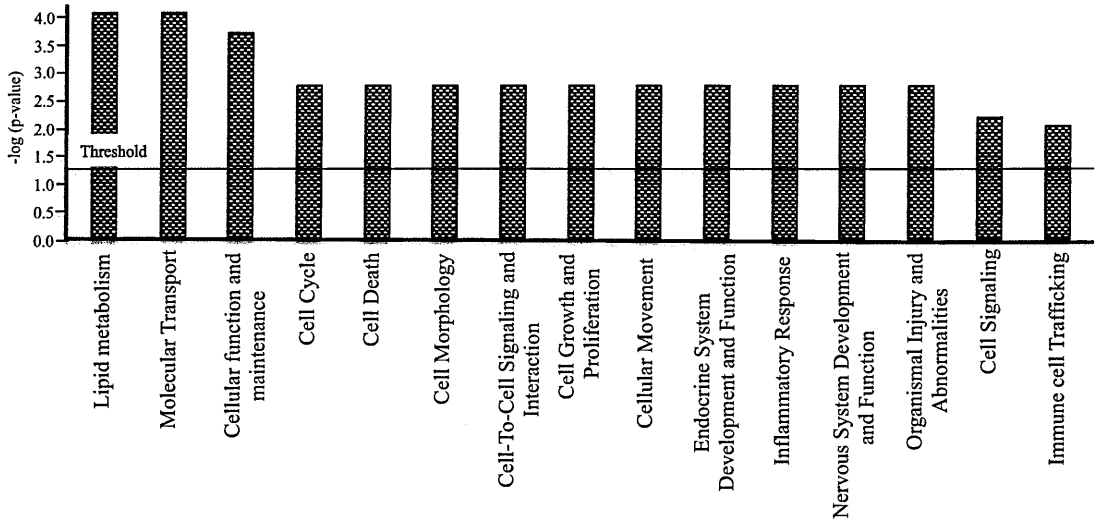

Figure 3.3. IPA based biofunctions: Brain proteins (n = 5 per group) that were differentially expressed in response to GW agent exposure were further interrogated using IPA and a "Core Analysis" was performed. Line designated by the term "threshold" indicates statistical significance cut-off of -log (p-value) of 1.5 or below. This figure represents biofunction categories differentially regulated in response to GW agent exposure at post-exposure day 150, a timepoint which immediately followed observations of cognitive impairment. *Note: Image already published (Abdullah et al 2011).*

and *antigen presentation.* Other related biofunctions included *neurological diseases* and *lipid metabolism.*

3.2.4. Discussion

Given the heterogeneity of GW exposures, symptom profiles vary with different exposures and produce a complex clinical presentation. As described in Chapter 2 above, mouse model B of GW agent exposure (PB+PER) demonstrates cognitive and psychomotor-based CNS symptoms; such symptoms are also observed in veterans with GWI (Binns et al 2008). Given the complexity of the clinical presentation observed in veterans with GWI, it is possible that biological changes that correlate with these symptoms are also complex. It is expected that the proteomic findings that are discussed below may provide a global view of the underlying biological disturbances associated with GW agent exposure.

Table 3.2. GW-agent induced differentially expressed proteins in plasma

IPI accession number	Entrez Gene Name	p-value	Fold Change	Type(s)
IPI00222011.1	Chromosome 9 open reading frame 43	0.01	-1.71	Other
IPI00896683.1	Immunoglobulin heavy chain (gamma polypeptide)	0.01	-1.33	Other
IPI00457431.1	Ig heavy chain V-III region U61	0.04	-1.32	Other
IPI00109876.1	Growth Factor receptor(GRB)-bound protein 2-related adaptor protein	0.01	-1.15	Other
IPI00473912.4	GRB10 interacting GYF protein 2	0.02	-1.11	Other
IPI00420972.2	Immunoglobulin heavy constant gamma 2A	0.00	-1.10	Other
IPI00227455.2	Potassium channel tetramerisation domain containing 8	0.04	-1.10	Other
IPI00128030.1	Antigen p97 (melanoma associated) identified by monoclonal antibodies 133.2 and 96.5	0.05	-1.07	Other
IPI00128484.1	Hemopexin	0.00	-1.04	Transporter
IPI00308213.3	Immunoglobulin heavy constant gamma 1 (G1m marker)	0.01	1.04	Other
IPI00123920.2	serpin peptidase inhibitor, clade A (alpha-1 antiproteinase, antitrypsin), member 1	0.00	1.06	Other
IPI00131830.1	Serine (or cysteine) peptidase inhibitor, clade A, member 3K	0.00	1.08	Other
IPI00139788.2	Transferrin	0.00	1.09	Transporter
IPI00123223.2	Murinoglobulin 1	0.03	1.17	Transporter
IPI00114958.1	Kininogen 1	0.01	1.20	Other
IPI00121209.1	Apolipoprotein A-I	0.04	1.20	Transporter
IPI00624663.3	Pregnancy zone protein	0.00	1.21	Other
IPI00322463.3	Apolipoprotein H (beta-2-glycoprotein I)	0.02	1.22	Transporter
IPI00115867.4	Carboxylesterase 1G	0.02	1.30	Enzyme
IPI00177214.2	Immunoglobulin heavy constant mu	0.00	1.30	Transmembrane receptor
IPI00556788.1	Immunoglobulin heavy constant gamma 2A	0.00	1.73	Other
IPI00856876.1	CAS1 domain containing 1	0.03	1.79	Enzyme
IPI00877236.1	Apolipoprotein A-I	0.00	1.91	Transporter

Note: A list consisting of IPI accession numbers, names, types and p-values for proteins shown to be differentially modulated in plasma in GW agent exposed mice compared to control mice. A ratio of ln-transformed value for each protein was calculated for GW agent exposure/control and the corresponding fold change is indicated using color, where red indicates up-regulation and blue indicates down-regulation.

Proteomic findings from brain and blood support a role of immune and inflammatory dysfunction in the pathogenesis of GWI and are also supported by neuropathology data presented in Chapter 2. For instance, in plasma APOA1 was increased by 1.6 fold and was associated with modulating immune responses after

Ingenuity analyses based biofunctions

Figure 3.4

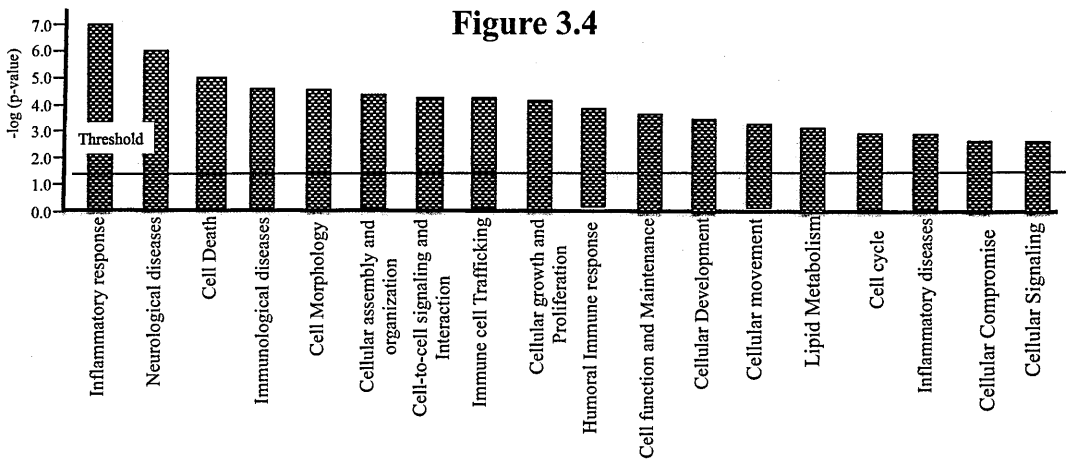

Figure 3.4. IPA based biofunctions: Plasma proteins (n = 5 for each of the exposed and the control group) that were differentially expressed in response to GW agent exposure to mice in model B were further interrogated using IPA and a "Core Analysis" was performed. Line designated by the term "threshold" indicates statistical significance cut-off of -log(p-value) 1.5 or below. The figure above represents biofunction categories modulated in response to GW agent exposure at post-exposure day 150, a timepoint that immediately followed observations of cognitive impairment. A number of humoral and cellular immunity related biofunctions were affected in response to GW agent exposure.

exposure to GW agents. As expected, the *humoral immune response* was only present in plasma but not in the brain. In both blood and brain, biofunctions that were modulated in response to GW agent exposure included *immune cell trafficking* and *inflammatory response.* A number of studies have shown that each PB and PER can modulate both the cell-mediated and humoral immunity (Peden-Adams et al 2004; Punareewattana et al; Prater et al 2005). Administration of PER to mice is shown to affect cell-mediated immunity by depressing splenic T-cell proliferative response and thymic cellularity, as well as affecting humoral responses by reducing splenic B lymphocyte-specific antibody production (Prater et al 2002; Prater et al 2003). Exposure to PB is shown to affect humoral immunity where responses to IgM antibody were dampened in mice after 14 days of PB exposure. These findings are in agreement with the evidence of immune dysfunction observed in veterans with GWI. Several studies report a persistent Th1 immune response (pro-inflammatory cytokine production by Type-1 T-helper cells) that is accompanied by

an increased expression of the pro-inflammatory cytokines on CD4 T-cells in veterans with GWI (Skowera et al 2004). Although Th2 immune response (reflected by production of anti-inflammatory cytokines by Type-2 T-helper cells) was observed in blood of veterans with GWI compared to well-veterans from GW era (Broderick et al 2011). Low CD3 T-cell and natural killer cell counts have been observed in ill veterans (Zhang et al 1999; Whistler et al 2009). These studies clearly support a role of immune/inflammation imbalance with respect to GW agent exposure and are currently being evaluated as a new line of investigation at the Roskamp Institute aimed at characterizing immune/ inflammation profiles associated with GW agent exposure (PI: Ait-Ghezala, CDMRP award).

Fatty acid binding proteins

Lipid metabolism was also one of the biofunctions shown to be affected in both the brain and blood of mice exposed to GW agents. Among the proteins associated with lipid metabolism, of particular interest is the observation of a reduction in fatty acid binding protein 3 (FABP3) in the brain of GW agent exposed mice. Fatty acid binding protein 3 is expressed in neurons within the hippocampus and cortex (Motohashi et al 2009). Clinical studies suggest that FABP3 levels are decreased in the brain but increased in the CSF and serum of patients with neurocognitive disorders (Chiasserini et al 2010; Wada-Isoe et al 2008). FABP3-deficient mice show increased fear and anxiety, also observed in GW agent exposed mice. Therefore, the observed decrease in FABP3 provides evidence for a dysregulation of lipid metabolism in response to GW agent exposure. Furthermore, FABP3 is involved in the uptake of AA (Murphy et al 2005). Metabolites of AA have a well-defined role in propagating inflammation, and thus it can be hypothesized that changes in lipids and lipid metabolites may be of importance in understanding the pathobiology of GWI.

Apolipoproteins

In blood, lipid metabolism was also modulated in response to GW agent exposure. In particular, lipoproteins, APOH and APOA1, were associated with this biofunction and are highly relevant to lipid metabolism. For instance, APOA1 plays a critical role in cholesterol efflux by acting as a cofactor of lecithin-cholesterol acyltransferase (a phospholipase) and solubilizing phospholipids to facilitate cholesterol absorption (Phillips et al 1998). Apolipoprotein H, also known as beta2-glycoprotein 1, is shown to be an anti-phospholipid antibody that is present in autoimmune diseases (Matsuura et al 2010; Yasuda et al 2000). Hence both brain and plasma proteomic profiling suggest that lipid metabolism may be affected in response to GW agent exposure.

Growth Hormone

Proteomic findings show lower GH levels in the brain of exposed mice compared to controls. Growth hormone (GH) is regulated by the neuroendocrine system and GH deficiency is associated with impaired cognition (Maruff, & Falleti 2005). Several studies suggest that the cholinergic system controls ghrelin induced GH release where a number of studies have shown that administration of pyridostigmine can increase circulating GH levels (Broglio et al 2004) (Ghigo et al 1990). Therefore, additional evaluation of the molecular pathways associated with GH may be helpful in providing an understanding of the pathobiology of GWI.

These exploratory proteomic studies provided a global view of the biological changes and identified key areas of focus. However, additional validation of these studies is required using alternative techniques, such as western blot or ELISA (where available). Immune/inflammatory-based changes identified are consistent with current GWI research and this aspect of GWI is being investigated as a separate project at the Roskamp Institute which is geared towards discovery and validation of novel treatments against CNS symptoms of GWI. Findings pertaining to lipid metabolism provide a novel avenue for

exploration, particularly since lipid metabolites are upstream of many inflammatory cascades. Further evaluation of lipid changes using lipidomic approaches are presented in the next chapter of this thesis.

4.0. Chapter 4 Application of lipidomics technology to lipid profiling of mice exposed to GW agents

The studies presented in this thesis reflect the lipidomics work performed as part of the implementation of the lipidomics platform at the Roskamp Institute and also provide data which will be helpful in increasing the awareness of the role that lipids play in the CNS disorders. Given that the proteomic findings in Chapter 3 suggested that lipid metabolism pathways may be affected in response to GW agent exposure, the primary focus of the lipidomics work was to understand lipid changes in relation to GW agent exposure. Therefore, lipidomics technology was applied to examine brain and blood samples from mouse models of GW agent exposure. Lipid profiling was performed on the brain and blood samples from mouse models of other neurological illnesses (in comparison to their respective control groups) to determine if phosphatidylcholine (PC) and sphingomyelin (SM) profiles of GW agent exposed mice were distinct from those observed in mouse models of other neurological conditions. Lipid profiles from mouse models of GW agent exposure were further interrogated to identify molecular pathways that may underlie the CNS symptoms associated with GW agent exposure and whether these pathways are targetable by therapies.

4.1. Introduction

4.1.1. Lipid characteristics

Glycerophospholipids and sphingomyelin together are defined as phospholipids (PLs) and represent 20-25% of the dry weight of the adult brain and nearly 60% of the neuronal membrane mass (Farooqui et al 2007). Phospholipids have side chains that are linked to a backbone composed of either a glycerol or a sphingosine (in the case of sphingomyelin only) and also contain a phosphoric acid and a polar head-group. Phospholipids are amphipathic molecules that have both polar and non-polar components

and can be further divided into subclasses, such as PC, phosphatidylethanolamine (PE), SM, phosphatidylserine (PS), phosphatidylinositol (PI), phosphatidic acid (PA) and phosphatidylglycerol (PG). Each PL subclass has a unique polar head-group. For example, PC and SM both contain a choline moiety in their head-groups, while PE has ethanolamine, PS has serine and PI has an inositol group.

Within each PL class, there are a large number of distinct molecular species, which arise from a combination of different fatty acid side chains with various head-group structures. It is estimated that a mammalian lipidome may contain about 3000 distinct PL species (Brouwers 2011). The polar end is charged due to the presence of a phosphate and sometimes a nitrogenous base. In a lipid bilayer, the PLs are organized in a way where the polar head-groups of PLs face the intracellular and extracellular spaces of the lipid bilayer and the hydrophobic side chains are packed within the inter-membrane faces of the lipid bilayer. These hydrophobic chains are connected to glycerol of PL through acyl, alkenyl and alkyl bonds. In general, the first position of the glycerol backbone (sn1) contains saturated fatty acid (e.g., palmitic or stearic acid) and the second position of the glycerol backbone (sn2) contains unsaturated fatty acids, such as AA and DHA (Farooqui et al 2007). Among other things, the degree of saturation of these lipids affects membrane fluidity where an increase in saturated lipids would make it more viscous but an increase in unsaturated lipids would increase membrane fluidity (Farooqui et al 2007). Figure 4.1 shows examples of PL and ether PL (ePL) structures.

4.1.2. Lipid role in cellular function and signaling pathways:

Cellular PLs have a key role in maintaining structural function and integrity of the membrane. The lipid bilayer, much of which is composed of PC and SM, maintains the integrity of the cell membrane. Fluidity of this lipid bilayer is critical in allowing passage of certain molecules and solutes in and out of the cells. Membrane permeability is affected by an increase in saturation of fatty acid chains, making it more rigid and less fluid

(Tymoczko et al 2012). Phospholipids also play an important role in membrane fusion, which is a critical requirement of many cellular processes including fertilization, cell division, exocytosis, endocytosis and intracellular membrane transport. Phospholipids also form specialized subcellular structures and are essential for proper functioning of membrane bound proteins (Adibhatla, & Hatcher 2008; Wenk 2005).

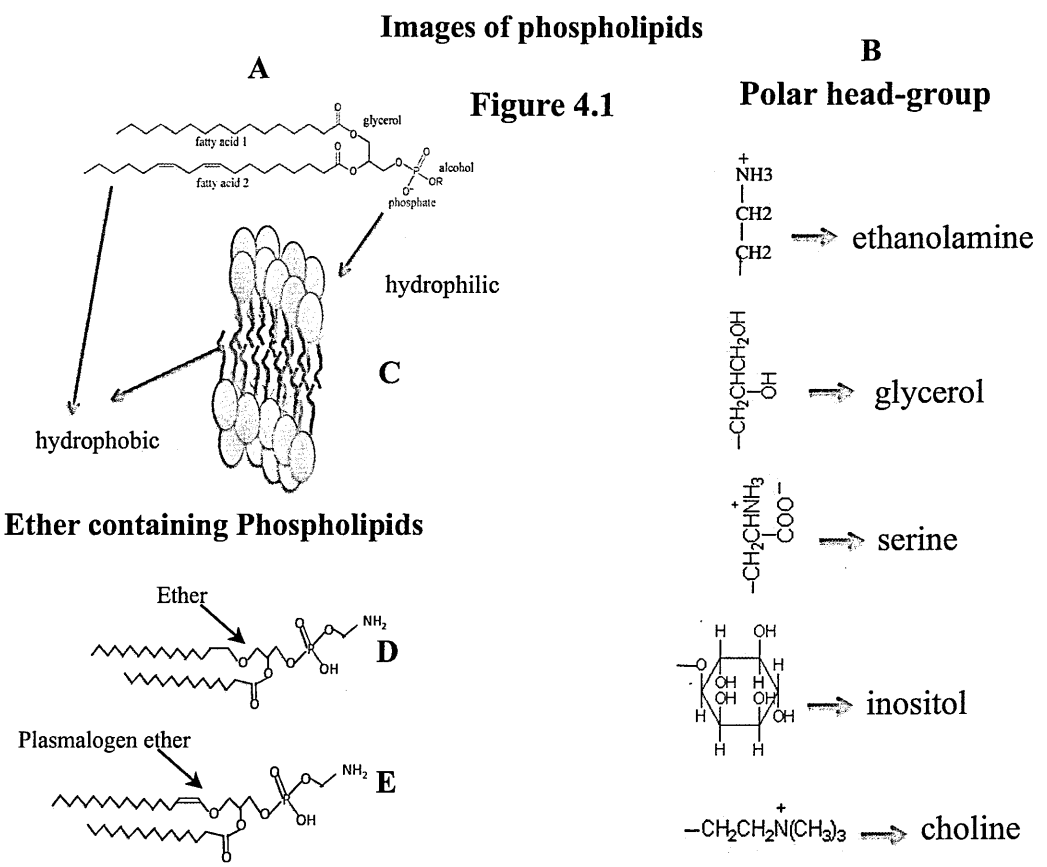

Figure 4.1. Images of phospholipids: (A) An image of diacyl PL containing ester linked fatty acid side chains connected to a glycerol backbone and a phosphate group that combines with different polar head-groups (R). Each fatty acid side chain can vary in carbon numbers, generally even numbers from 14-22 carbons with various double bonds. Fatty acid side chain 1 (C16:0 - containing 16 carbons and no double-bond) is connected to the first carbon in the glycerol backbone and fatty acid side chain 2 (C18:2 - containing 18 carbons and 2 double bonds) is connected to the second carbon in the glycerol backbone. (B) Examples of different polar head-groups include glycerol, inositol, choline, serine and ethanolamine. (C) A cross-section of plasma membrane. Polar headgroups are present in the intracellular and extracellular sides where fatty acid side chains are sandwiched between them in the hydrophobic region of the lipid bilayer. (D) An example of ether PC that contains O-alkyl linked ether bonds at the sn-1 and ester linkage at the sn2 position. (E) An example of plasmalogen PC which contains a vinyl ether at the sn1 and an ester linkage at the sn2 position.

Over the last few decades, fundamental discoveries have been made with regard to the role that PLs and their metabolites play in a variety of biological functions and cellular signaling pathways. One of the most important discoveries pertains to arachidonic acid (AA - an omega-6 fatty acid/fatty akyl where the final carbon-carbon double bond is at the 6^{th} carbon position from the terminal methyl group), which is liberated from PL by phospholipase A2 (PLA_2). Subsequent metabolism of AA to prostaglandins and leukotrienes (collectively referred to as eicosanoids) is facilitated by the enzymatic activity of cyclooxygenase (COX) and lipooxygenase (LOX), respectively. The eicosanoids are upstream of pro-inflammatory pathways and have been widely targeted for therapeutic modulation of inflammation, including the use of COX inhibitors (Adibhatla, & Hatcher 2008). More recently, similar enzymatic pathways for DHA, an omega-3 fatty acid (where the final carbon-carbon double bond is at the 3^{rd} carbon position from the terminal methyl group), have been shown to generate anti-inflammatory mediators, such as resolvins and protectins. These bioactive DHA metabolites can resolve inflammation at low nanomolar concentrations (Serhan et al 2008). See Figure 4.2 for a schematic presentation of PL metabolism pathways.

Lysophopholipids (LPL) are generated by the action of phospholipases on PLs and a number of these are novel mediators of inflammatory and immune responses. Among these, LPC is the most abundant LPL and is shown to affect immune cell functioning. There is a high concentration of LPC in blood but most of it is found bound to serum albumin and lipoproteins (Kabarowski 2009). A review of the literature suggests that LPC is capable of eliciting both pro- and anti-inflammatory (mixed inflammatory) responses where acyl LPCs (LPC16:0 and LPC18:0) have been shown to increase expression of CD40 (which belongs to the TNF-α super family) in mature dendritic cells and cause an upregulation of inflammatory and/or anti-inflammatory cytokines (Bach et al 2010).

Image of phospholipid metabolic pathways

Figure 4.2

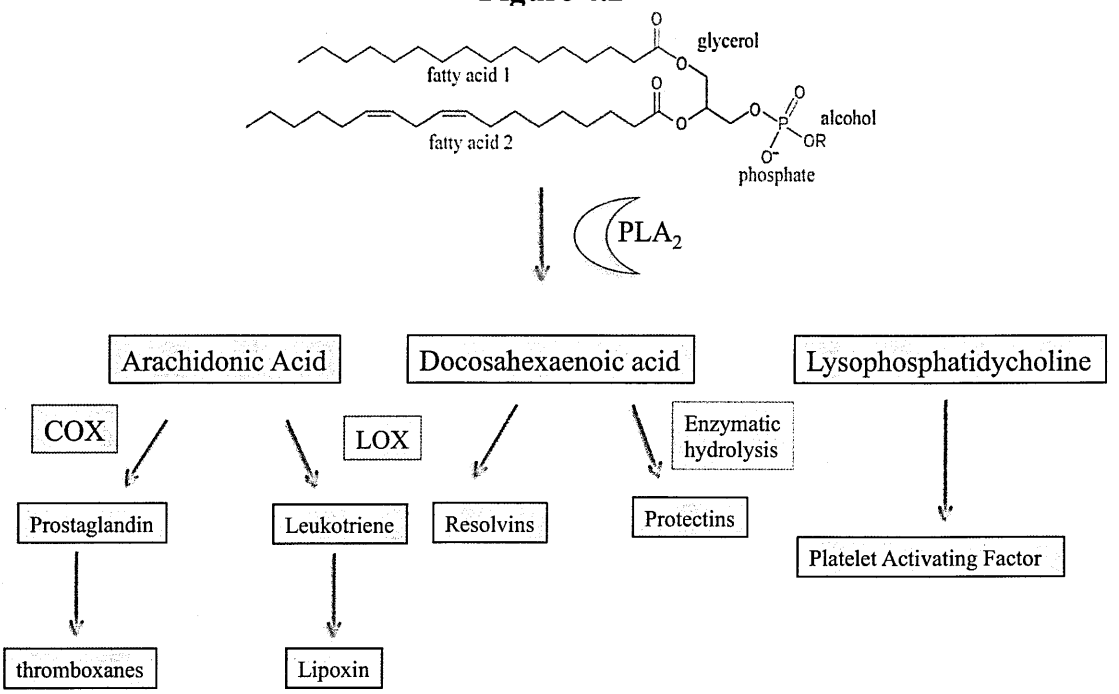

Figure 4.2. Image of phospholipid metabolic pathways: (A) This image shows that PL can be metabolized by PLA_2 which can generate AA, DHA and LPCs. Arachidonic acid can be further metabolized by COX and LOX to generate prostaglandins and leukotrienes. Prostaglandins and leukotrienes are further metabolized to produce thromboxanes and lipoxin, respectively. Docosahexaenoic acid can be enzymatically converted to protectins or to resolvins via the LOX pathway. Upon action of PLA_2 on PC, certain LPC products are converted to PAF.

Treatment with LPC16:0 and LPC18:0 *in vitro* resulted in an increase in IFN-γ, a pro-inflammatory cytokine (Th1), and an increase in IL-13 (Type Th2) and IL-5 (Type Th2), both of which are considered anti-inflammatory cytokines. *In vivo*, an increase in the production of IL-6 (Th1/Th2) and IL-5 was reported in response to LPC16:0 and LPC18:0 exposure (Bach et al 2010). In addition, LPC16:0 or LPC20:2 can cause secretion of GM-CSF from natural killer cells (Fox et al 2009). Collectively, these studies suggest that metabolites of PC can modulate both immune and inflammatory responses and may represent upstream targets of these biological functions.

There are two varieties of PLs, those that contain acyl chains at both the sn-1 and sn-2 positions and those that are ether lipids which contain either O-alkyl or O-alk-1-enyl, specifically at the sn1 position (Vance, & Vance 2008). In general, ether PLs are abundant

in PC and PE and the presence of ether bonds allows for a tighter packaging of these lipids in cell membranes. Ether PLs are thought to play a role in membrane reorganization and vesicle formation. Among ether PLs, plasmalogens are those that contain O-alk-1-enyl at sn1, generally contain more polyunstaturated fatty acids (PUFA) and play a role in cholesterol esterification and maintenance of myelin covered axonal nodes (Mankidy et al 2010; Gorgas et al 2006). A deficiency of the plasmalogen content within PL is considered to be a prominent feature of several CNS disorders, including Niemann Pick type C disease (NPCD), Zellweger's disease (ZD) and AD (Gorgas et al 2006).

Another lipid metabolite, PAF, was originally named due to the initial discoveries showing that it was released from Immunoglobulin E (IgE) stimulated basophils and caused aggregation of platelets. This bioactive lipid is now shown to be present in a number of cells and can be produced in the brain via de novo synthesis or remodeling pathways which consist of biochemical reactions involving PLA_2 and acetyltransferase (MAclennan KM et al 1996). Studies have shown that PAF can affect a number of physiological and biological functions, such as BBB permeability, inflammation and ACh release (MAclennan KM et al 1996).

In summary, cellular signaling mediated by these lipids and their metabolites is upstream of several key intracellular cascades in biological functions, which include modulation of inflammatory and immune responses. Therefore, examination of PLs and their metabolites represents a highly relevant area for further examination of neurobehavioral and neuropathological features of GW agent exposure.

4.1.3. Lipidomics technology

The advances in lipid research have been greatly facilitated by recent developments in MS instrumentation and techniques that allow accurate identification and quantification of several thousands of lipids and their molecular subspecies in complex biological samples with relative ease. MS-based lipidomic approaches have largely displaced other

methods for lipid analysis because of their higher sensitivity, information content and efficiency (Brouwers 2011).

Individual PLs and their molecular species can be identified and quantified using LC/MS (Brouwers 2011). A number of approaches are available that rely solely on mass spectrometry, but use of LC/MS is particularly advantageous since it allows for the separation and quantification of PLs in much higher detail than that achievable by using MS alone (Brouwers 2011). While an LC-free shot-gun lipidomics approach is quicker, ion suppression, particularly for shot-gun methods that employ direct infusion of crude extracts, can become troublesome and reduce accurate detection of molecules that don't compete well for the charge during the ionization process. In these shot-gun methods, ion suppression by other molecules in the biological matrix that can carry the charge better than PLs is also a problem for accurate detection and quantification of PL. On the other hand, use of normal phase LC in conjunction with MS separates PL subclasses based on the polarity of their head-group which is tremendously useful in resolving issues pertaining to ion suppression. Many of the commonly used chromatographic procedures published today are based on work from the early 1990s, which applied a binary gradient using a combination of hexane, 2-propanol and water as mobile phase with increasing water amounts to achieve separation of major PLs within 20 minutes. However, these studies were limited by poor run-to-run reproducibility, which was possibly due to the absence of chemicals to prevent column degradation (Brouwers 2011). In recent years, a number of these difficulties have been overcome by the use of varying combinations of chloroform, methanol and buffered ammonium hydroxide to improve separation, and with the use of diol-modified silica to achieve greater stability and quicker regeneration of the stationary phase (Brouwers 2011).

The experiments detailed in this thesis not only take advantage of these advances in LC/MS methods, but also use a novel approach of applying in-source collision induced

dissociation (SCID) to generate partial fragmentation of lipids to obtain structural information during the full scan mode of data acquisition. This method is tremendously useful in (1) the quantification of molecular species with overlapping mass-to-charge ratios (m/z) across different classes of PL and (2) reducing the number of LC/MS/MS runs required for the identification of individual molecular species. With this SCID LC/MS approach, separation, identification, and quantification of the seven major PL classes and SM can be accomplished in a single experiment. In addition, identification and quantification of dozens of molecular species over a 1,000 fold concentration range can be obtained within each class of PL.

Given that the chemicals that were used to develop mouse models of GW agent exposure affect ACh turnover and ACh-related signaling pathways, PLs that contain choline represent relevant targets to explore in the pathobiology of GWI. Phosphatidylcholine and SM (both containing choline in their head-groups) were characterized using this novel SCID LC/MS approach. Studies described in this Chapter include comparisons of brain and blood from mouse models of GW agent exposure with their respective control groups. Phosphatidylcholine and SM in brain and blood samples from mouse models of other CNS illnesses (AD and Traumatic Brain Injury [TBI]) were also examined in order to understand how lipid changes may overlap or differ between these mouse models and models of GW agent exposure. Based on this lipidomic-based target identification approach, a pilot study was conducted to determine if lipid abnormalities can be normalized with treatments that affect lipid metabolism and whether such treatments can normalize lipid metabolism dysfunction associated with GW agent exposure.

4.2. Materials and methods

4.2.1. Mouse models

Whole brain homogenates from mouse models A (n = 5 per exposure/control) and B (n = 4 per exposure/control) of GW agent exposure were prepared as described above in Chapter 3. Brain extracts were from the same mice on which exploratory biomolecular (mouse model A) and proteomic studies (mouse model B) were conducted. The post-exposure interval for mouse model A was 42 days (approximate age 4 months) and for mouse model B (CD1 mice) it was 150 days (approximate age 7 months). Both brain and plasma samples were analyzed for mouse model A and mouse model B of GW agent exposure. A mouse model of AD (PSAPPswe mice containing both the Swedish mutation K595N/M596L in APP and the M146L Presenilin [PS] mutation) was used for comparing AD-dependent lipidomics changes against GW agent dependent lipidomic changes. Six-month old PSAPPswe mice were compared to B6SJL/F1 wild-type mice (n = 5 per group), a timepoint at which the PSAPPswe mice have high brain levels of soluble and insoluble Aβ levels and show Thioflavin S positive plaques and astrocytosis (Kumar-Singh et al 2005; McGowan et al 1999). Only brain samples were available for lipidomics analyses from this AD mouse model.

The other comparison groups included two mouse models of Traumatic Brain Injury (TBI), one that received controlled cortical impact (CCI) and another which received a closed head injury (CHI) which mimics mild TBI (mTBI). Administration of CCI TBI to mice is described in detail elsewhere (Crawford et al 2012). Briefly, mice were administered anesthesia at 1L/min O_2 mixed with 3% isoflurane. Once each mouse was deeply anesthetized, it was individually mounted in a stereotaxic frame and the temperature was monitored throughout the surgery. A midline incision was made, followed by a 5-mm craniectomy that was adjacent to the central suture, midway between lambda

and bregma, with the dura kept intact over the cortex. A single severe injury was administered as reported (Crawford et al 2012) using an electromagnetic device and an injury was delivered to the right cortex with a 3-mm diameter tip at a rate of 5 m/sec and depth of 1.8mm. Sham mice for the CCI procedure received anesthesia and craniectomy without receiving an injury. For the lipidomic studies described below, 8 mice were utilized (n = 4 per group), the injury was administered at 3-months of age and a post-injury timepoint of 3-months was examined (approximate age 6 months). Lipidomic studies were performed on both brain and plasma samples.

For mTBI studies, the same equipment was used but injury was delivered as a closed head injury on the midline at a lesser force than CCI to avoid skull fracture (Mouzon et al 2012). The injury was administered to the head using a strike velocity of 5m/s, a strike depth of 1.0mm and dwell time of 200ms. Animals either received a single mTBI (s-m-TBI) or repeated mTBI (r-mTBI) for which additional injuries were administered at days 3, 5, 7 and 9 after the original injury. A control group for each injury was used where single anesthesia (s-sham) and repetitive anesthesia (r-sham) was administered to derive matching groups for comparison. This mTBI injury was administered to 10-week old C57BL6 male mice (n = 3/4 per injury/sham). Mice were euthanized after the 24hrs post-injury timepoint and only plasma samples were used for the lipidomic studies described below.

Based on the findings from lipidomics work aimed at pathway identification, pilot treatment studies were performed. A dihydropyridine calcium channel blocker (DHP-CCB), nilvadipine, was chosen based on the support from the literature showing an impact of this drug on opposing LPC induced adverse biological affects (Takayama et al 2009). As described in Chapter 2, it is anticipated that C57BL6 mice will be used for subsequent GWI work to be conducted at the Roskamp Institute, and thus this strain was chosen for

these studies. Included in the aims was the need to determine if the brain and plasma PL and SM changes observed in CD1 mice from mouse model B can be observed in this C57BL6 strain and whether nilvadipine treatment can normalize PL abnormalities (if observed in this strain) associated with GW agent exposure. Briefly, 0.7mg/kg of PB and 200mg/kg of PER were administered to C57BL6 mice for 10 days while unexposed animals received vehicle (DMSO) only. At 3-months post-exposure (approximate age 6 months), a subset of unexposed (n = 5) and exposed mice (n = 5) received i.p. nilvadipine 2 mg/kg in 70% DMSO for 10 days while the control group received vehicle only (n = 4 exposed, n = 5 unexposed). This dose of nilvadipine was chosen based on work conducted at the Roskamp Institute showing efficacy in AD mouse models without any toxic side-effects (unpublished work). Mice were immediately euthanized after 10 days of treatment and both brain and blood samples were analyzed for lipidomic analyses.

All animal procedures were approved by the Roskamp Institute IACUC and were conducted in accordance with the guidelines described in Chapter 2.

4.2.2. Lipidomic analyses

The Folch method (Folch et al 1957) was used to extract lipids from 50µl of crude mouse brain homogenate in mammalian protein extraction reagent (Pierce, IL) for mouse models A and B of GW agent exposure. For these two mouse models of GW agent exposure, only the insoluble fractions were examined for lipidomic studies. One whole left hemisphere was used for the PSAPPswe mouse model studies. For the CCI TBI mouse model, lipids were extracted from each ipsilateral cortex, hippocampus and cerebellum separately for injured mice and the corresponding hemisphere from sham mice. Each brain region was homogenized separately in PBS and then lipids were extracted from 50µl of homogenate from each region for each mouse. For plasma lipidomic studies, 50µl of plasma was used for all mouse models. The Folch extraction was performed following an addition of di-14:0 fatty acid PC and 14:0-LPC (Avanti Polar Lipids) as the internal

standards (IS), at 1μg/5μl concentration. The Folch lower (organic) phase was evaporated and redissolved in 2:1 chloroform-methanol for LC/MS analysis. For mouse model A and B and for PSAPPswe mice, each sample was analyzed by LC/MS in duplicate. All other samples (brain samples of mouse models of CCI TBI and plasma samples of mTBI and C57BL6 mouse model B of GW agent exposure) were analyzed in triplicate. Brain lipids from PSAPPswe and models A and B of GW agent exposure were eluted isocratically with hexane:2-propanol:water:formic acid-ammonium hydroxide (30:60:9:1:0.12, v/v) at a flow rate of 50μl/min using a 1mm x 10cm column packed with 3μm Pinnacle II silica particles (Restek) maintained at 25°C. Additional methodological developments were subsequently performed to obtain a better separation of PLs. Subsequent to that, lipidomic analyses were performed for the experiments pertaining to brain and plasma samples from TBI mouse models and C57BL6 mouse model of GW agent exposure B. For these experiments, a solvent gradient was run from 10% solvent B (80% methanol, 10 mM formic acid, 5 mM ammonium hydroxide) in solvent A (chloroform-acetonitrile, 2:1) to 60% B in 13 min with a 4 min hold at the final conditions. The flow rate and column specifics were same as above. Full scan MS analyses were performed using a Thermo LTQ linear ion trap mass spectrometer, which was equipped with a Thermo Surveyor pumping system and Micro AS autosampler. Alternate positive (40% relative energy) and negative (90% relative energy) ion spectra were acquired from m/z 70 to 1,200 with SCID. All spectra were obtained with a 200 msec maximum ion time and 5 microscans. The fatty acid composition of individual lipid molecular species was determined by separate DDA LC/ MS/MS analyses (1 full scan followed by 3 DDA scans of the most intense ions from the full scan, ions sampled were excluded from further analysis for 1 min, 30% relative CID energy, 3 microscans, 500 msec max injection time) under the above LC conditions. Spectra of PC and SM molecular species were located on the chromatogram using

retention time (RT) and m/z 184 ion plots to locate the fragment ion of the phosphocholine head-group. These mass spectra were summed over the peak for each lipid class, converted to listings with a threshold of 0.01% base ion intensity, exported to Microsoft EXCEL and then analyzed using LipidomeDB on-line (Zhou et al 2011)(http://lipidome.bcf.ku.edu:9000/Lipidomics/) to identify and quantify (with reference to the added internal standards) each lipid molecular species. Dimension reduction and multi-collinearity issues were resolved using principal component analysis (PCA), which is routinely used to evaluate lipidomic data (Graessler et al 2009). Variables with eigenvalues of ≥ 1 were retained and PCA was used for extracting components (a composite variable that contains original lipid variables that are grouped based on correlations of the original lipid outcome variables with each other and variance explained in the dataset). The Anderson-Rubin method was used for exporting uncorrelated scores in order to perform MLM regression analyses on each component (the outcome measure) while adjusting for fixed (exposure and replication) and random (mouse) factors. Additional analyses were also performed by grouping individual PC molecular species based on the saturation status, where PC species containing saturated fatty acids (SFA), monounsaturated fatty acids (MUFA) and polyunsaturated fatty acids (PUFA) were each grouped as separate variables. Statistical analyses were performed using MLM as described above for these outcome variables.

4.2.3. Free fatty acid and 2-arachidonylglycerol quantification

Total brain homogenate from mouse model B of GW agent exposure was used for quantification of free fatty acids (FFA) and 2-arachidonylglycerol (2AG) using reverse phase LC (RPLC)/MS procedures. Brain homogenate (60µl) was diluted with 240µl of PBS, followed by an addition of 700µl of ethanol. To this, 100µg of 15-(S)HETE-$_{d8}$ (Cayman Chemicals) was added as an IS. We used this IS as the goal was to expand the RPLC method to include examination of FFA metabolites (i.e., prostaglandins, leukotrienes

and resolvins). Next, the samples were vortexed for 1 min and heated at 80°C for 2 min, followed by centrifugation at 21,000 x g for 10 minutes. The supernatant was transferred to a new tube, mixed with 2 ml of hexane and then vortexed again for 1 min. This mixture was left to stand for 1 min to allow the phases to separate. The upper phase (hexane) was discarded and lower phase was taken to dryness using a speed vac. The dried lower phase was then resuspended in 100µl of 75% methanol and 25% 10mM ammonium acetate (NH_4OAc). For LC/MS analyses, free fatty acids were eluted using a solvent gradient of 100% solvent A (10mM NH_4OAc) in pH 4.5 in 40% of 33% methanol (MeOH) in acetonitrile (ACN) and solvent B (33% MeOH in ACN) at 200µl/min using a 2.1mm x 3µM Kinetix column packed with 2.6 µm C18 particles (Phenomenex) maintained at 25°C. The gradient was maintained at 100% solvent A for 2 min. From 2-12.5 min a linear gradient was run to 70% B and then to 82% B from 12.5 min to 18 min. A reverse gradient to initial conditions was then run over the next 6 min. As above, LC/MS analyses were performed using a Thermo LTQ linear ion trap mass spectrometer. Full scan negative ion mode was used to quantify FFA. LC/MS/MS was performed for monitoring 2AG, where the m/z 379 MH^+ precursor ion was isolated using an isolation width of 2.7 with CE of 25V applied. The m/z 287.3 product ion was used to monitor 2AG. Similarly, LC/MS/MS was performed for monitoring the 15-(S)HETE-$_{d8}$ internal standard; m/z 327 was used for isolating product ion 227 using the same isolation width and CE as above. The total peak area of each analyte of interest was divided by the peak area for the IS for quantification. MLM regression was used for statistical analyses as described above for LC/MS.

4.3. Results

4.3.1. General lipidomics strategy

Figure 4.3 displays a chromatogram from an LC/MS run showing individual peaks for each PC, SM, PI, PE, LPE, and LPC subclasses of PL. As described in the methods

section, m/z values corresponding to the fragment ions from each head-group were used to locate peaks for each PL class on the chromatogram. Use of m/z 184 (the phosphocholine fragment ion produced by SCID) in the positive ion mode assisted with identifying the PC, SM and LPC peaks. Similarly, PE and LPE were located on the chromatogram using m/z 140 for phosphoethanolamine fragment ion. Phosphatidylinositols were identified using the m/z 241 phosphoinositol fragment ion. Figure 4.4A shows a spectrum of PC in the positive ion mode. This figure demonstrates that all PC molecular species in a run can be visualized on the chromatogram using m/z 184. Figure 4.4B shows that the use of SCID in the negative ionization mode yields a m/z 168 for the head-group of PC and provides additional information about the fatty acid composition of individual PC molecular species. This strategy facilitates localization of each PL class peak on the chromatogram and assists

SCID LC/MS lipidomic analysis

Figure 4.3

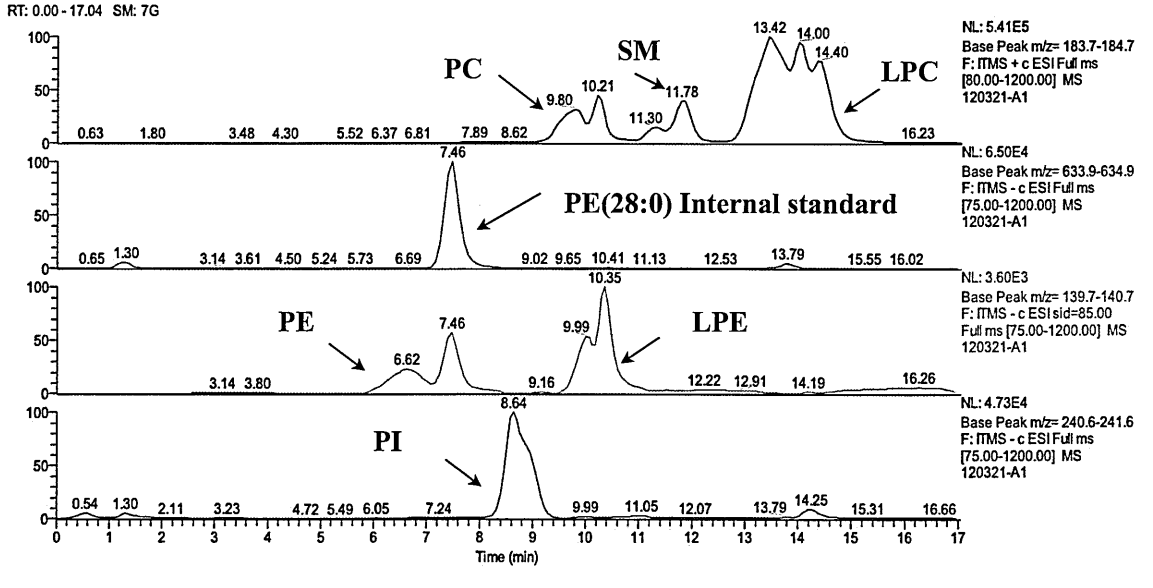

Figure 4.3. Schematics of LC/MS lipidomics approach: A chromatogram of a LC/MS run showing PL identified in both the negative and positive ionization mode. In the top panel, all three phosphocholine moiety containing lipids, PC, SM, and LPC, were localized with m/z 184 on the chromatogram in the positive ionization mode. Similarly, PE and LPE peaks (3rd panel from the top) were localized using m/z 140 in the negative ionization mode. In the last panel, the PI peak was localized on the chromatogram using m/z 241 in the negative ionization mode.

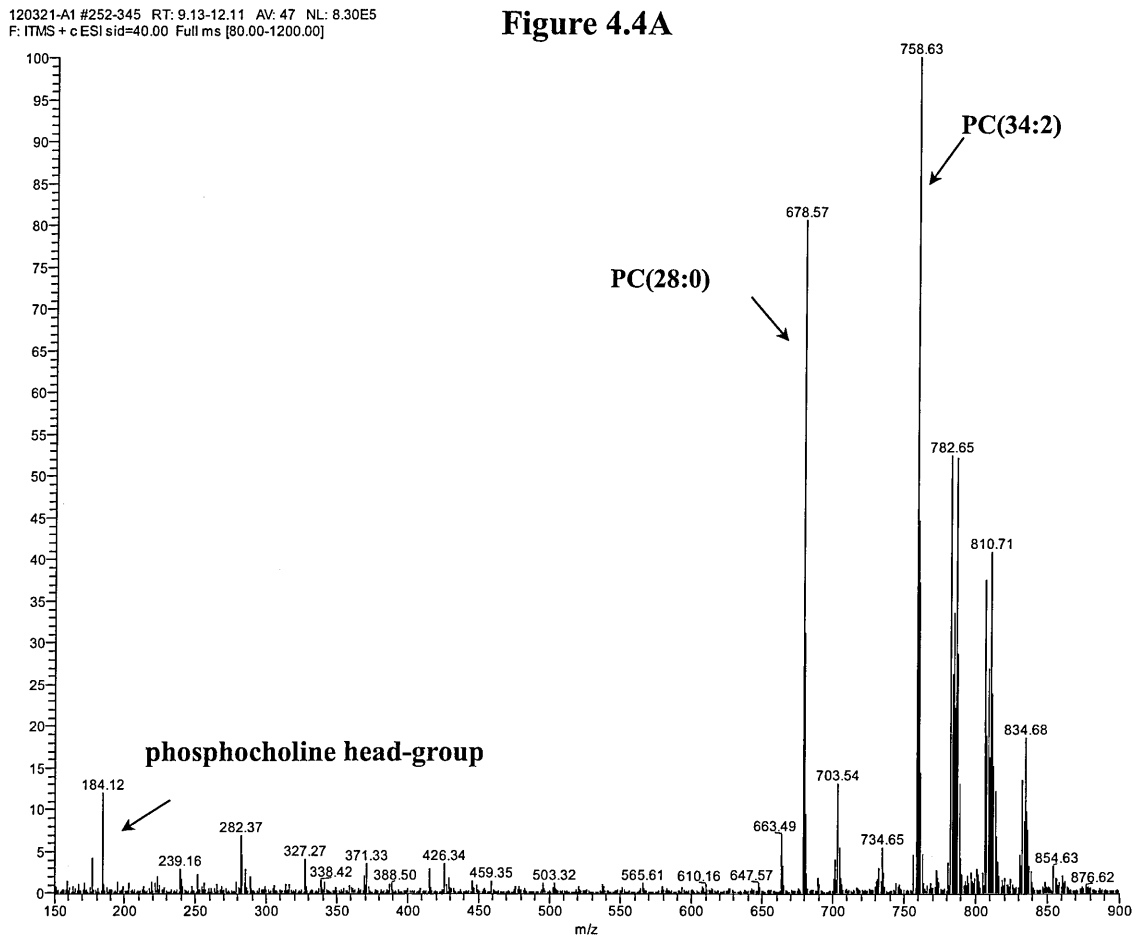

Figure 4.4B

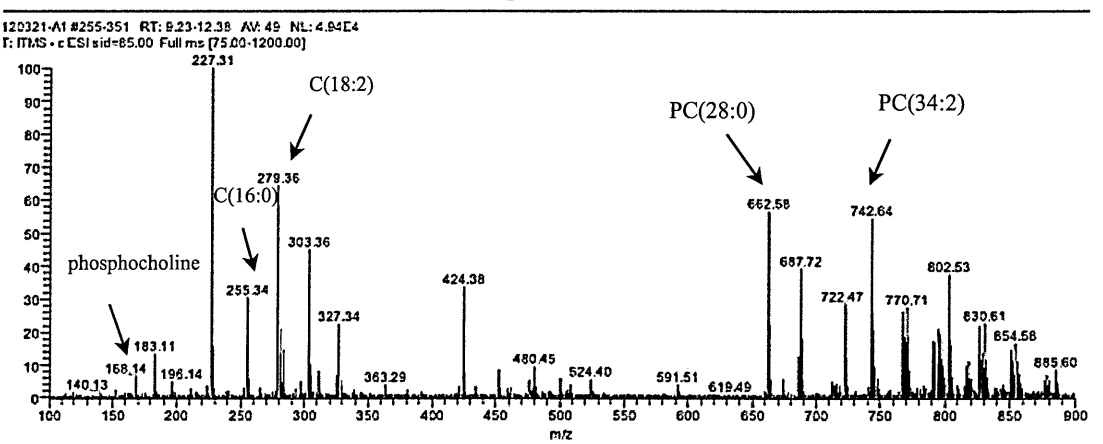

Figure 4.4. Schematics of LC/MS lipidomics approach: (A) MS spectra summed over the chromatogram in positive ionization scanning mode. Detection of PC and SM was facilitated using SCID to generate fragment ion m/z 184, corresponding to the phosphocholine head-group. The m/z 678.5 is the [M+H]+ ion for di-14:0 PC. (B) Summed MS spectra in negative ionization mode shows that SCID fragmentation can help distinguish between different subspecies of PC. The ePC(34:2) molecular species with $[M-15]^-$ m/z 742.6 contains a fatty acid (FA) C18:2 corresponding to m/z 279.4 and FA C16:0 with $[M-15]^-$ m/z 255.4.

with the identification of individual molecular species prior to performing an in-depth characterization using LC/MS/MS approach.

4.3.2. Profiling of brain PC and SM from model A of GW agent exposure:

Brain lipids from mouse model A exposed (n = 5 [3F, 2M]) and control (n = 5 [3F, 2M]) were analyzed using a multivariate approach of PCA, which isolated 7 components, of which component 1 accounted for 41% of the total variance in the dataset and component 2 accounted for 23% of the variance. Based on MLM regression analyses, component 2 was significantly associated with GW agent exposure ($F_{(1,17)} = 7.8$, $p = 0.01$). Among 18 PC and SM molecular species in component 2, 11 were diacyl PC molecular species, 2 were very-long chain fatty acid (VLCFA > 22 carbons) containing SM and 5 were ePC, of which 1 contained SFA and the remaining 4 contained MUFA. Figure 4.5 shows all PC and SM species detected and those that were specific to component 2. Additional univariate analyses were performed, focusing on molecular species that were in component 2. Univariate analyses support PCA analysis as ePC(34:0), ePC(36:2), ePC(36:1), one diacyl PC(36:0) and PC(40:4), all factors of component 2, were significantly elevated in exposed compared to control mice. Figure 4.4 also shows an increase of a 24:0 dihydrosphingomyelin (DSM) in exposed mice compared to control mice. Figure 4.6 shows that among significantly modulated PC species, those containing MUFA were more abundant compared to those with SFA or PUFA. Identifications of PC molecular species associated with GW agent exposure for this model is presented in Table 4.1 on page 143.

4.3.3. Profiling of brain PC and SM from model B of GW agent exposure

In mouse model B of GW agent exposure (n = 4 GW agent exposed and n = 4 controls), a different PC and SM profile was observed from that seen in model A. Total PC ($F_{(1,13)} = 7.87$, $p = 0.02$) and total SM ($F_{(1,13)} = 7.57$, $p = 0.02$) were significantly increased in the brain of exposed mice compared to control mice, see Figures 4.7A and B.

Mouse model A of GW agent exposure

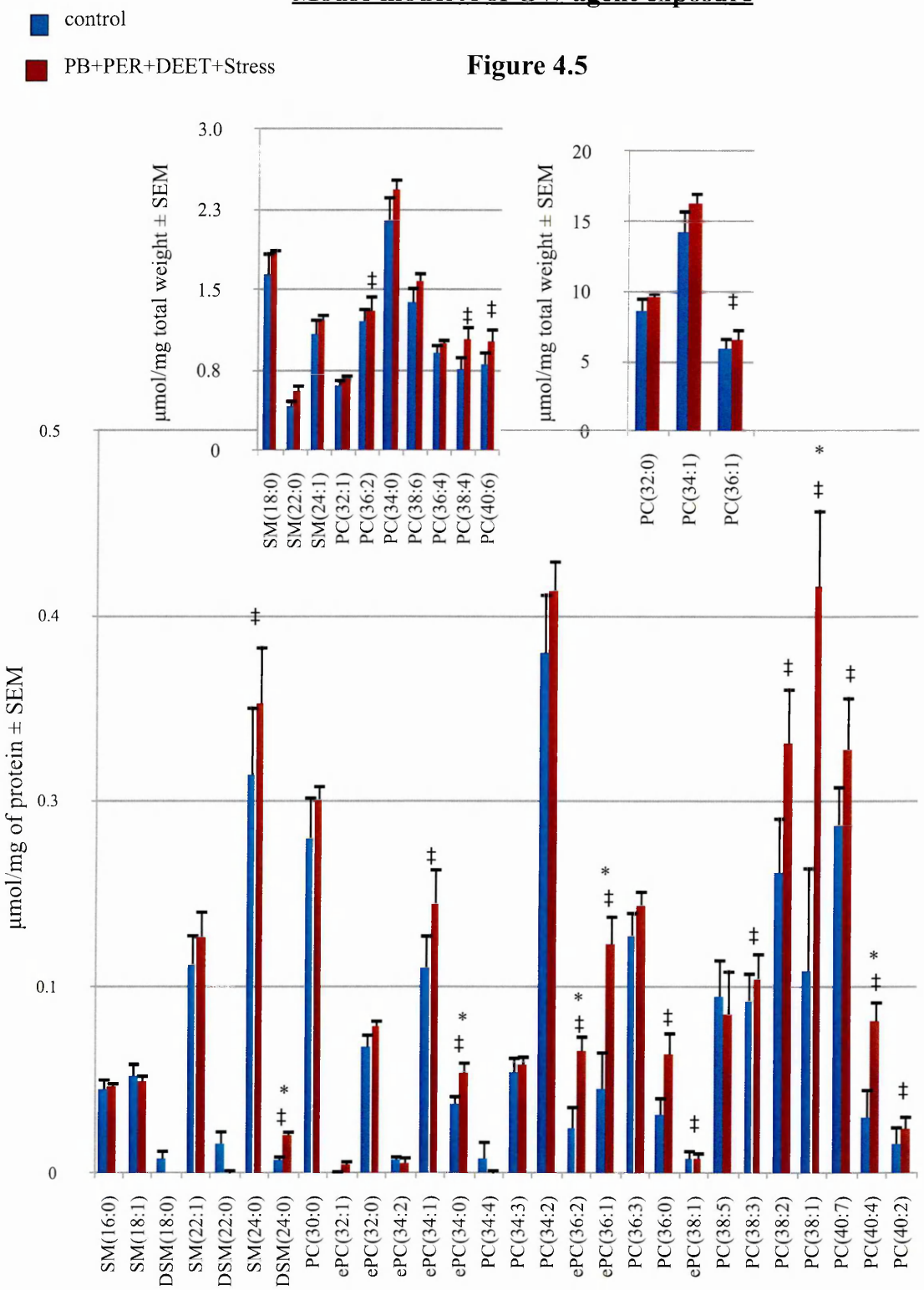

Figure 4.5

Figure 4.5. Brain phospholipid changes for mouse model A of GW agent exposure: Mean ± SEM (n = 5 per group) of all of the PC and SM molecular species identified during the LC/MS analysis and those denoted by ‡ were associated with component 2. Within component 2, univariate MLM analyses showed that ether PC: ePC(34:0), ePC(36:2), ePC(36:1) were significantly higher in the exposed mice than in the controls. Species with LCFA, PC(38:1) and PC(40:4) were also elevated in exposed mice compared to controls, *denotes $p < 0.05$ for a main exposure effect. PC(38:4) was marginally elevated in exposed vs. control, $p = 0.08$. A VLCFA containing DSM (24:0) was also significantly elevated in exposed mice vs. controls, *denotes $p < 0.05$ for the main exposure effect. Inserts contain lipids with different concentrations than those shown in the main image.

Degree of unsaturation of brain PC for mouse model A of GW agent exposure

Figure 4.6

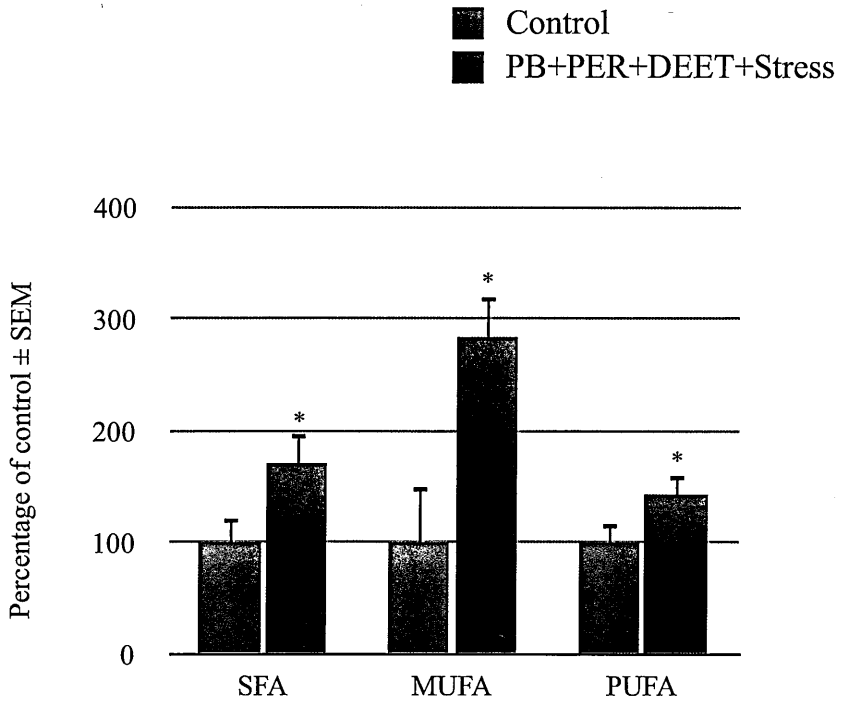

Figure 4.6. Degree of unsaturation of brain PC molecular species for mouse model A of GW agent exposure: Mean ± SEM (n = 5 per group) presented as percentage of control. Figure shows that among significantly modulated PC molecular species, MUFA containing PC were nearly 300% relative to controls, SFA containing species were 170% and PUFA were 143% in exposed relative to control animals, *denotes $p < 0.05$ for a main exposure effect (based on MLM where exposure was included as a fixed main factor).

Multivariate PCA showed that component 1 explained 44% of the variance, component 2 explained 21% of the variance and component 3 explained 14% of the variance. Collectively, these three components explained the largest total variance within the data. Of these, component 3 was significantly associated with the exposure ($F_{(1,10)} = 16.2$ $p = 0.002$). Figure 4.8 shows the individual molecular species and demonstrates that most PC molecular species were increased in GW agent exposed mice compared to control mice. For component 3, although both diacyl and ePC were increased in exposed mice compared to controls, those with diacyl side chains were greatly affected, where 9 diacyl PCs were elevated but only 1 ePC was elevated. In addition, PC molecular species with long chain fatty acids (LCFA; 14-20 carbons) appeared to be affected. Figure 4.8 shows distribution

of individual SM molecular species; none of the SM species were part of component 3. Examination of degree of unsaturation status of PC molecular species showed that molecular species containing SFA ($F_{(1,13)} = 4.5$ $p = 0.06$), MUFA ($F_{(1,10)} = 7.4$ $p = 0.02$) and PUFA ($F_{(1,12)} = 16.2$ $p = 0.002$) were all similarly increased in exposed animals relative to controls (Figure 4.9).

Mouse model B of GW agent exposure

Figure 4.7A

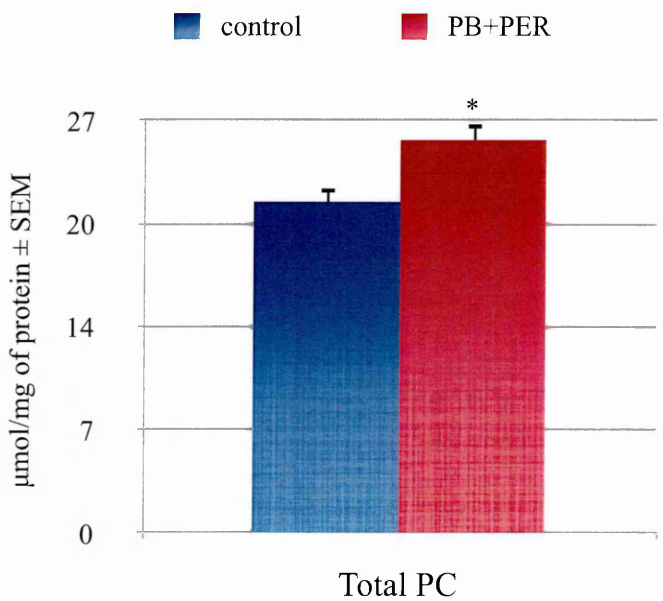

Total PC

Figure 4.7B

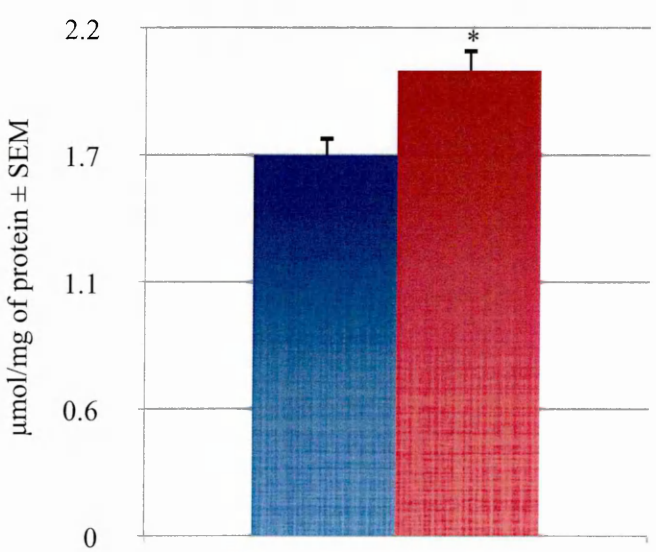

Total SM

Figure 4.7. Total brain PC and SM for mouse model B of GW agent exposure: Mean ± SEM of PC and SM in exposed (n = 4) and control mice (n = 4) for mouse model B of GW agent exposure. Individual molecular species of PC and SM identified by LC/MS were summed after lipidome DB analyses to generate total PC and total SM levels, respectively. (A) A nearly 1.20 fold increase in total PC was noted in exposed mice in model B compared to control mice, *denotes $p < 0.05$ for a main exposure effect (based on MLM where exposure was included as a fixed main factor). (B) For total SM, a 1.22 fold increase was observed in exposed animals compared to controls, *denotes $p < 0.05$ (based on MLM analyses as described above for A).

Mouse model B of GW agent exposure

Figure 4.8

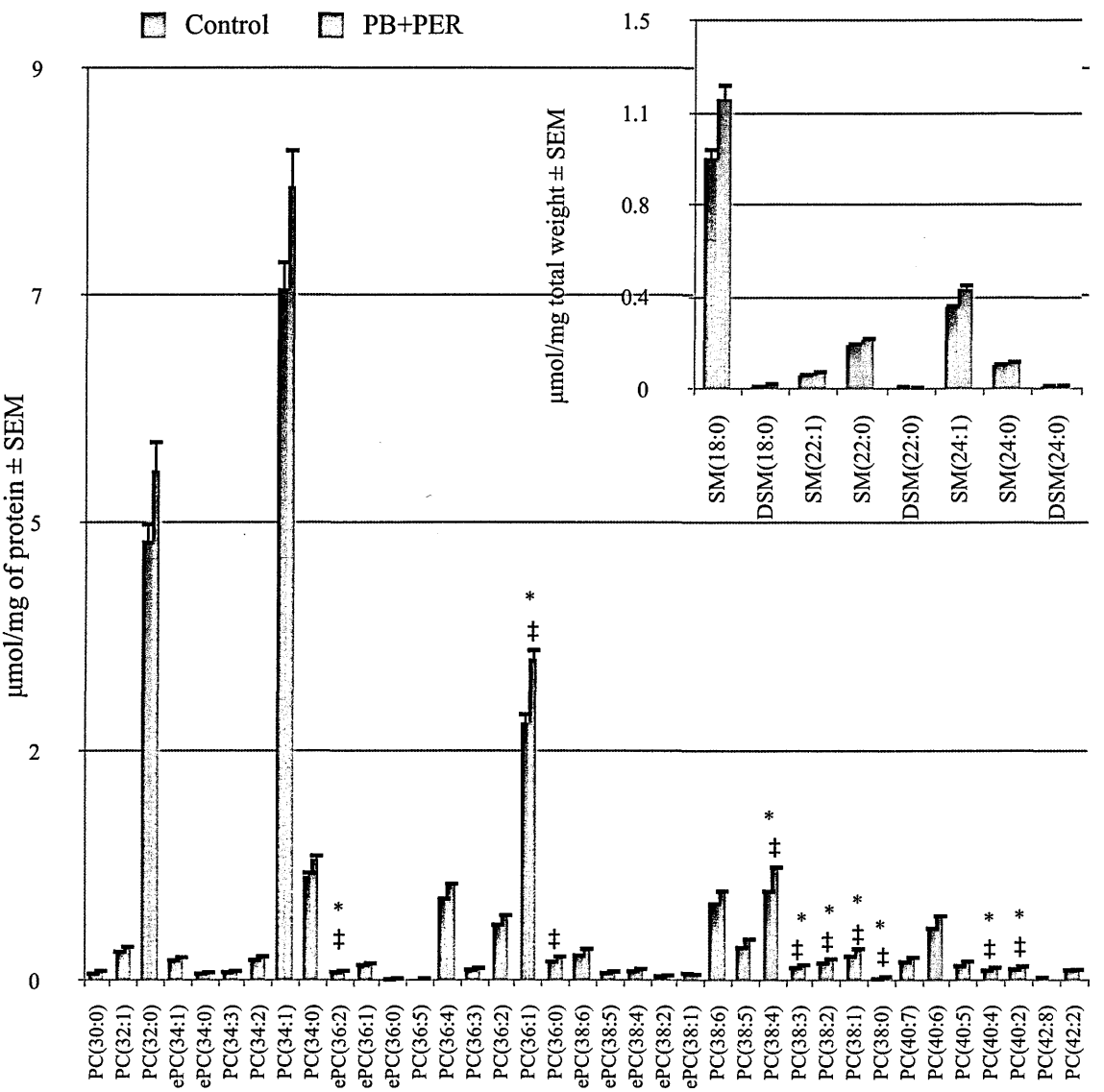

Figure 4.8. Brain phospholipid changes for mouse model B of GW agent exposure: Mean ± SEM (n = 4 per group) of all of the PC and SM molecular species identified by LC/MS analysis; those denoted by ‡ were associated with component 3. (A) Univariate analyses show that all molecular species in component 3 (indicated using asterisks) were significantly different between exposed and control animals, *denotes $p < 0.05$ for a main exposure effect (based on MLM where exposure was included as a fixed main factor). (B) Although SM(18:0) and SM(24:1) were also increased in response to GW agent exposure, none of the SM species were associated with component 3. Insert contains lipids with different concentrations than those shown in the main image.

Degree of unsaturation of brain PC for mouse model B of GW agent exposure

Figure 4.9

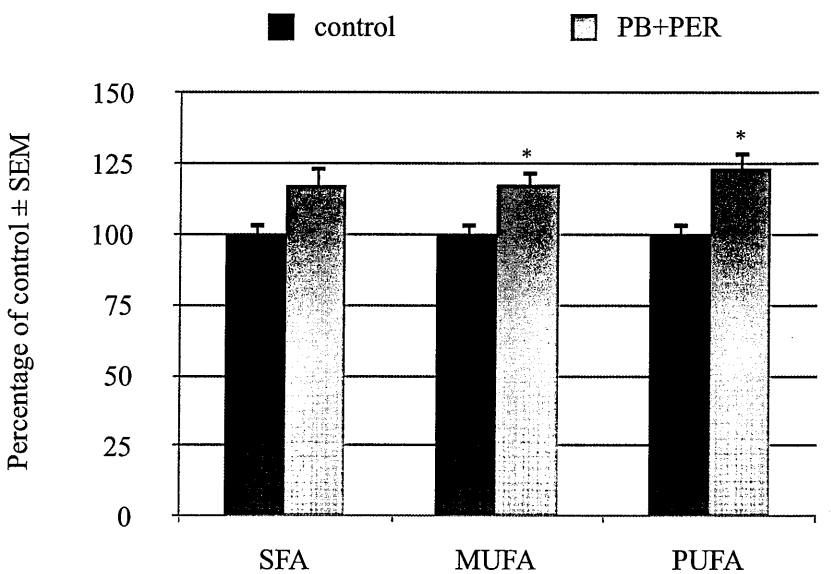

Figure 4.9. Degree of unsaturation of brain PC molecular species for mouse model B of GW agent exposure: Mean ± SEM (n = 4 per group) presented as percentage of control. The figure represents percent SFA, MUFA and PUFA containing PC molecular species exposed relative to control. Phosphatidylcholine containing SFA and MUFA were nearly 117% relative to controls and PUFA containing PC molecular species were 123% relative to controls in exposed mice compared to controls in mouse model B. *denotes $p < 0.05$ for a main exposure effect (based on MLM where exposure was a fixed main factor).

4.3.4. Profiling of brain PC and SM from the PSAPPswe mouse model

Brain lipid extracts from 6-month old PSAPPswe mice (n = 5, [3F, 2M]) and wild-type mice (n = 5, [2M, 3F]) were examined to compare PC and SM profiles in order to determine if detected changes are similar to those observed in mouse models of GW agent exposure. Total PC levels were decreased in PSAPPswe mice compared to wild-type mice, but the differences were not significant ($F_{(1,24)} = 2.8$, $p = 0.1$, Figure 4.10A). Similarly, total SM levels were lower in PSAPPswe mice compared to wild-type mice ($F_{(1,24)} = 2.6$, $p = 0.1$, Figure 4.10B). Figures 4.11 and 4.12 show individual PC and SM molecular species. Univariate analyses showed that a number of PC and SM molecular species were lower but PCA analyses did not reveal a particular underlying pattern in the dataset that was associated with PSAPPswe status. Examination of degree of unsaturation showed that

compared to control mice, PC molecular species with SFA were reduced by 16% ($F_{(1,25)}$ = 6.3, p = 0.02), MUFA ($F_{(1, 24)}$ = 3.3, p = 0.08) were marginally reduced and PUFA ($F_{(1, 23)}$ = 2.7, p = 0.1) were generally similar (Figure 4.13).

4.3.5. Profiling of brain PC and SM from the CCI TBI mouse model

For these studies, lipid extracts from cortex, hippocampus and cerebellum were examined separately at the 3-months post-injury timepoint. For total PC, a significant main injury effect was observed ($F_{(1, 33)}$ = 9.3, p = 0.004) and an effect of brain regions ($F_{(1, 33)}$ = 150, p <0.001) and an interaction between injury and brain regions ($F_{(1, 29)}$ = 24.2, p < 0.001) were observed as well. Similarly, for total SM, there was a main effect of injury ($F_{(1, 34)}$ = 8.4, p = 0.007), a brain region effect ($F_{(1, 32)}$ = 124, p < 0.001) and an interaction between injury and brain regions ($F_{(1, 32)}$ = 20.7, p < 0.001). Figure 4.14 shows that total PC and SM species are modulated in response to CCI TBI at this 3-month post-exposure timepoint, where PC and SM levels are lower in the hippocampi and cerebella and are elevated in the cortices of injured mice compared to sham mice. Figure 4.15 shows an example of a subset of individual molecular species changes with a similar pattern for each

PSAPPswe AD mouse model

Figure 4.10A

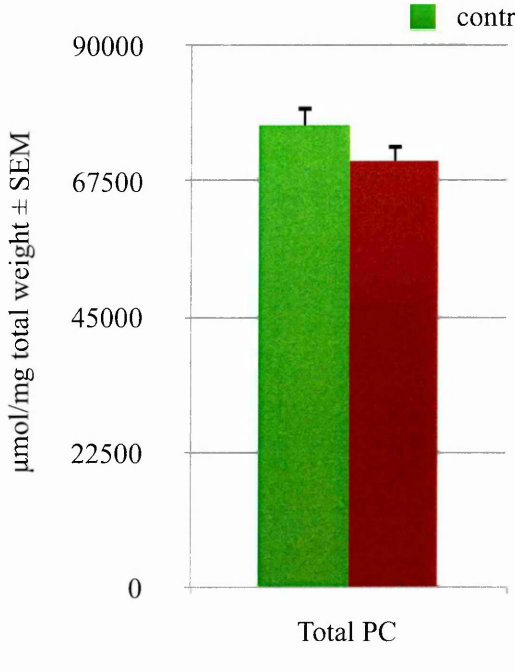

Figure 4.10B

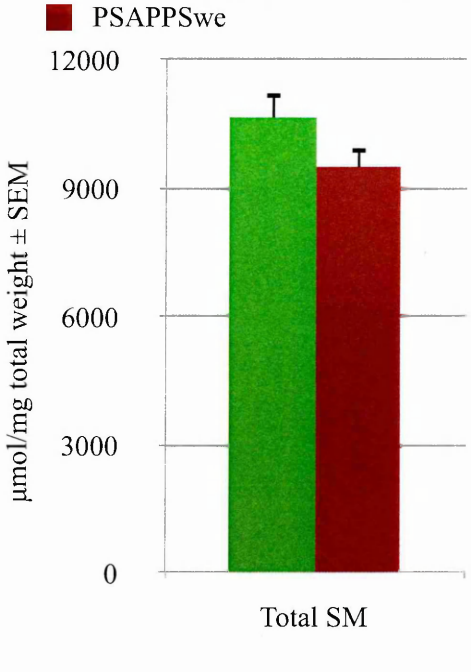

Figure 4.10. Brain total PC and SM for PSAPPswe mouse model of AD: Mean ± SEM of in PSAPPswe (n = 5) and control mice (n = 5). (A) Individual molecular species of PC and identified by LC/MS analyses were summed after lipidome DB analyses to generate total PC and total SM levels, respectively. A nearly 1.08 fold decease in total PC was noted in PSAPPswe compared to control mice. (B) For total SM, a 1.12 fold decrease was observed in PSAPPswe compared to controls, $p > 0.05$.

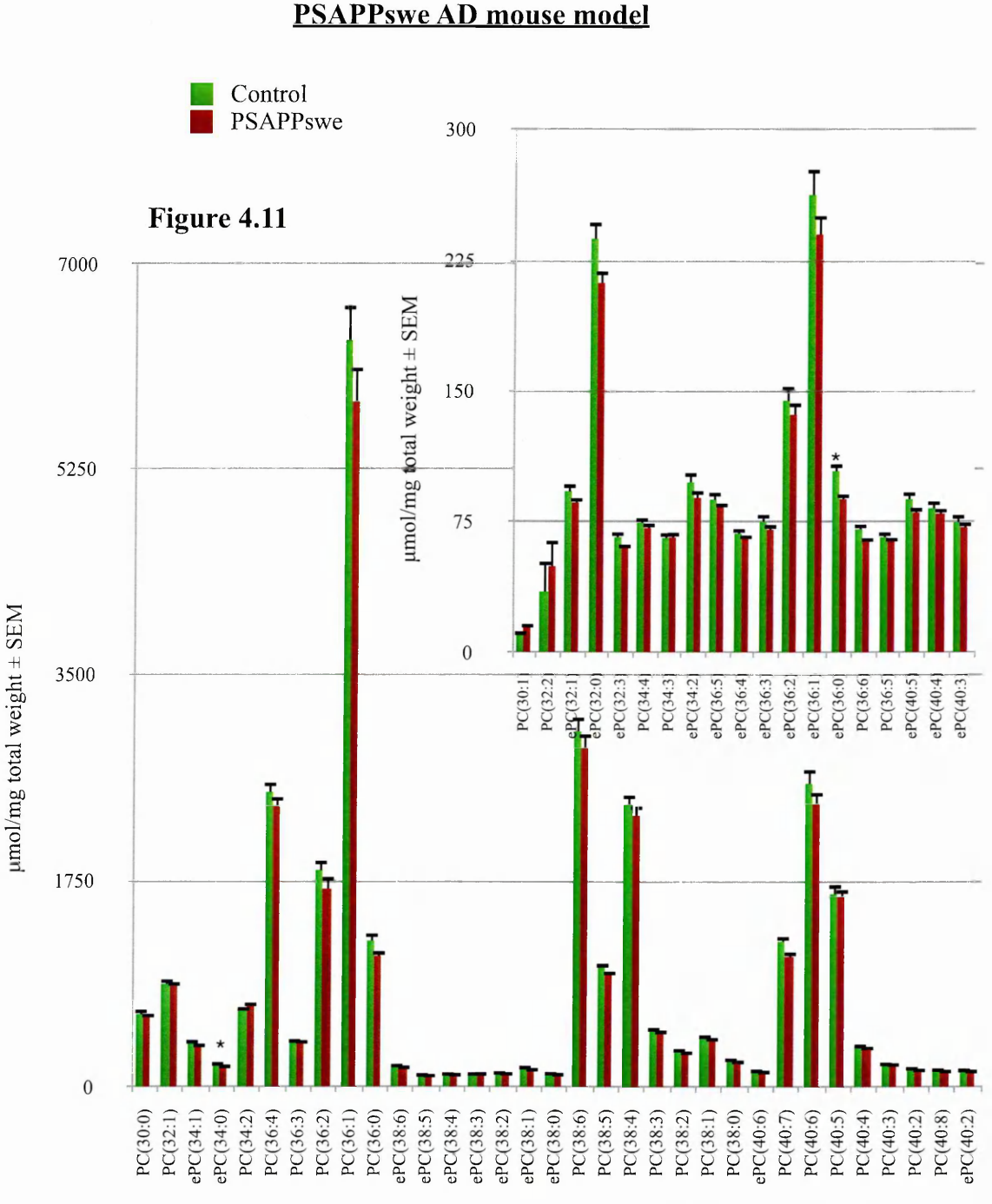

Figure 4.11. Brain phospholipid changes for the PSAPPswe mouse model of AD: Mean ± SEM (n = 5 per group) of all of the lipids identified by LC/MS analyses. ePC32:0, ePC(36:1), ePC(36:0) and ePC(34:0) were significantly lower in PSAPPswe mice compared to control mice, *denotes $p < 0.05$ for a main exposure effect (based on MLM where exposure was a fixed main factor). Insert contains lipids with different concentration than those shown in the main image.

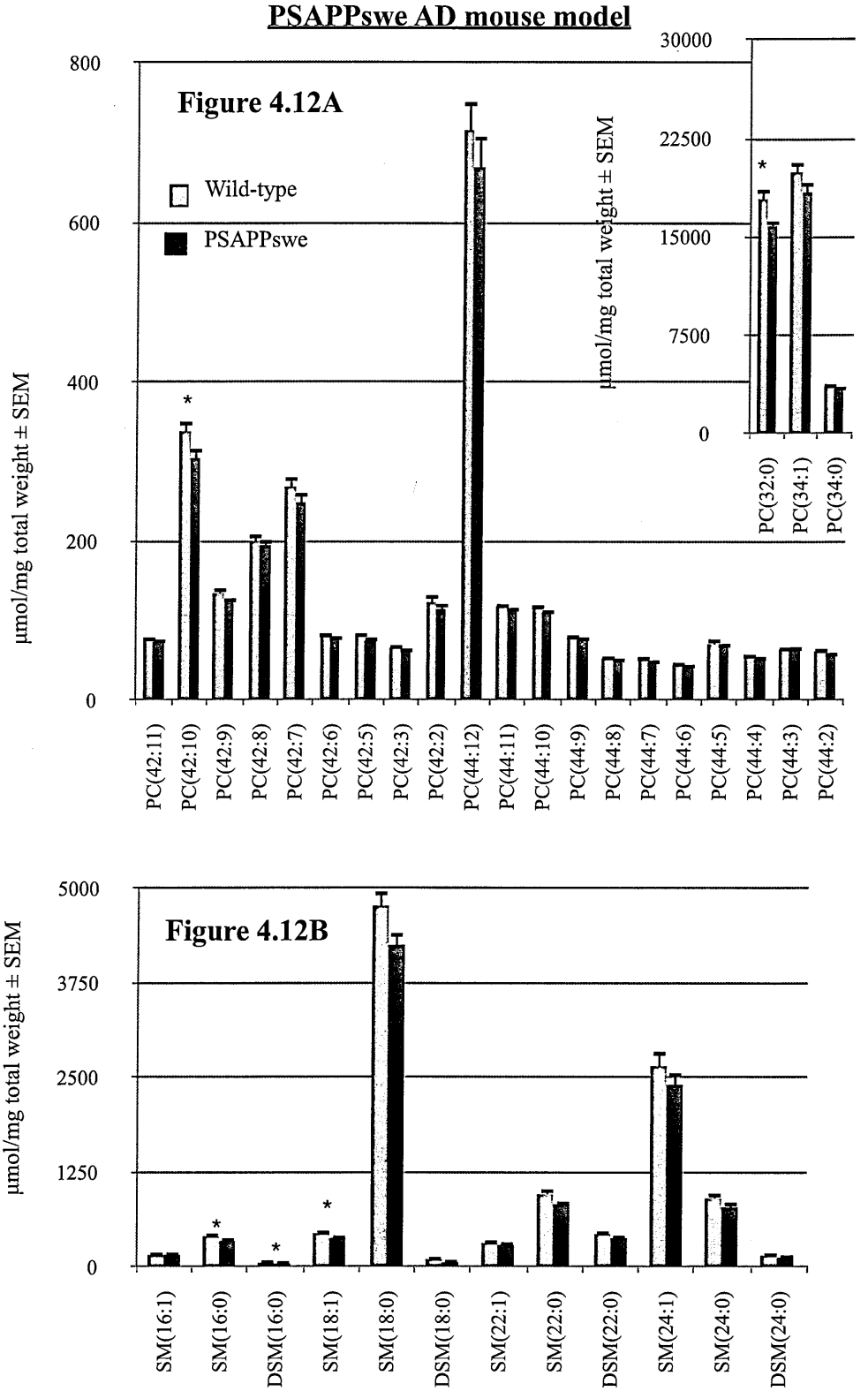

Figure 4.12. Brain phospholipid changes for the PSAPPswe mouse model of AD: Mean ± SEM (n = 5 per group) of all of the lipids identified by LC/MS analyses. (A) PC(32:0) and PC(42:10) and (B) SM(16:0), DSM(16:0), and SM(18:1) were all significantly lower in PSAPPswe mice compared to control mice, *denotes $p < 0.05$ for a main exposure effect (based on MLM where exposure was a fixed main factor). Insert contains lipids with different concentration than those shown in the main image.

Degree of unsaturation of brain PC PSAPPswe AD mouse model

Figure 4.13

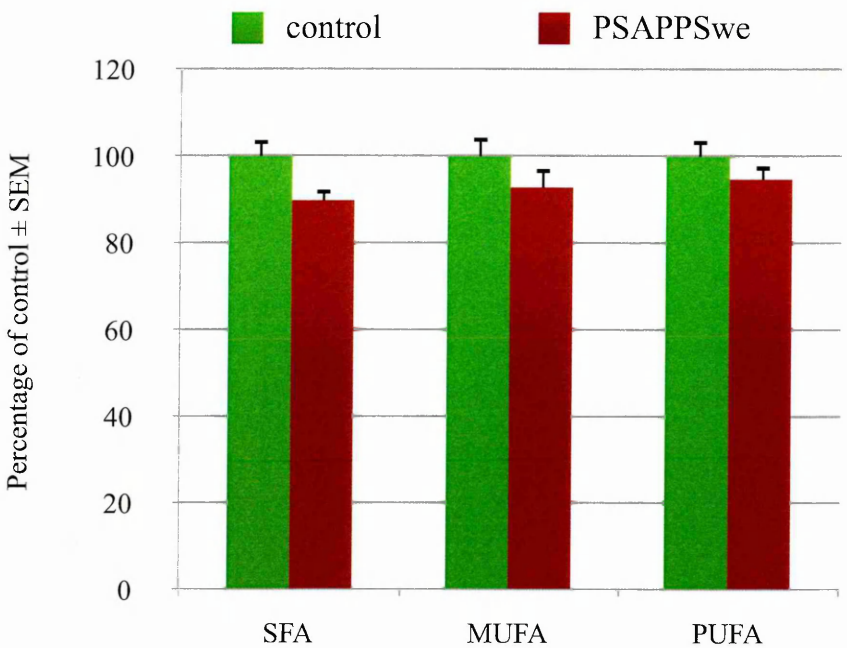

Figure 4.13. Degree of unsaturation status of brain PC for PSAPPswe mouse model of AD: Mean ± SEM (n = 5 per group) presented as percentage of control. Figure shows that SFA, MUFA and PUFA containing species did not differ from wild-type control mice and were generally similar to each other, $p > 0.05$.

CCI TBI mouse model

Figure 4.14A

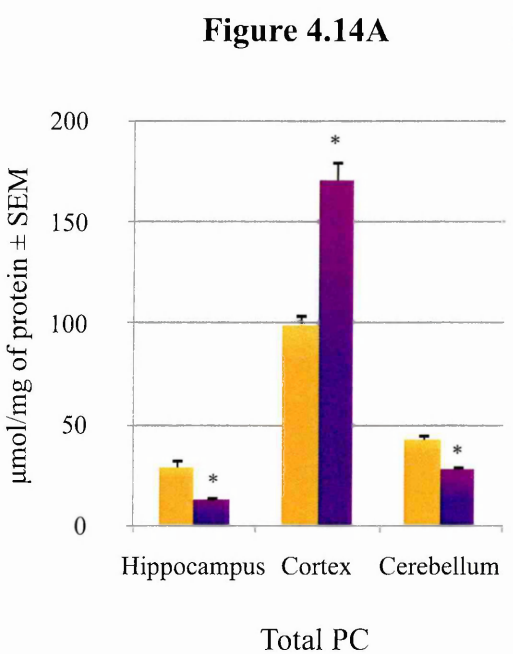

Figure 4.14B

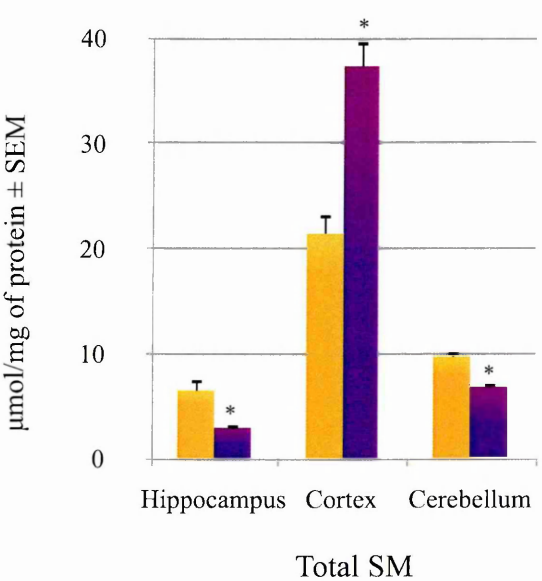

Figure 4.14. Brain total PC and SM for CCI TBI mouse model: Mean ± SEM of in CCI TBI (n = 4) and sham mice (n = 4). Individual PC molecular species identified by LC/MS were summed after lipidome DB analyses to generate total PC and total SM levels, respectively. (A) In the hippocampus and cerebellum, a nearly 2.3 and 1.5 fold decrease, respectively, in total PC was noted in CCI injured mice compared to control mice, $p < 0.05$. In the cortex, a 1.7 fold increase was noted in injured mice compared to sham mice, $p < 0.05$. (B) Similar observations were made for SM, a decrease of about 1.5 and 1.4 was noted respectively in the hippocampi and cerebella of injured mice compared to sham mice, $p < 0.05$. A 1.7 fold increase was again noted for SM in the cortices of injured mice compared to sham mice, *denotes $p < 0.05$ for a main injury effect (based on MLM with injury and region were fixed main factors).

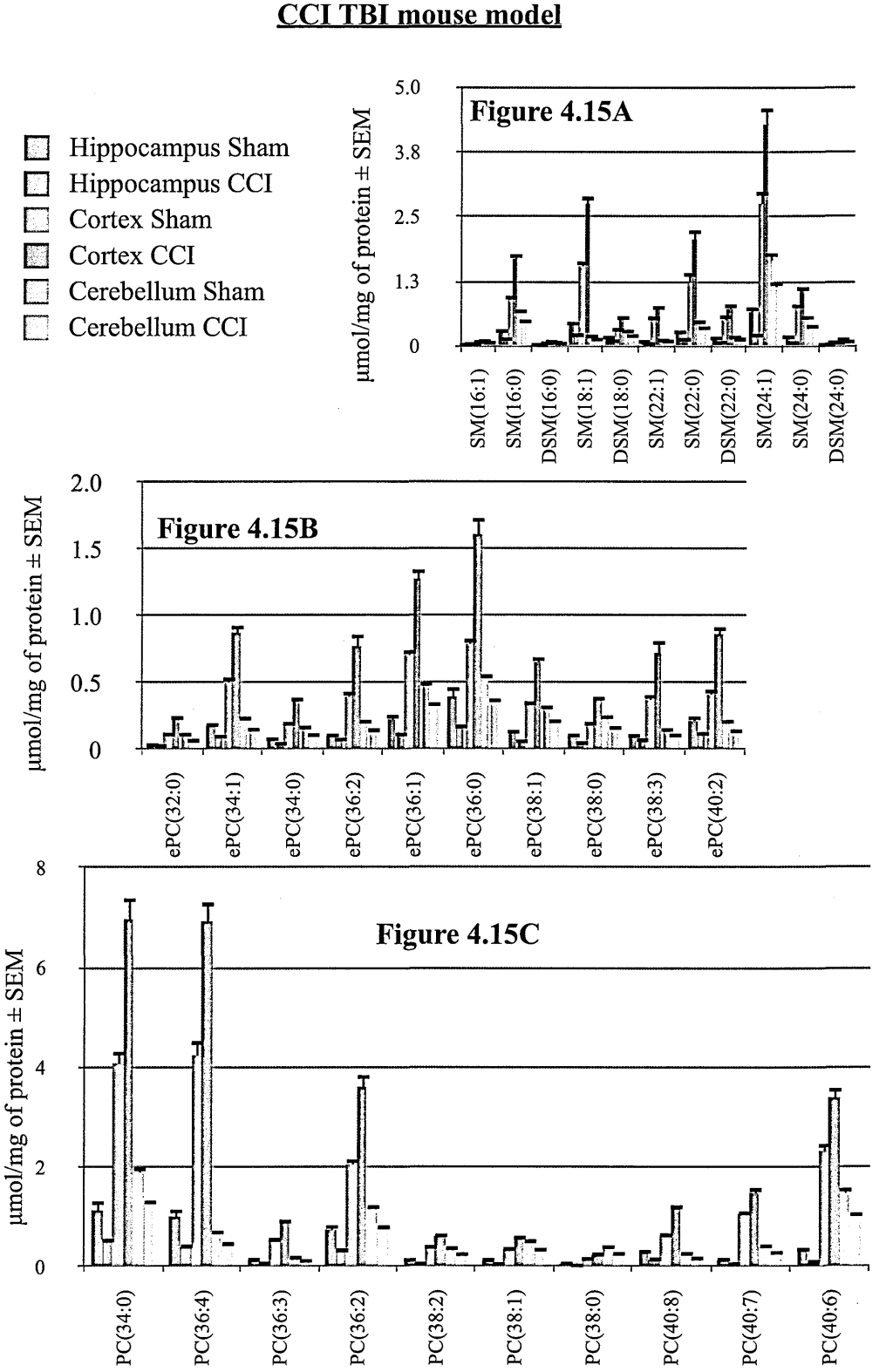

Figure 4.15. A representative image of some of the brain PC and SM molecular species for CCI TBI model: Mean ± SEM (n = 4 per group). (A-C) As in total PC and SM graphs, region specific differences are observed where in the hippocampus, lipid levels are decreased in the TBI group compared to sham mice. However, in the cortex, PC and SM levels are increased in TBI compared to controls. Note, figure is a representative image only and no statistical analyses were performed on individual species given that total PC and SM levels were significant and each species appeared to behave in exactly the same pattern.

Unsaturation status of CCI TBI mouse model

Figure 4.16

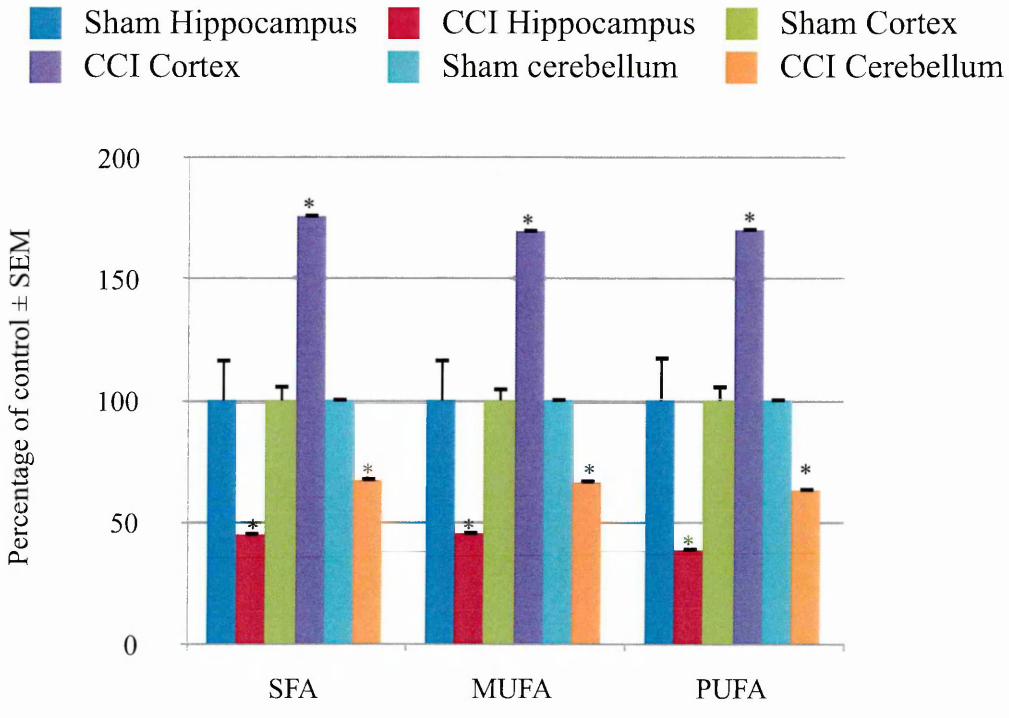

Figure 4.16. Degree of unsaturation of brain PC for the CCI TBI mouse model: Mean ± SEM (n = 4 per group) presented as percentage in CCI injured mice relative to sham mice. Within the hippocampus SFA were 45%, MUFA were 45% and PUFA were 39% in injured mice relative to controls. Within the cortex, SFA were 176%, MUFA were 170% and PUFA were 170% in injured mice relative to controls. In the cerebellum, SFA were 67%, MUFA were 67% and PUFA were 63% in injured mice relative to controls, *denotes $p < 0.05$ for a main injury effect (based on MLM with exposure and brain regions were fixed main factors).

lipid species within each brain region as that observed for total PC and SM. Examination of the degree of unsaturation of PC molecular species did not show any differential changes after injury where SFA, MUFA and PUFA were equally lowered in the hippocampi and the cerebella but were increased in the cortices of injured mice compared to sham mice, see Figure 4.16.

4.3.6. Profiling of plasma PC and SM from mouse model A of GW agent exposure:

Plasma PC and SM from model A were examined to determine if changes in their levels could serve as biomarkers of GW agent exposure (n = 4 exposed and n = 4 controls). As was observed in the brain tissue samples, total PC levels did not differ between exposed and control animals ($F_{(1, 22)} = 2.5$, = 0.1). Total levels of SM individual molecular species were elevated in exposed animals compared to controls ($F_{(1,19)} = 7.92$, $p = 0.01$). Figure

Plasma lipidomics of mouse model A of GW agent exposure

Figure 4.17

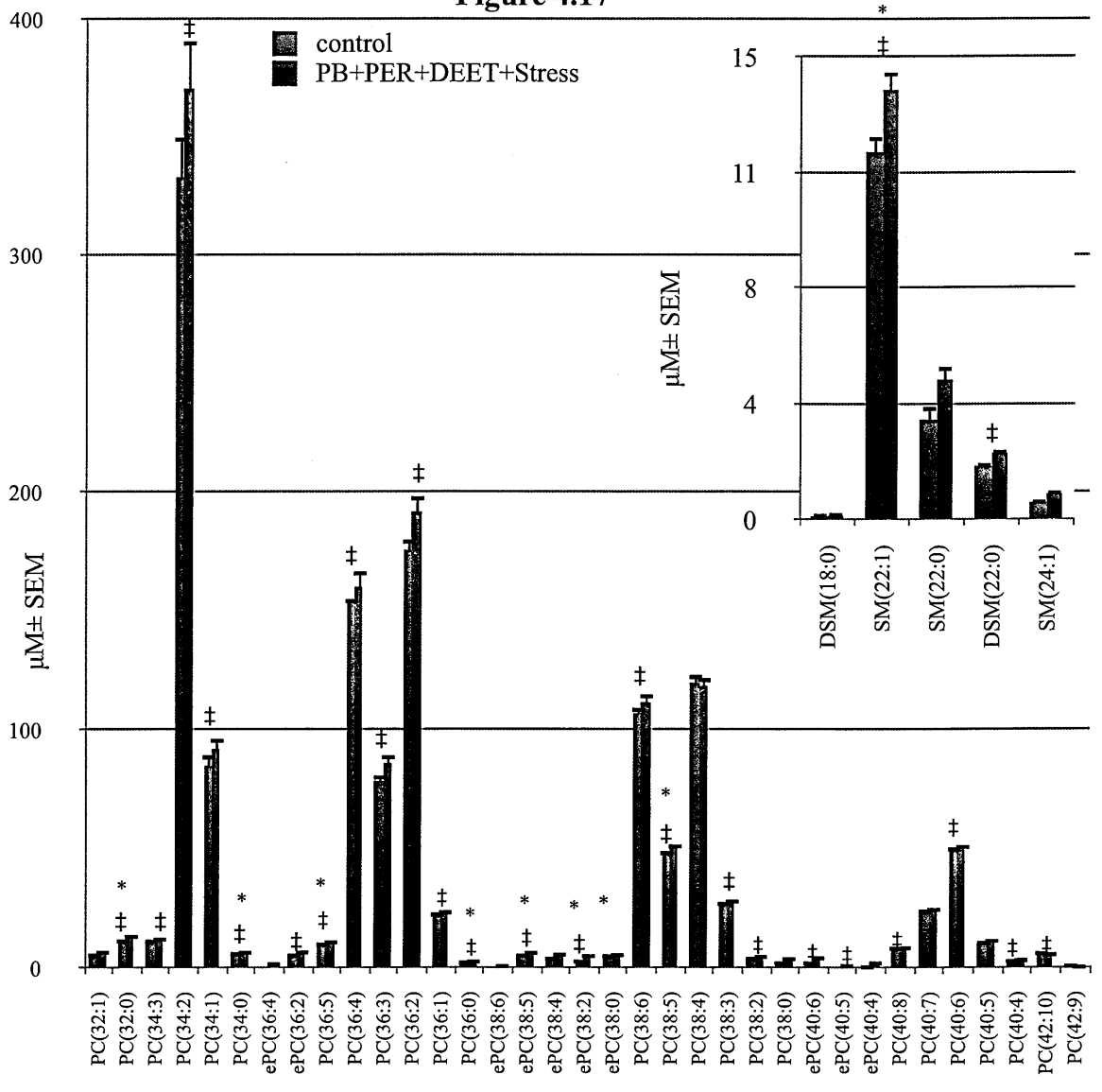

Figure 4.17. Plasma PC and SM changes for mouse model A of GW agent exposure: Mean ± SEM (n =4 per group) of all of the PC and SM identified by LC/MS analyses. Note, ‡ denotes those species that were associated with component 1 from PCA. Univariate analyses of species from component 1 show that PC(32:0), PC(34:0), ePC(36:2), SM(22:1), PC(36:0), ePC(38:5), ePC(38:2), ePC(38:0), and PC(38:5) were significantly different between PB+PER+DEET +Stress and control mice, *denotes $p < 0.05$ for a main exposure effect (based on MLM where exposure was a fixed main factor). Insert contains lipids with different concentration than those shown in the main image.

4.17 shows all individual PC and SM molecular species that were identified in this experiment. A data reduction strategy using PCA suggested that component 1 explained the largest variance, 39% and was associated with GW agent exposure in model A ($F_{(1, 21)}$ = 5.0, p = 0.04). Examination of the degree of unsaturation of individual PC molecular species revealed that SFA ($F_{(1, 20)}$ = 20.7, p < 0.001) containing PC molecular species were significantly elevated but MUFA ($F_{(1, 23)}$ =1.05, p = 0.32) and PUFA ($F_{(1, 22)}$ = 2.1, p = 0.2) containing PC species were similar between exposed and control animals, see Figure 4.18.

Degree of unsaturation of plasma PC for mouse model A of GW agent exposure

Figure 4.18

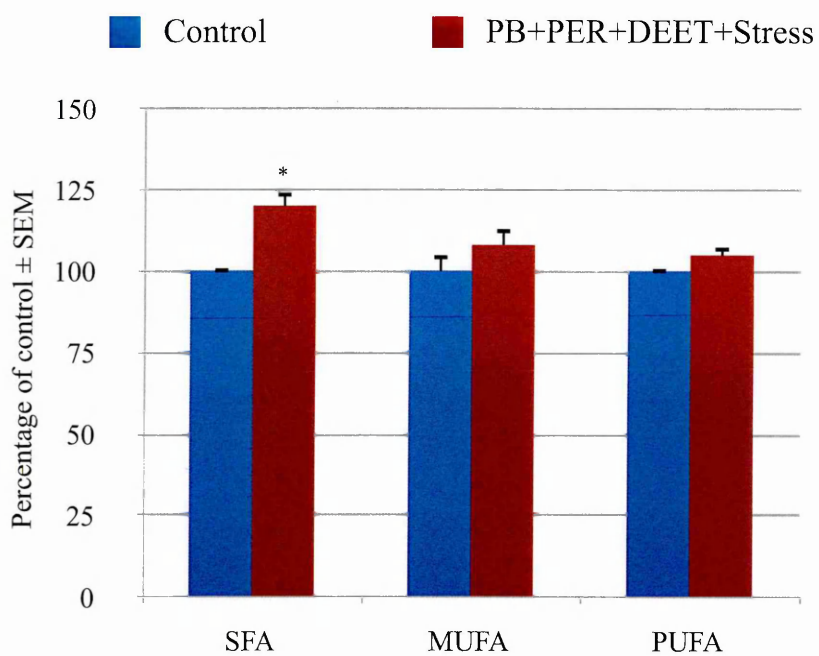

Figure 4.18. Degree of unsaturation status of plasma PC for mouse model A of GW agent exposure: Mean ± SEM (n = 4 per group) presented as percentage in exposed relative to control showing that SFA containing species were 120% MUFA were 108% and PUFA containing species were 105% in plasma of exposed mice relative to controls, * denotes p < 0.05 for a main exposure effect (based on MLM where exposure was a fixed main factor).

4.3.7. Profiling of plasma PC and SM from mouse model B of GW agent exposure

As in model A of GW agent exposure above, lipidomic profiling was performed to determine if plasma PC and SM changes can serve as biomarkers of GW agent exposure (n = 4 GW agent, n = 4 control). There were no significant differences between exposed and

Plasma lipidomics of mouse model B of GW agent exposure

Figure 4.19

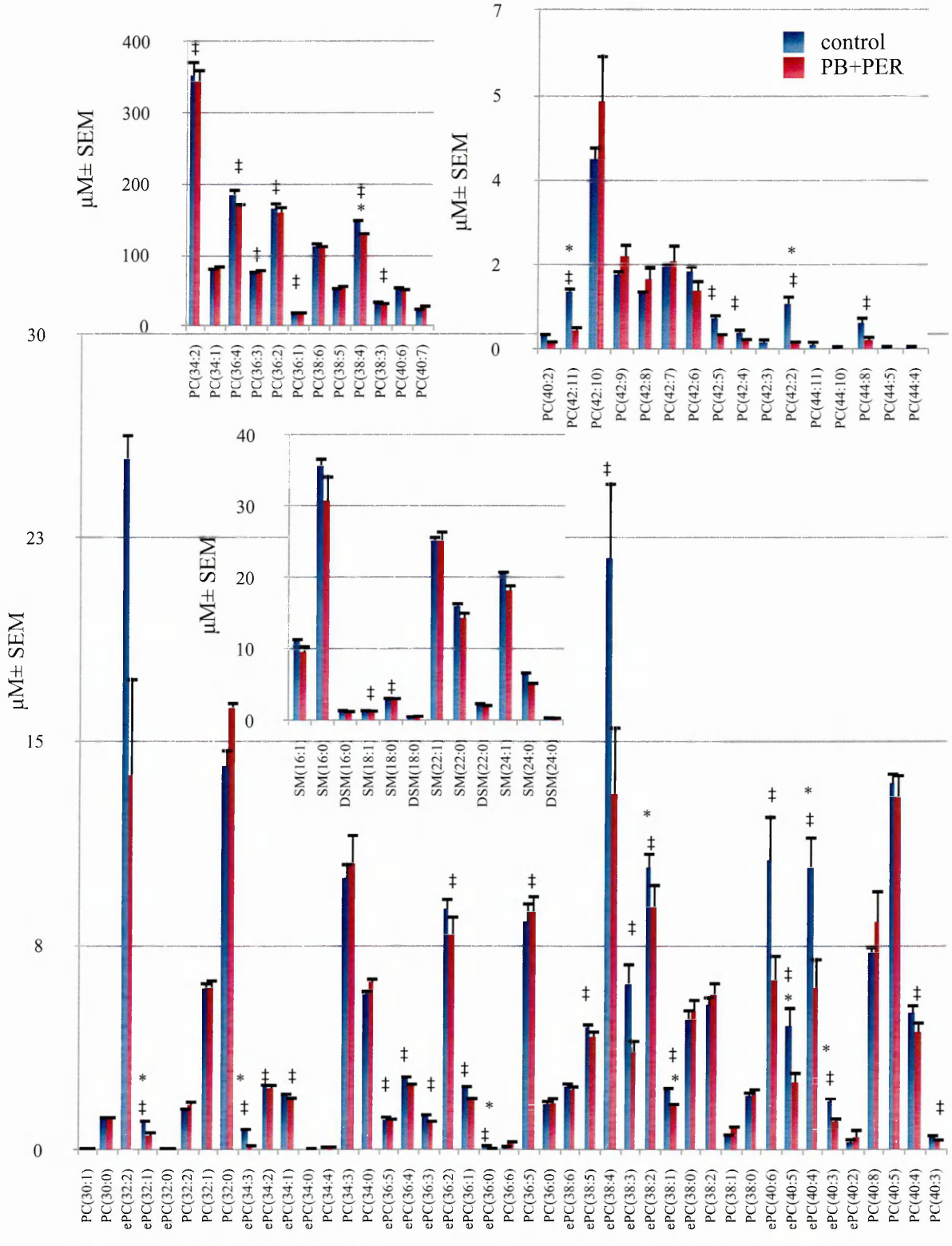

Figure 4.19. Plasma PC and SM changes for mouse model B of GW agent exposure: Mean ± SEM (n = 4 per group) of all of the PC and SM identified by LC/MS analyses. Note, symbol ‡ denote those species that were associated with component 1 from PCA. Univariate analyses of species from component 1 show that ePC(32:1), ePC(34:3), ePC(36:1), ePC(36:0), ePC(38:2), ePC(38:1), PC(38:4), ePC(40:5), ePC(40:4), ePC(40:3), PC(42:11), PC(42:2) and PC(44:8) were significantly different between PB+PER and control mice, *denotes $p < 0.05$ for a main exposure effect (based on MLM where exposure was a fixed main factor). Inserts contain lipids that have different concentration than that in the main figure.

Degree of unsaturation of plasma PC of mouse model B for GW agent exposure

Figure 4.20

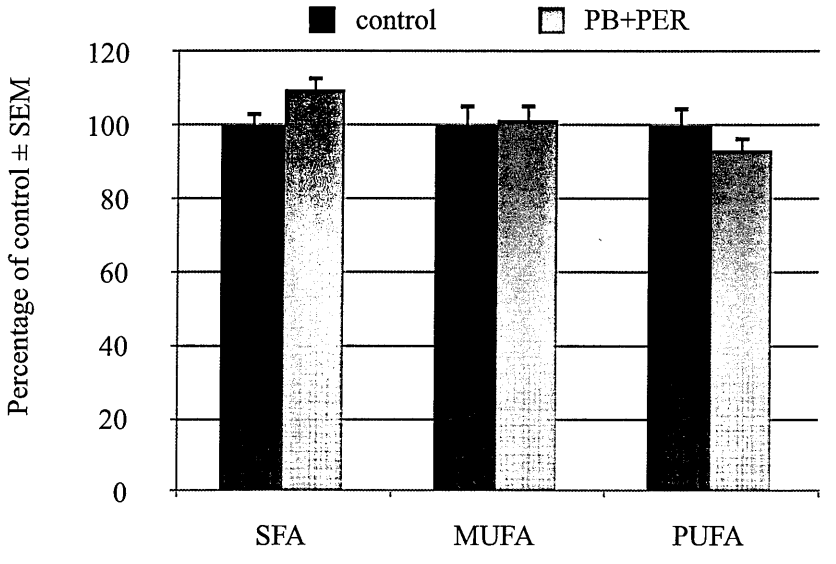

Figure 4.20. Degree of unsaturation of plasma PC for mouse model B of GW agent exposure: Mean ± SEM (n = 4 per group) presented as percentage in exposed relative to control showing that molecular species containing SFA were 109%, MUFA were 101% and PUFA were 93% in exposed mice relative to controls, $p > 0.05$.

control mice either for total PC ($F_{(1, 15)} = 0.026$, $p = 0.9$) or total SM levels ($F_{(1, 16)} = 1.13$, $p = 0.3$). The multivariate approach of using PCA showed that component 1 explained 30.1 % of variance in the dataset and was associated with GW agent exposure in this model ($F_{(1, 13)} = 7.25$, $p = 0.02$). Figure 4.19 shows individual PC and SM species and those that were specific to PCA component 1. There was also a marginal effect of degree of unsaturation, where SFA containing PC molecular species were marginally increased in exposed mice compared to controls ($F_{(1, 14)} = 3.9$, $p = 0.07$). However, MUFA ($F_{(1, 14)} = 0.4$, $p = 0.5$) and PUFA ($F_{(1, 13)} = 0.3$, $p = 0.6$) did not differ between exposed and control animals, see Figure 4.20.

4.3.8. Profiling of plasma PC and SM from CCI TBI mouse model

In the CCI mouse model of TBI (n = 4 CCI, n = 4 sham), there were no differences between injured and sham mice for the total PC ($F_{(1, 20)} = 1.17$, $p = 0.3$) and SM levels ($F_{(1,}$

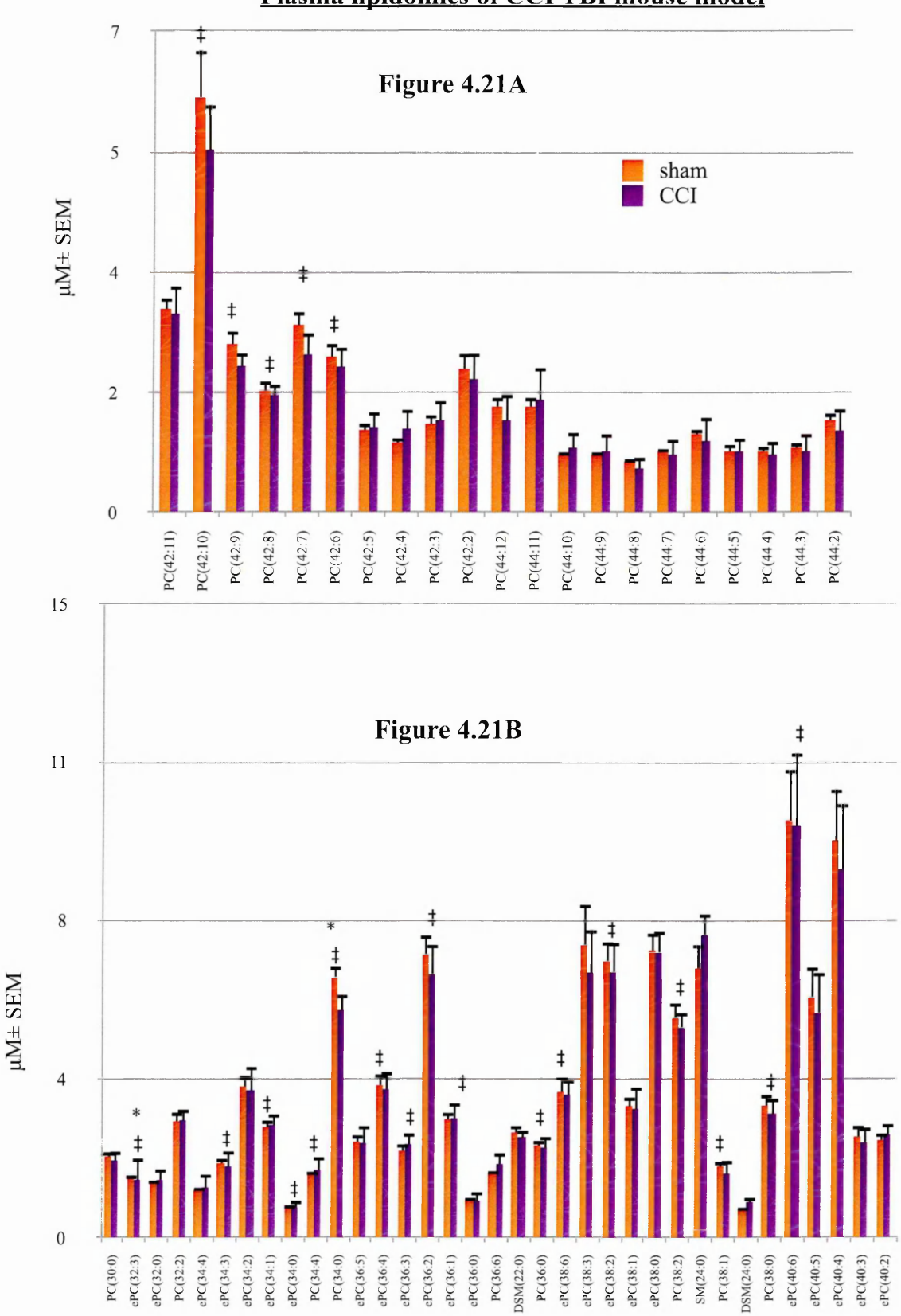

Figure 4.21. Plasma PC and SM changes for the CCI TBI mouse model: Mean ± SEM (n = 4 per group) of all of the lipids identified during the LC/MS run. The symbol ‡ denote those species that were associated with component 1 from PCA. (A-B) Univariate analyses of species from component 1 show that ePC(32:3) and PC(34:0),were significantly different with injury compared to controls, *denotes $p < 0.05$ for a main injury effect (based on MLM with exposure as a fixed main factor).

Figure 4.22A

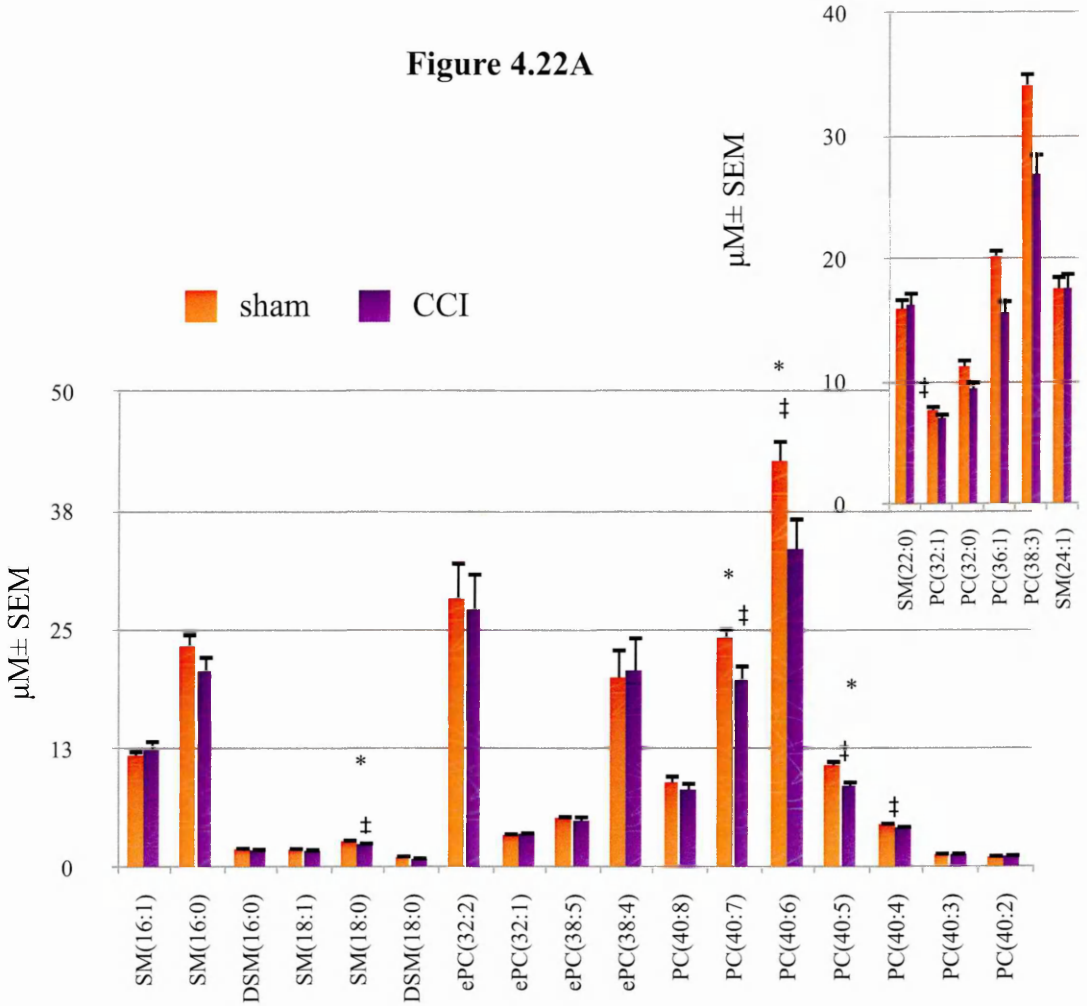

Figure 4.22B

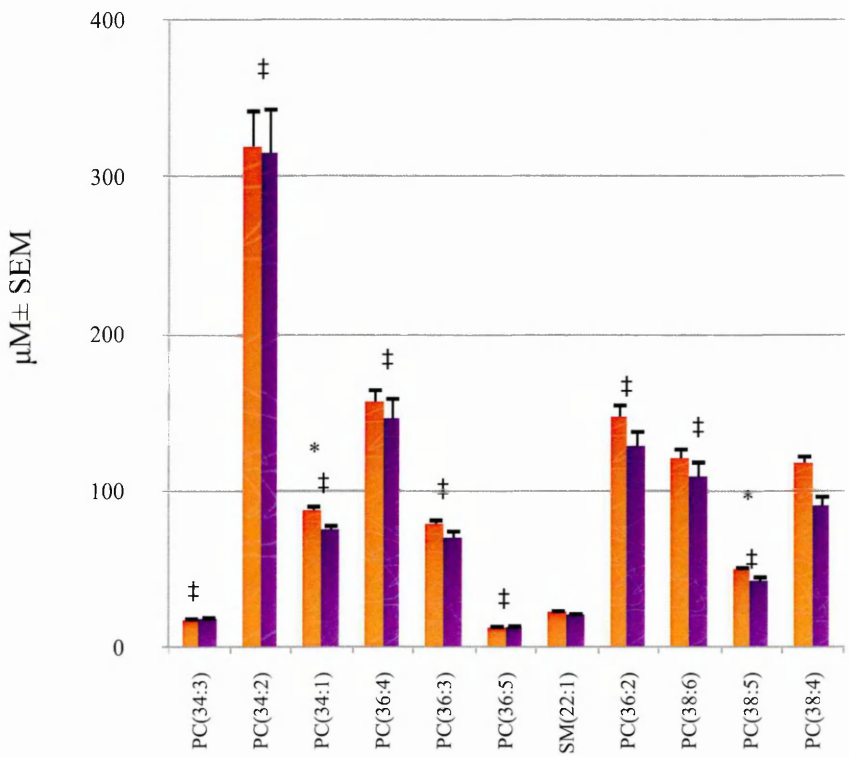

Figure 4.22. Plasma PC and SM changes for the CCI TBI mouse model: Mean ± SEM (n = 4 per group) of all of the lipids identified during the LC/MS run. The symbol ‡ denote those species that were associated with component 1 from PCA. (A-B) Univariate analyses of species from component 1 show that SM(18:0) and PC(34:1), PC(38:5), PC(40:5), PC(40:6), PC(40:7) were significantly different with injury compared to controls, *denotes $p < 0.05$ for a main injury effect (based on MLM with exposure as a fixed main factor). Insert contains lipids that have different concentration than that in the main figure.

Degree of unsaturation of plasma PC for CCI TBI mouse model

Figure 4.23

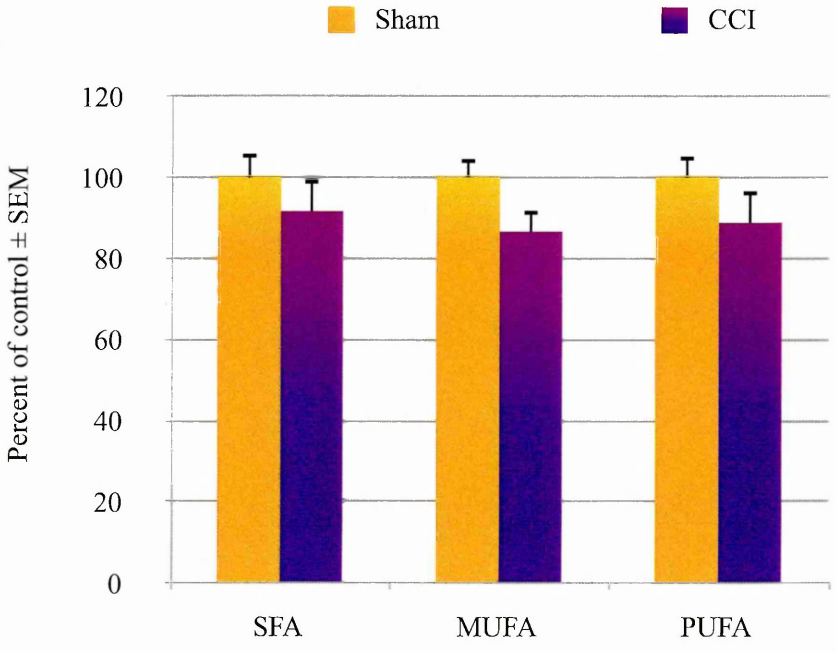

Figure 4.23 Degree of unsaturation of plasma PC for the CCI TBI mouse model: Mean ± SEM (n = 4 per group) presented as percentage of sham showing that MUFA containing PC molecular species were decreased in injured animals 87% relative to sham injured mice and that SFA (91%) and PUFA (88%) were also slightly decreased in injured animals relative to sham but these differences were not significant, $p > 0.05$.

$_{20)} = 0.3$, $p = 0.6$). Figure 4.21 and 4.22 show individual molecular species of PC and SM. As above, PCA was performed but for PC species only which showed that component 1 explained the largest variance (44%) and was significantly associated with injury ($F_{(1, 5)} = 16.3$, $p = 0.01$). Figure 4.23 shows an effect on the degree of unsaturation, where SFA levels were similar between injured and sham mice ($F_{(1, 20)} = 1.1$, $p = 0.3$). However, MUFA containing PC molecular species were marginally decreased in injured mice

compared to controls ($F_{(1, 15)} = 4.2$, $p = 0.06$) but with no significant difference in PUFA containing PC species between injured and sham animals ($F_{(1, 17)} = 0.9$, $p = 0.3$).

4.3.9. Profiling of plasma PC and SM from mTBI mouse model:

Total PC and SM from plasma samples from single and repetitive mTBI mouse model (n = 4 s-sham, n = 4 s-m-TBI, n = 3 r-sham and n = 4 r-m-TBI) are presented in Figure 4.24. For total PC levels, a significant main effect of injury was observed ($F_{(1, 28)} = 38.5$, $p < 0.001$) and *post-hoc* analyses showed significant differences between s-sham and s-mTBI ($p < 0.001$) as well as differences between r-sham and r-mTBI ($p < 0.001$) (Figure 4.24A). For total SM levels, a significant main effect of injury was observed ($F_{(1, 34)} = 4.7$, $p = 0.01$) and *post-hoc* analyses showed significant differences between s-sham and s-mTBI ($p < 0.001$) and between r-sham and r-mTBI ($p < 0.05$), see Figure 4.24B. Examination of the degree of unsaturation in PC provided evidence that PC molecular species that contained

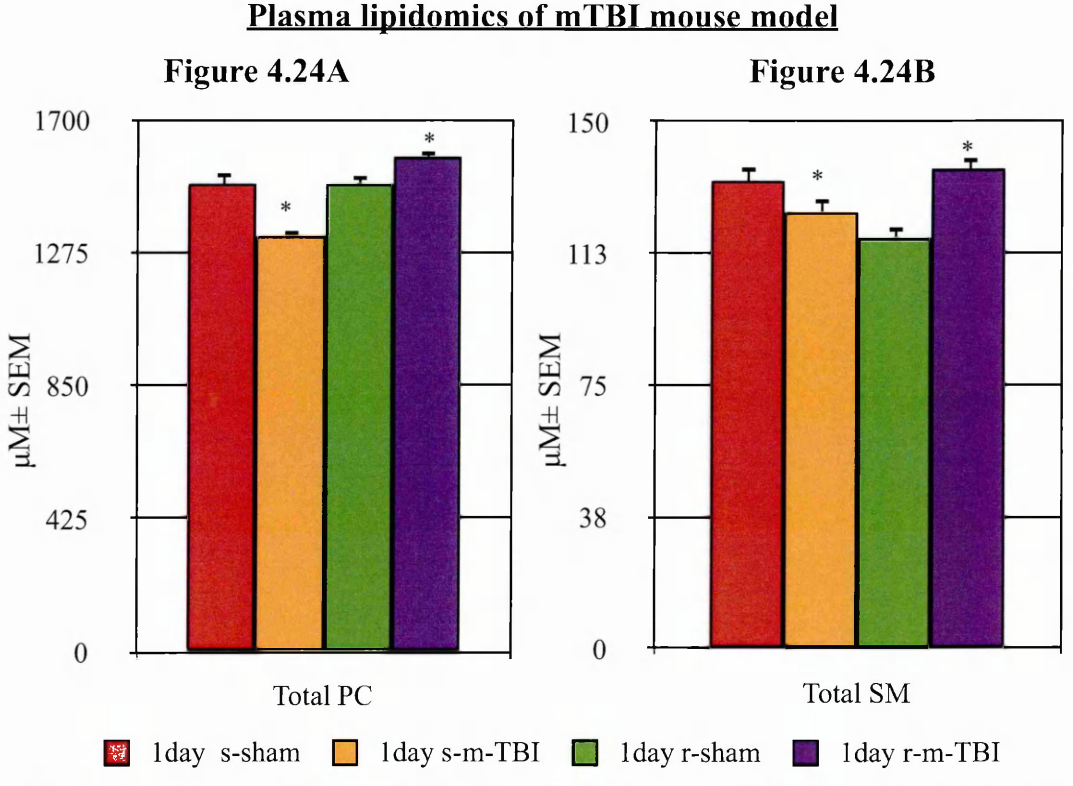

Figure 4.24. Plasma PC and SM for the mTBI mouse model: Mean ± SEM of in s-m-TBI (n = 4), s-sham (n = 4), r-m-TBI (n = 4) and r-sham (n = 3). (A) Individual molecular species of PC and identified during the LC/MS were summed after lipidome DB analyses to generate total PC and total SM levels. A significant decrease in s-m-TBI mice was observed compared to s-sham mice and an increase in r-sham and r-m-TBI mice for total PC, *$p < 0.05$ denotes a main injury effect (based on MLM where exposure was included as a fixed main factor). (B) For total SM, a decrease was observed in s-mTBI compared to s-sham and an increase in r-sham and r-mTBI animals compared to shams, * $p < 0.05$ (based on MLM where exposure was included as a fixed main factor).

SFA did not differ by injury ($F_{(1, 35)} = 1.1$, $p = 0.4$). On the other hand, those that contained MUFA ($F_{(1, 35)} = 25.3$, $p < 0.001$) or PUFA ($F_{(1, 29)} = 38.8$, $p < 0.001$) were decreased in injured compared to uninjured mice. *Post-hoc* analyses revealed that there were significant differences between s-sham and s-mTBI ($p < 0.001$) in MUFA containing PC species and for PUFA containing molecular species ($p < 0.001$). These differences were not significant for r-sham compared to r-mTBI (Figure 4.25).

Degree of unsaturation status of plasma PC for mTBI mouse model

Figure 4.25

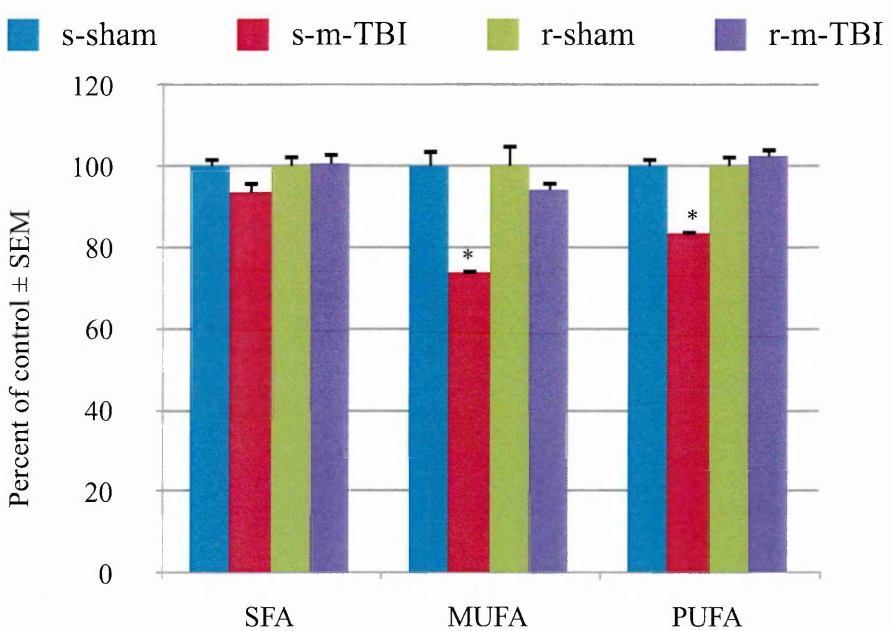

Figure 4.25. Degree of unsaturation of plasma PC for the mTBI mouse model: Mean ± SEM (n = 3/4 per group) presented as percentage in s-m-TBI relative to s-sham and r-m-TBI relative to r-sham. PC species containing MUFA were decreased in s-mTBI, 73% relative to s-sham mice. There were no differences for SFA between the four groups. For PUFA, s-mTBI mice showed a decrease, 83% relative to control, *denotes $p < 0.05$ for a main injury effect (based on MLM where injury was included as a fixed main factor). There were no significant differences between r-sham and r-mTBI mice, $p > 0.05$.

4.3.9. Lipidomic approaches for target identification for mouse model B of GW agent exposure

Since one of the main goals of this project was to determine if lipidomic technology can be useful in identifying molecular targets for therapeutic interventions, additional

analyses were focused on mouse model B of GW agent exposure. From brain tissue, FFAs, C16:0 (palmitic acid [PA]), C18:2 (linoleic acid [LA]), 18:1 omega-9 (oleic acid [OA]), C20:4 omega-6 (arachidonic acid, [AA]), and C22:6 omega-3 (docosahexaenoic acid, [DHA]) and a bioactive lipid 2-arachidonoylglycerol (2AG) were examined using the RPLC/MS and the RPLC/MS/MS. There were significant increases in PA ($F_{(1, 16)} = 4.5$, $p = 0.05$), OA($F_{(1, 19)} = 6.8$, $p = 0.02$), AA ($F_{(1, 16)} = 9.1$, $p = 0.01$), DHA ($F_{(1, 20)} = 18.7$, $p < 0.001$) and 2AG ($F_{(1, 20)} = 8.0$, $p = 0.01$) in exposed mice compared to controls. There were no differences between the two groups for LA ($F_{(1, 19)} = 2.5$, $p = 0.13$). Figure 4.26 shows an increase in several FFA and 2AG in the brains of exposed animals expressed as a percentage of control levels. Examination of the PC/SM ratio showed a small but significant decrease ($F_{(1,9)} = 5.7$, $p = 0.04$) in exposed animals (mean ratio = 12.79, SE ±

Free fatty acid and 2AG from mouse model B of GW agent exposure

Figure 4.26

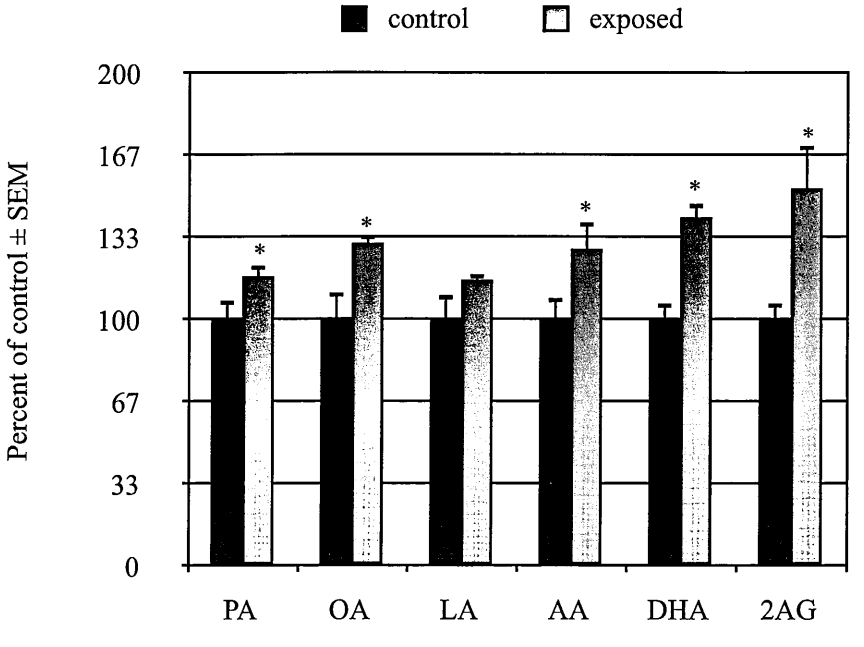

Figure 4.26. Brain free fatty acids and 2AG for mouse model B of GW agent exposure: Mean ± SEM (n = 4 per group) presented as percentage of control. Brain PA levels were 117%, OA levels were 130% LA levels were 116%, AA levels were 128% and DHA levels were 140% in PB+PER exposed mice relative to control mice from mouse model B. Brain 2AG levels were 153% relative to controls, * denotes $p < 0.05$ for a main exposure effect (based on MLM with exposure as a fixed main factor.

Additional plasma lipids from mouse model B of GW agent exposure

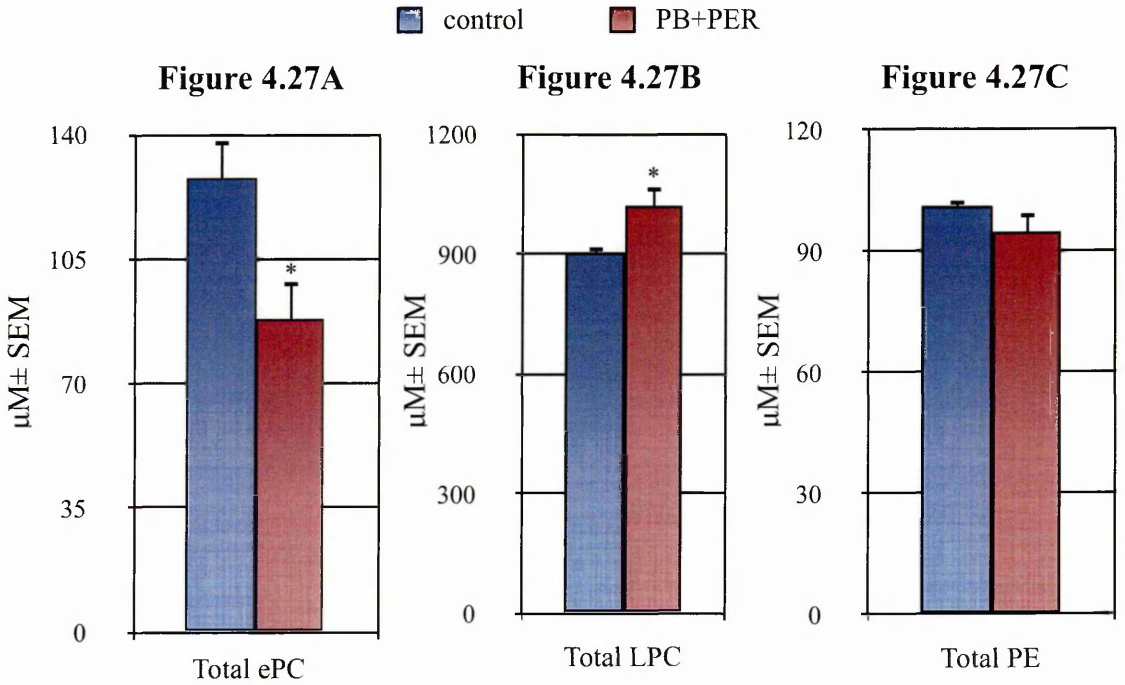

Figure 4.27. Plasma ePC, PE and LPC comparisons for mouse model B of the GW agent exposure: Mean ± SEM in exposed (n = 4) and control (n = 4). There was (A) 1.44 decrease in ePC and (B) 1.13 fold increase for LPC. (C) There was no differences in total PE levels between exposed animals compared to controls, *denotes $p < 0.05$ for a main exposure effect (based on MLM where exposure was included as a fixed main factor).

Plasma LPC and free fatty acids from mouse model B of GW agent exposure

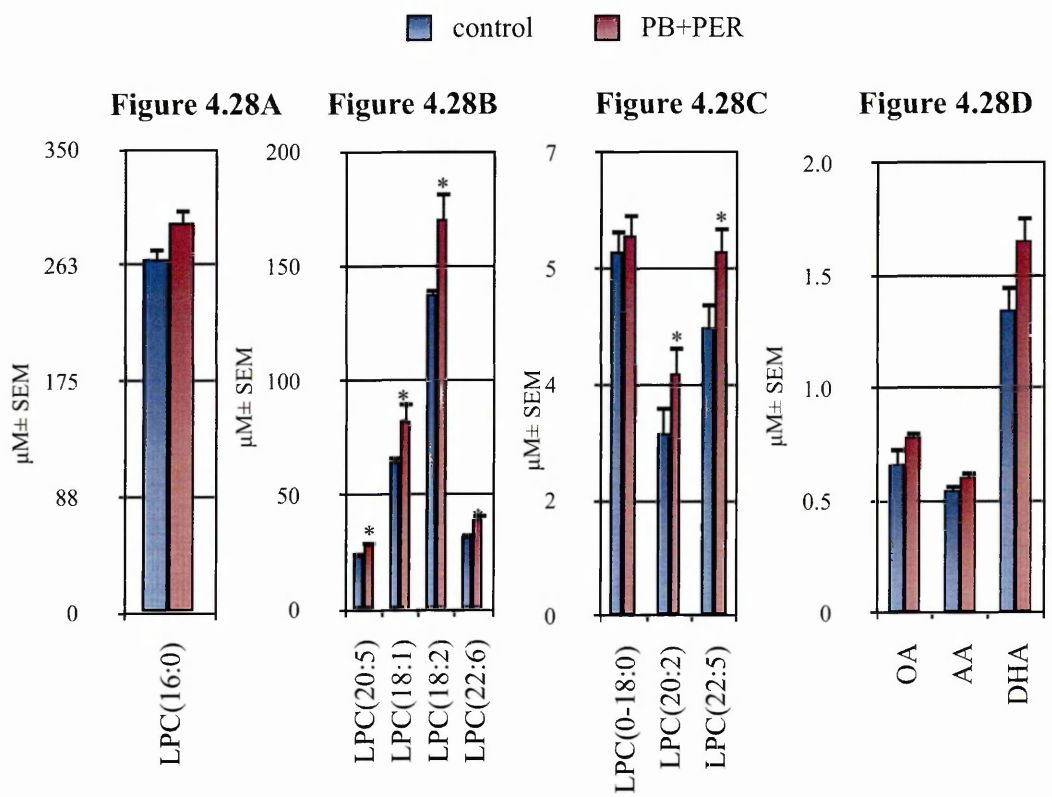

Figure 4.28. Plasma FFA and LPC molecular species comparisons for mouse model B of GW agent exposure: Mean ± SEM in exposed (n = 4) and control (n = 4). (A), LPC(16:0) was only marginally increased in exposed compared to controls (p = 0.07). (B-C) LPC(18:1), LPC(18:2) LPC(20:5), LPC(20:2), LPC(22:6) and LPC(22:5) were significantly increased in exposed mice compared to controls, *denotes $p < 0.05$ for a main exposure effect (based on MLM where exposure was included as a fixed main factor). (D) A number of FFA, AA and DHA showed a trend for an increase in exposed animal compared to controls, $p > 0.05$.

0.29) compared to controls (mean ratio = 13.20, SE ± 0.21).

In plasma, FFA as well as ePC, PE and LPC were examined using the lipidomic LC/MS approach employed above for PC and SM quantification. Total ePCs were further examined since the profiling data suggested that several ether PC molecular species were decreased in exposed animals compared to controls. Total ePC levels were significantly lower in exposed animals compared to controls ($F_{(1, 15)} = 5.3$, $p = 0.04$). Total PE levels did not differ between exposed and control mice ($F_{(1, 17)} = 2.4$, $p = 0.14$). Total LPC levels were significantly elevated in exposed mice compared to controls ($F_{(1, 19)} = 5.5$, $p = 0.03$, Figure 4.27). However, LPC molecular species that contained PUFA were significantly elevated in exposed mice compared to controls ($F_{(1, 19)} = 6.8$, $p = 0.02$, see Figure 4.28). Examination of FFA from plasma showed a significant increase in OA ($F_{(1, 12)} = 4.6$, $p = 0.05$), and a marginal increase in DHA ($F_{(1, 18)} = 4.2$, $p = 0.06$) and in AA ($F_{(1, 16)} = 3.6$, $p = 0.08$) in exposed animals compared to controls, see Figure 4.28.

4.3.10. Pilot studies of the effects of a potential treatment on recovery of normal lipid profiles in mouse model B of GW agent exposure

There were 4 comparison groups in this study, those treated with nilvadipine (n = 5 exposed and n = 5 unexposed) and those that received vehicle only (n = 4 exposed, n = 5 unexposed). For plasma lipid profiles, there was a main effect of GW agent exposure on PC levels ($F_{(1, 42)} = 21.09$ $p < 0.001$), no main effect of nilvadipine treatment ($F_{(1, 42)} = 0.6$, $p = 0.4$) and an interaction between GW agent exposure and nilvadipine treatment ($F_{(1, 42)} = 29.15$, $p < 0.001$). Figure 4.29A shows that PC in unexposed controls were similar to unexposed nilvadipine treated mice. GW agent exposed mice had higher PC levels than

Lipidomics data from pilot nilvadipine treatment studies in mouse model B of GW agent exposure

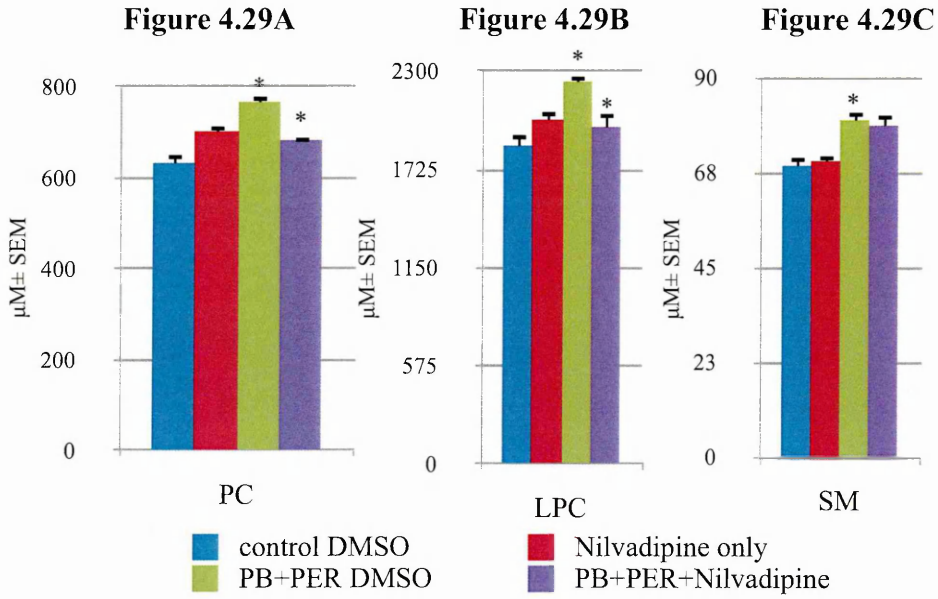

Figure 4.29. Plasma PC, LPC and SM comparisons from nilvadipine treatment studies for mouse model B of the GW agent exposure: Mean ± SEM in PB+PER (n = 5), control DMSO (n = 4), PB+PER+Nilvadipine (n =5), and Nilvadipine (n = 5). (A-B) Total PC and LPC levels were increased in PB+PER exposed mice compared to controls and Nilvadipine treatment significantly reduced LPC and PC levels in PB+PER exposed mice compared to controls, *denotes $p < 0.05$ (based on MLM with PB+PER and nilvadipine treatment as fixed main factors). (C) There was an effect of PB+PER exposure on SM levels (*$p < 0.05$) but no treatment affect of nilvadipine in GW agent exposed mice.

Table 4.1. Lipid Identifications obtained from lipid map for PC molecular species that were significantly different in mouse model A of GW agent exposure

Lipid	(M+H)+ m/z	ID	M-sn1 m/z	M-sn2 m/z	Sn1 FA	Sn2 FA
*ePC(34:0)	748.6	PC(O-16:0/18:0)	-	480	-	283
		PC(O-18:0/16:0)	-	508	-	255
ePC(36:2)	772.6	PC(P-16:0/20:1)	-	478	-	309
		PC(O-18:0/18:2)	-	508	-	279
		PC(P-18:0/18:1)	-	506	-	281
*ePC(36:1)	774.6	PC(O-18:0/18:1)	-	508	-	281
*PC(36:0)	790.6	PC(18:0/18:0)	522	522	283	283
*PC(38:4)	810.6	PC(18:0/20:4)	542	522	283	303
		PC(16:0/22:4)	570	552	255	331
*PC(38:1)	816.6	PC(16:0/22:1)	576	494	255	337
*PC(40:4)	838.6	PC(18:0/22:4)	570	522	283	331
PC(40:2)	842.7	PC(20:1/20:1)	548	548	309	309
		PC(22:0/18:2)	518	578	339	279
		PC(18:1/22:1)	576	520	281	337

Note: *Indicates molecular species for which product ions were observed to confirm identification using LC/MS/MS in data dependent analysis that was performed in conjunction with LC/MS SCID in negative ion mode. [M+H]+ indicates m/z value + 1 hydrogen in positive ion. (M-sn1) indicates lyso fragment ion corresponding to the loss at the first glycerol position. (M-sn2) indicates lyso fragment ion corresponding to the loss at the second glycerol position. Sn1 FA (fatty acid at the sn1 position and Sn2 FA (fatty acid at the sn2 position.

Table 4.2. Summary table showing fold-change of individual PC and SM molecular species identified from brain samples using SCID LC/MS

	Model A	Model B	PSAPPswe
SM(16:0)	1.03	ND	-1.17
PC(30:1)	1.90	ND	1.39
PC(30:0)	1.11	1.43	-1.03
ePC(32:1)	7.33	ND	-1.08
ePC(32:0)	1.16	ND	-1.12
SM(18:1)	-1.06	ND	-1.16
SM(18:0)	1.12	1.26	-1.12
PC(32:1)	1.10	1.18	-1.01
DSM(18:0)	ND	2.00	-1.54
PC(32:0)	1.11	1.16	-1.13
ePC(34:2)	-1.31	ND	-1.10
ePC(34:1)	1.31	1.15	-1.09
ePC(34:0)	1.45	1.18	-1.13
PC(34:3)	1.08	1.13	1.00
PC(34:2)	1.12	1.18	1.06
PC(34:1)	1.14	1.15	-1.08
PC(34:0)	1.13	1.16	-1.05
ePC(36:2)	2.70	1.21	-1.06
ePC(36:1)	2.71	1.11	-1.09
ePC(36:0)	ND	2.00	-1.18
PC(36:4)	1.10	1.18	-1.05
PC(36:3)	1.13	1.17	-1.02
SM(22:1)	1.13	1.19	-1.07
PC(36:2)	1.08	1.18	-1.09
SM(22:0)	1.35	1.12	-1.16
PC(36:1)	1.11	1.25	-1.09
DSM(22:0)	ND	-1.32	-1.14
PC(36:0)	2.02	1.26	-1.12
ePC(38:6)	ND	1.27	-1.09
ePC(38:5)	ND	1.24	-1.06
ePC(38:4)	ND	1.25	-1.05
ePC(38:2)	ND	1.25	-1.07
ePC(38:1)	1.00	-1.17	-1.13
PC(38:6)	1.14	1.17	-1.05
PC(38:5)	-1.11	1.25	-1.07
PC(38:4)	1.37	1.27	-1.04
PC(38:3)	1.13	1.22	-1.05
SM(24:1)	1.12	1.22	-1.10
PC(38:2)	1.43	1.24	-1.07
SM(24:0)	1.18	1.11	-1.15
PC(38:1)	2.90	1.31	-1.06
DSM(24:0)	2.82	1.06	-1.21
PC(38:0)	ND	2.15	-1.08
PC(40:7)	1.22	1.24	-1.12
PC(40:6)	1.27	1.24	-1.07
PC(40:5)	ND	1.30	-1.01
PC(40:4)	2.71	1.30	-1.06
PC(40:3)	ND	1.26	-1.03
PC(40:2)	1.50	ND	-1.10

Note: Fold-change (exposed over controls, PSAPPswe over wild-type and injured over sham) values are displayed for each molecular species. Those indicated with ND (Not Detected) and were not detected in the SCID LC/MS run. (-) downregulated (+) upregulated

Table 4.3. Summary table showing fold-change of individual PC and SM molecular species identified from plasma samples using SCID LC/MS

	Model A	Model B	CCI TBI	s-m-TBI	r-m-TBI
SM(16:1)	ND	-1.17	1.04	-1.14	3.10
SM(16:0)	ND	-1.16	-1.13	1.07	1.30
PC(30:1)	ND	-1.00	1.28	ND	ND
DSM(16:0)	ND	-1.11	-1.06	1.06	1.64
PC(30:0)	ND	-1.00	-1.05	1.05	1.13
ePC(32:3)	ND	ND	-1.03	ND	ND
ePC(32:2)	ND	-1.85	-1.04	-1.43	1.06
ePC(32:1)	ND	-1.91	1.03	-1.32	1.32
ePC(32:0)	ND	-1.00	1.05	1.02	1.57
SM(18:1)	ND	-1.06	-1.07	1.06	1.04
PC(32:2)	ND	1.12	1.01	-1.56	-1.29
SM(18:0)	ND	-1.01	-1.12	-1.00	1.01
PC(32:1)	1.23	1.00	-1.09	-1.71	-1.23
DSM(18:0)	1.35	1.12	-1.23	-2.40	1.05
PC(32:0)	1.17	1.15	-1.19	-1.03	-1.05
ePC(34:3)	ND	-5.00	-1.04	-1.33	1.66
ePC(34:2)	ND	-1.04	-1.03	1.11	1.16
ePC(34:1)	ND	-1.08	1.02	-1.10	1.17
PC(34:4)	ND	-1.00	1.06	ND	2.67
PC(34:3)	1.08	1.05	1.05	-1.62	-1.13
PC(34:2)	1.11	-1.02	-1.01	1.01	1.08
PC(34:1)	1.08	1.04	-1.16	-1.40	-1.12
PC(34:0)	1.09	1.08	-1.14	-1.26	1.07
ePC(36:5)	ND	-1.00	-1.01	1.53	2.18
ePC(36:4)	ND	-1.11	-1.03	1.19	1.12
ePC(36:3)	ND	-1.23	1.08	-1.09	1.18
ePC(36:2)	1.25	-1.12	-1.08	-1.01	1.24
ePC(36:1)	ND	-1.23	1.01	-1.13	1.15
ePC(36:0)	ND	-3.00	-1.02	-1.18	2.00
PC(36:6)	ND	2.40	1.15	1.16	1.85
PC(36:5)	1.09	1.04	1.04	-1.09	-1.00
PC(36:4)	1.04	-1.08	-1.07	-1.25	-1.05
PC(36:3)	1.09	1.03	-1.12	1.04	-1.02
SM(22:1)	1.17	-1.01	-1.09	-1.06	-1.04
PC(36:2)	1.09	-1.03	-1.14	-1.07	1.24
SM(22:0)	1.40	-1.11	1.02	-1.26	-1.06
PC(36:1)	1.04	-1.01	-1.29	-1.28	1.10
DSM(22:0)	1.24	-1.12	-1.05	-1.14	1.31
PC(36:0)	1.21	1.01	-1.03	-1.03	1.01
ePC(38:6)	ND	-1.05	-1.02	1.38	1.21
ePC(38:5)	1.21	-1.08	-1.06	1.16	1.23
ePC(38:4)	1.43	-1.66	1.04	-1.36	1.18
ePC(38:3)	ND	-1.69	-1.10	-1.45	1.08
ePC(38:2)	1.90	-1.16	-1.04	1.04	1.14
ePC(38:1)	ND	-1.35	-1.02	1.01	1.25
ePC(38:0)	1.10	1.06	-1.01	-1.33	-1.18
PC(38:6)	1.04	-1.01	-1.11	-1.15	-1.05
PC(38:5)	1.06	1.05	-1.18	-1.27	-1.09
PC(38:4)	-1.01	-1.14	-1.30	-1.38	1.09
PC(38:3)	1.04	-1.06	-1.27	-1.15	1.06
SM(24:1)	1.53	-1.14	1.00	-1.06	1.11
PC(38:2)	1.20	1.07	-1.05	-1.14	-1.00
SM(24:0)	ND	-1.28	1.12	-1.28	1.22
PC(38:1)	ND	1.53	-1.11	1.22	-1.45

Table 4.3 continued

DSM(24:0)		-1.10	1.27	-1.03	2.00
PC(38:0)	1.99	1.02	-1.07	1.21	1.07
ePC(40:6)	2.18	-1.70	-1.01	-1.32	1.09
ePC(40:5)	ND	-1.83	-1.07	-1.15	1.10
ePC(40:4)	7.62	-1.74	-1.08	-1.39	1.32
ePC(40:3)	ND	-1.71	-1.06	-1.42	1.29
ePC(40:2)	ND	1.63	1.05	-1.09	1.08
PC(40:8)	1.02	1.15	-1.09	-1.33	-1.23
PC(40:7)	1.03	1.18	-1.23	-1.08	-1.11
PC(40:6)	-1.00	-1.05	-1.28	-1.07	1.31
PC(40:5)	1.08	-1.04	-1.25	-1.35	1.04
PC(40:4)	1.20	-1.16	-1.08	-1.64	1.03
PC(40:3)	ND	-1.45	-1.00	-1.26	1.55
PC(40:2)	ND	-2.00	1.06	-1.27	2.16
PC(42:11)	ND	-3.00	-1.02	-1.21	1.30
PC(42:10)	-1.08	1.30	-1.14	-1.87	-1.17
PC(42:9)	-3.70	1.24	-1.15	-1.37	-1.01
PC(42:8)	ND	1.23	-1.04	1.00	1.22
PC(42:7)	ND	1.04	-1.19	1.05	-1.07
PC(42:6)	ND	-1.32	-1.07	-1.31	1.08
PC(42:5)	ND	-2.17	1.04	-1.62	1.64
PC(42:4)	ND	-1.75	1.20	-1.29	1.54
PC(42:2)	ND	-6.33	-1.08	-1.47	1.22
PC(44:8)	ND	-2.75	-1.15	-1.20	2.38

Note: Fold-change (exposed over control, injured over sham) values are displayed for each molecular species. Those indicated with ND (Not Detected) and were not detected in the SCID LC/MS run. (-) downregulated (+) upregulated

unexposed mice and nilvadipine treated GW agent exposed mice. For LPC (see Figure 4.29B), there was a main exposure effect ($F_{(1, 50)} = 6.82$, $p = 0.01$), no main effect of nilvadipine treatment ($F_{(1, 50)} = 0.7$, $p = 0.4$) and an interaction between GW agent exposure and nilvadipine treatment ($F_{(1, 50)} = 9.8$, $p = 0.003$). Similar to PC findings, Figure 4.29 also shows that LPC levels were elevated in GW agent exposed mice compared to unexposed control mice. LPC levels were lower in nilvadipine treated GW agent exposed mice compared to untreated GW agent exposed mice. For SM levels (see Figure 4.29C), there was a main effect of GW agent exposure ($F_{(1, 51)} = 17.14$, $p < 0.01$), no main effect of nilvadipine treatment ($F_{(1, 51)} = 0.00$, $p = 0.9$) and no interaction between nilvadipine treatment and GW agent exposure ($F_{(1, 51)} = 0.25$, $p = 0.62$). Total PC and SM levels from one whole brain hemisphere were also examined but there were no differences between

GW agent exposed mice compared to controls, no main effect of nilvadipine and no interaction between GW agent exposure and nilvadipine treatment.

Tables 4.2 and 4.3 provide fold-change and the direction of change information on each individual PC and SM molecular species for brain and plasma, respectively.

4.4. Discussion

Lipidomic analyses were performed on phosphocholine-containing lipids, PC and SM, since metabolism of these lipids is linked to ACh production and turnover as well as to activation of the ACh receptor signaling system, which is altered in response to various combinations of GW agent exposure. For example, Abou-Donia and colleagues have shown an increase in mAChR and nAChR ligand binding in the cortices of rats that received combined exposure to PB, PER and DEET (Abou-Donia et al 2004). Studies also suggest that after chronic exposure to AChE inhibitors there is a compensatory increase in AChE mRNA levels (Bansal et al 2009). Lamproglou and colleagues showed a decrease in phosphocholine levels in rats exposed to PB and stress compared to non-stressed rats (Lamproglou et al 2009). Interestingly, a number of studies have shown that early-life exposure to PER in rats increased membrane fluidity of heart cells, which was accompanied by an increase in plasma cholesterol levels as well as an increase in the production of inflammatory cytokines, such as IL-1β, IL-12, IFN-γ and IL-10 (Vadhana et al 2011). These studies suggest that the GW agent utilized may affect cellular membrane PL levels and their metabolism.

4.4.1. Relevance of lipids and lipid mediated pathways to GWI:

As described in Chapter 3, impaired peripheral immune and inflammatory responses are among key biological features of GWI. While initial hypotheses by Rook and Zumla proposed a Th2 shift in the immune system (Rook and Zumla 1997), clinical studies so far show a mixed profile with both pro-inflammatory and anti-inflammatory

cytokines being increased after stimulation of lymphocytes from veterans with GWI compared to control (Broderick et al 2011; Skowera et al 2004).

Phospholipids and their metabolites are involved in mediating a number of immune and inflammatory responses and are capable of eliciting both Th1 and Th2 type immune responses. As described above, LPC can stimulate production of both pro- and anti-inflammatory cytokines (Bach et al 2010). While prostaglandins that are AA metabolites initiate pro-inflammatory events, DHA metabolites are generally associated with anti-inflammatory events. Findings presented in this Chapter support the hypothesis that lipid metabolites (that are downstream of AA and DHA) could contribute to the immune and inflammatory imbalance observed in veterans with GWI. Therefore, a future examination of lipids and their metabolites is expected to be useful for identifying biological processes that are upstream of the aberrant immune and inflammatory changes observed in veterans with GWI. An in-depth discussion of the lipid changes that were observed in each mouse model follows.

4.4.2. Brain lipid profiling

4.4.2.1. Brain lipid profile of mouse model A of GW agent exposure

In this study, we observed that among PC and SM molecular species quantified in this experiment, several ePC and PC containing LCFA and SM containing VLCFA were increased in the brains of exposed animals compared to controls. Among the myriad of potential mechanisms for these lipid changes, (such as altered transport, uptake, storage, synthesis and turnover), alterations in peroxisomal function best explain these observations (Wenk 2005; Farooqui et al 2007). Changes in ePC and SM containing VLCFA are generally indicative of peroxisome malfunction (Singh et al 2009). This is supported by genomic work performed at the Roskamp Institute showing a decrease in message RNA for peroxisomal biogenesis factor 10 (PEX-10) by nearly two-fold in response to PB, PER, and DEET exposure of SH-SY5Y neuronal cells (Crynen et al 2012). A study in mice

showed that exposure to PB and stress resulted in an increase in lipid peroxidation, further supporting the hypothesis that peroxisomal dysfunction may be associated with GW agent exposure (Somani et *al.,* 2000). In exposed animals, while SFA and PUFA were also increased compared to controls, MUFA containing PC species were nearly 300% relative to control. This could be through an increase in Stearoyl-CoA desaturase (SCD) enzyme activity, a lipogenic enzyme catalyzing the synthesis of MUFA. This is also supported by the genomic studies conducted at the Roskamp Institute showing downregulation of the SCD mRNA levels by nearly two-fold (Crynen et al 2012) - possibly a consequence of negative feedback inhibition (this requires further examination). Collectively, these studies suggest that peroxisome malfunction and SCD activity might be an interesting target for further investigation in GW agent exposure associated with mouse model A.

4.4.2.2. Brain lipid profile of mouse model B of GW agent exposure:

Brain lipid examination of mouse model B of GW agent exposure shows an increase in total PC and SM levels in the brains of exposed mice compared to control mice. PC and SM are generally found in the outer plasma membrane leaflet and changes in total PC levels may affect membrane fluidity of the outer plasma membrane (Vance, & Vance 2008; Farooqui et al 2007). A more detailed examination of membrane fractions as well as other PLs may help determine if membrane integrity is affected in response to GW agent exposure. These studies will be informative since the literature suggests that PER can affect membrane fluidity. Lipid data analysis using PCA showed that PC molecular species significantly associated with exposure included a large number of diacyl PC that contained PUFA. This is consistent with the examination of degree of unsaturation status of PC showing that PUFA containing species were increased by 123% in exposed animals relative to controls. Given that both AA (associated with downstream pro-inflammatory conditions) and DHA (anti-inflammatory conditions) can influence inflammation, additional investigation is required to determine if these PUFA containing PC molecular

species may be associated with the mixed inflammation profiles observed in veterans with GWI.

A review of the literature suggested that a ratio of PC/SM may be a useful index of membrane fluidity, where an increase in this ratio would indicate an increase in membrane fluidity. Examination of this index in mouse model B suggests a decrease in membrane fluidity. This is consistent with previous reports on PER's effect on cellular membranes. For instance, following neonatal exposure to PER, Vadhana and colleagues reported a decrease in membrane fluidity of heart cell membrane (and concomitant heart disease) in adult rats (Vadhana et al 2011).

4.4.2.3. Brain lipid profiles of other models of neurological illnesses:

The main objective of these studies was to determine if the changes observed in PC and SM in the brains of mouse models A and B were distinct from other models of neurological illness. A decrease was observed in several brain PC and SM molecular species in PSAPPswe mice compared to wild-type mice. A close examination suggested that ePC species or SM molecular species containing C16:0 and C18:0 were decreased in PSAPPswe mice compared to controls. However, there was an increase in PC and SM in exposed mice compared to controls for both mouse models of GW agent exposure. Among these, several ePC were increased in exposed animals compared to unexposed. Although these studies suggest that peroxisomal dysfunction may be present in both GW agent exposure models and in the AD mouse model, the direction of change in each models suggests that in this AD mouse model, there may be a decrease in peroxisomal function, while in the GW agent exposed mice there appears to be an increase in perxoisomal function. Furthermore, unlike mouse models of GW agent exposure, there were no differences between PSAPPswe mice and control mice with regard to the degree of unsaturation of PC.

A direct comparison cannot be made with the CCI TBI mouse model since brain

regions (cortex, hippocampus and cerebellum) were separately examined in this study. These data show brain region specific differences in PC and SM levels and brain region specific responses to the injury. Given that PC and SM levels were much higher in the cortex than in the hippocampus or the cerebellum, it would be expected that the net effect would be an increase in PC and SM given the size of the cortex in comparison to the hippocampus and the cerebellum. This would be similar to the findings observed in the CD1 mice from mouse model B of GW agent exposure. Nevertheless, these data suggest that future studies in the GW models should incorporate brain region specific lipid profiling to gain a more thorough understanding of the biochemical pathways that might be affected in response to GW agents. In particular, matrix assisted laser desorption/ ionization (MALDI)-MS imaging may be extremely valuable for identifying the underlying structural changes in response to GW agent exposure and other CNS injuries (Jackson, & Woods 2009).

4.4.3. Plasma lipid profiling

Diagnosis of GWI largely relies on clinical presentation of symptoms, and as yet, there are no objective biomarkers available for diagnosing GWI. Furthermore, nearly 50,000 veterans continuing to suffer from unexplained symptoms have had their disability claims denied or are still pending due to the challenges associated with providing an objective and accurate diagnosis of GWI. It is anticipated that availability of biomarkers would be useful in objectively diagnosing GWI and would also be extremely useful in correctly classifying veterans with GWI so that appropriate care and therapies could be provided. The main goal of these studies was to determine if differences in plasma PC and SM could be used to differentiate GW agent exposed mice from controls and whether these changes were specific to GWI, with the ultimate goal of translating these findings to human studies.

4.4.3.1. Lipid profiling of plasma PC and SM in mouse models A and B of GW agent exposure:

For mouse model A of GW agent exposure, changes in PC and SM molecular species observed in the plasma of exposed mice compared to control mice showed that ePC and diacyl PC containing LCFA were increased in GW agent exposed mice compared to control mice. For both mouse models, particularly mouse model B, PC changes show that a large number of ePC and PUFA containing PC molecular species were affected in exposed animals compared to controls. In the plasma of GW agent exposed mice from both models, PC molecular species that contained SFA were affected more than MUFA and PUFA containing species. In mouse model A, SFA were increased in exposed animals compared to controls. In mouse model B, a non-significant increase in SFA was observed in exposed animals compared to controls. There are a number of limitations associated with comparison of mouse model A to mouse model B given the differences in post-exposure time period, age and gender composition. Nevertheless, these studies provide evidence that plasma PC levels are affected by GW agent exposure in both mouse models of GW agent exposure. Future examination of biological pathways associated with peripheral synthesis of these lipids and brain transport may be useful in understanding possible inter-relationships between plasma and brain lipid changes in response to GW agent exposure.

4.4.3.2. Lipid profiling of plasma PC and SM from mouse models of other neurological illnesses

These studies show that plasma PC and SM changes observed in CCI and mTBI are distinct from those observed in mouse models A and B of GW agent exposure. For CCI TBI, a significant number of individual molecular species were lower in CCI injured mice compared to control mice. For s-mTBI, there was an increase in the levels of SM but a decrease in the levels of PC among injured mice compared to control mice. However, for r-mTBI, injured mice had an increase in PC and SM levels compared to uninjured mice.

Although a direct comparison of mTBI with CCI TBI is not possible given the post-injury time difference between the two studies, if time was not a factor, it can be postulated that different head injuries produce different profiles, particularly for PC since all three types of injury produced distinct effects on total PC levels. In addition, these lipid profiles are distinct from those in mouse model A of GW agent exposure where only an increase in certain PC species was observed in exposed animals and there was no change in total PC and SM in GW agent exposed animals compared to controls. Mouse model B showed a decrease in a number of PC and SM molecular species but no change in total PC and SM levels. All SFA, MUFA and PUFA containing species were decreased in CCI injured compared to control mice. Interestingly, despite the differences in total PC profiles between s-mTBI and r-mTBI, for both injuries, there was a tendency for a decrease in MUFA containing PC compared to respective controls. In addition, there was a decrease in PUFA containing PC molecular species in s-mTBI compared to s-sham. For both models of GW agent exposure, there was a tendency towards SFA containing PC species being increased in exposed animals compared to controls. Thus, it can be hypothesized that different CNS insults produce distinct changes in plasma lipid profiles, which may be useful in differential diagnoses, particularly since the veteran population may include individuals with TBI and GWI. Further studies are required to determine the potential of such an approach in the discovery of biomarkers for CNS illnesses.

4.4.4. Use of lipidomics for pathway identification and target validation

Lipid profiling of mouse model B of GW agent exposure was also performed to determine the downstream consequences of PC changes in the brain and plasma in order to identify potential treatment targets. In the brain, FFA profiling showed that both AA and DHA were increased in mice exposed to GW agents compared to controls. Since downstream metabolites of AA include prostaglandins, which have pro-inflammatory actions, and DHA metabolites, which are considered anti-inflammatory, these studies

support the observed mixed inflammatory profile in veterans with GWI. Also of interest is 2AG, which is a monoacylglycerol (MAG) that contains esterified AA at the sn2 position of glycerol. The action of MAG lipase (MAGL) liberates AA from 2AG. 2-arachidonylglycerol is a major endogenous ligand of cannabinoid receptors and the downstream pathways controlled by these receptors mediate anti-inflammatory processes in the brain (Ueda et al 2001). Collectively, these studies show that lipid metabolites that are upstream of both pro- and anti-inflammatory biological pathways may be affected in mouse model B of GW agent exposure which is consistent with findings of increased production of both pro- and anti-inflammatory cytokines (mixed inflammation) in veterans suffering from GWI (Skowera et al 2004). Examination of bioactive lipid metabolites of AA and DHA as well as Th1 and Th2 cytokines may help in understanding the consequence of changes in these lipids.

Examination of the plasma FFA and LPC results also supports a mixed inflammation profile in the periphery, since LPC molecular species (e.g., LPC (18:1)) are directly shown to cause pro-inflammatory changes. Furthermore, AA and DHA were increased in exposed mice compared to controls, also supporting a concept of a mixed inflammatory response. A decrease in a number of PC molecular species, particularly those that contain AA, DHA and ePC together with a net increase in LPC levels suggests an increase in the PLA_2 activity in the periphery. Based on these changes, it can be predicted that drugs that affect LPC levels and/or PLA_2 activity may be useful for treating lipid abnormalities associated with GW agent exposure.

The literature suggests that a number of DHP-CCB can block LPC induced endothelial dysfunction, oxidative stress, AA release and increased plasma membrane fluidity (Golfman et al 1999) (Takayama et al 2009; Matsubara et al 2006). Given these reports, nilvadipine, a DHP-CCB, was used to conduct pilot treatment studies in a mouse model of GW agent exposure. One of the main goals of these studies was to determine if

PC and SM changes observed in the brain, and PC and LPC changes observed in plasma from CD1 mouse model B at about the 4 month post-exposure timepoint, were also observed at the 3-month post-exposure in C57BL6 mouse model B. Each of these timepoints shortly followed the timepoint at which cognitive impairment was observed in exposed mice compare to controls in each CD1 and C57BL6 strain. The second objective was to test whether the increase in LPC observed in plasma of GW agent exposed mice (from CD1 strain) can be normalized by nilvadipine. Our results support the effectiveness of such an approach. These studies show that the elevated PC and LPC levels in the plasma of GW agent exposed mice (C57BL6 stain) were reduced after treatment with nilvadipine and levels of these lipids were normalized to being similar to those from unexposed mice, which did not receive GW agents or nilvadipine treatment. However, for this C57BL6 strain, there were no differences between GW agent exposed mice compared to control mice in the brain PC and SM levels. Hence findings of elevated PC and SM in mouse model B from the CD1 strain were not observed in the C57BL6 strain. Also, there was no effect of nilvadipine treatment on PC and SM levels in the brain. As indicated in Chapter 2, C57BL6 mice have cholinergic and PLA_2 deficiencies, it is possible that the pathological trajectory in this strain is different, particularly since a lower PB dose was utilized than that employed for the original studies conducted using the CD1 mouse strain. Nevertheless, plasma data do support partial translation of lipidomics findings from the CD1 strain to the C57BL6 strain and do support a potential usefulness of such an approach in identifying treatment targets for GWI.

The lipidomic studies described in this chapter, although preliminary, show that examination of PLs may be useful in profiling biological changes in brain and plasma after exposure to GW agents. These studies also show that such an approach can identify profiles that are unique in each mouse model of GW agent exposure. These studies also identify a number of tractable lipid-metabolism related biological pathways as potential

targets for therapeutic intervention. Further investigation is warranted to fully understand the biological mechanisms that underlie these lipid changes and the treatment responses observed in this mouse model of GW agent exposure.

Chapter 5 - General discussion

Now nearly twenty years since the first Persian Gulf War conflict, veterans with GWI continue to suffer from this persistent and debilitating illness, which is characterized by the presence of widespread pain, headaches and cognitive difficulties (Binns et al 2008). Previously, GWI was thought to be a primarily somatic disorder; however, a number of recent findings show a prominent CNS component to this illness. In fact, it would appear that GWI has distinct CNS subtypes, which seem to differ from each other based on the presence of cognitive problems or motor related symptoms. Although a number of treatment approaches are being evaluated, currently there are no approved treatments available for GWI that can either provide symptomatic relief or target the underlying pathology. Similarly, there are no biomarkers available to assist with the diagnosis of GWI, as additional 50,000 GW veterans continue to suffer from unexplained illnesses but have not received a formal diagnosis of GWI. In addition, biomarkers are also needed to objectively diagnose GWI as the current diagnostic criteria rely heavily on self-report of symptoms which can be subject to reporting bias given that a long time has now elapsed since the original GW agent exposure and disease onset. Availability of a biomarker panel for diagnosing GWI may also be useful in developing and providing personalized care where the level of care and interventions provided to veterans could be tailored based on their diagnostic classification and severity of illness. Biomarkers of GWI may also be helpful in monitoring treatment response in future clinical trials for testing therapies against GWI.

According to a DoD report, in 1993, the Deputy Under Secretary of Defense introduced pest management initiatives which have resulted in improved standards and practices whereby there is now a 50% reduction of pesticides use on military installations,

improved training of pesticide applicators and an increased awareness among military personnel of pesticide use. For instance, only a 20-33% DEET formulation is now provided to military personnel involved in Operation Iraqi Freedom compare to the 75% DEET that was issued during the first Gulf War. However, troops in current deployments have had access to uniforms that were pretreated with PER (Binns et al 2008).

In the civilian population, use of pesticides is of concern and has been implicated in a number of neurological illnesses. For instance, findings from a prospective longitudinal study of a Cache county (Utah, USA) cohort provide evidence that the use of organophosphate AChE inhibitors can increase the risk of AD and related disorders (Hayden et al 2010). Results from a 4-year prospective study conducted on agriculture workers in the Bordeaux region of France provide compelling evidence for an increased risk of neurocognitive decline among individuals with direct exposure to pesticides in midlife (Baldi et al 2011). In recent years, the Environmental Protection Agency (EPA) has initiated a phaseout of urban uses of organophosphates (OP) (2002). This has consequently resulted in a switch to other easily available pesticides and nearly 100 million applications of PER are made each year in US homes (Power, & Sudakin 2007; Cox1998). Data from the American Association of Poison Control Centers Toxic Exposure Surveillance System (TESS) show an increase in reporting of pyrethroid exposure related adverse events correlating with a decline in reporting of OP related incidences (Power, & Sudakin 2007). As such, exposure to these chemicals may further increase the incidence of neurological disorders. Therefore, understanding the molecular mechanisms of such exposures may help identify pesticide-related neurocognitive dysfunction so that appropriate corrective measures may be taken to reduce the CNS complications associated with pesticide use. Although the current work is performed within the context of GWI, these findings provide novel insights into the neurotoxic mechanisms associated with these chemicals.

A series of well-conducted epidemiological studies provide excellent support for the theory that a combined exposure to PB, pesticides and an insect repellent (DEET) may be one of the main causative factors in this illness. The current scientific consensus is that an increased risk of GWI is associated with combined exposure, to PB and pesticides/insect repellents (Binns et al 2008). Studies by Haley and colleagues suggest that perhaps exposure to different combinations of these GW agents may have produced different sub-syndromes of GWI; one that is generally characterized by cognitive impairment and associated with combined PB and PER exposure, and the other characterized by confusion, ataxia and motor type impairment and associated with PB and DEET (Haley et al 1997). Hence, a complicated symptom presentation and the heterogeneity of the original exposures are two major challenges for studies that are aimed at elucidating the pathogenic mechanisms and the discovery of suitable treatments.

A considerable time has elapsed since the original exposure and therefore it is imperative that studies focus on long-term outcomes associated with GWI. The work performed as part of this thesis presents a systematic attempt to identify the underlying chronic pathological features of GWI by examining chronic timepoints in rodents after GW agent exposure. Data presented in Chapter 2 show that various combinations and doses of PB, PER, DEET and stress, when given to mice, can produce a number of neurobehavioral changes that are similar to the symptoms observed in veterans with GWI. For example, in mouse model A of GW agent exposure, combined exposure to PB, PER, DEET and stress produced significant motor and anxiety-like symptoms that are consistent with symptoms observed in veterans with GWI. These studies also provide novel insight into gender differences in the presentation of neurobehavioral symptoms after GW agent exposure. However, no cognitive deficits were evident in this model. This profile appears similar to GW Syndrome 3 associated with PB and DEET and includes symptoms such as confusion, ataxia and motor related problems (Haley et al 1997). In order to determine if

GW agent exposure can produce cognitive neurobehavioral deficits, mouse model B was developed, in which mice were exposed to high doses of PB and PER. In this model, neurobehavioral testing showed a delayed appearance of cognitive symptoms, at 115 days post-exposure. Also, there was some evidence for psychomotor and anxiety related problems. However, no sensorimotor deficits were observed in mouse model B of GW agent exposure. This symptom profile and exposure combination appears similar to GW Syndrome 1 that was associated with PB and PER exposure and included cognitive impairment as a symptom (Haley et al 1997). Pathological examination revealed a presence of astrogliosis but no overt neuronal death or microgliosis. Collectively, these studies show that exposure to different combinations of GW agents produces distinct CNS symptom profiles but may share most of the same underlying pathology. This is evident by neuropathological studies showing profound astrogliosis in both mouse models of GW agent exposure but no neuronal loss or microgliosis.

In Chapter 3, exploratory proteomic approaches were found to be extremely useful in identifying global biological changes. This approach was particularly useful in these GWI research studies given the complexity of clinical presentation and the diversity of etiological exposures, and an unknown course of the disease progression. Examination of several biological pathways using proteomics provided a comprehensive view of the pathological mechanisms in a single experiment. Proteomic studies coupled with bioinformatic analyses suggested that in mouse model B, a number of immune and inflammatory related changes may be present in the brain and blood of exposed mice compared to control mice. These findings are supported by studies conducted on blood cells from veterans with GWI that show an increased presence of both pro- and anti-inflammatory cytokines in ill veterans compared to controls.

These studies resulted in additional support to the Institute (PI: Ait-Ghezala) from the DoD to explore immune and inflammation related dysfunction associated with GW agent

exposure. Proteomic findings from mouse model B also support endocrine dsyfunction, which is already being evaluated as an avenue for identifying potential treatments and biomarkers for GWI by Dr. Golier at the Bronx Veterans' Administration (VA) Hospital.

The data in Chapter 4 of this thesis presented lipidomic studies that were undertaken to examine biological pathways that may be upstream of ACh-related biological changes. As a number of lipid metabolites are upstream of immune and inflammation pathways, examination of phospholipids (particularly those containing choline) may also be helpful in understanding mixed inflammation (both pro- and anti-inflammatory) and related changes that are observed in veterans with GWI. Lipid profiling showed that changes in PC and SM from mouse models of GW agent exposure were distinct from those observed in other neurological illnesses. In general, compared to their respective control groups, both models of GW agent exposure showed an increase in PC and SM levels where the PSAPPswe mouse model of AD showed a decrease in PC and SM levels. Brain region dependent lipidomic studies showed considerable differences in total PC and SM levels and a differential response to head injury within these brain regions. These studies highlight that future examination of lipidomic profiles by brain region in may provide some important information on the pathological consequences of GW agent exposure.

From the aspect of biomarker discovery, plasma lipidomic work was undertaken as a follow-up to proteomic studies from mouse model B of GW agent exposure, which had detected a number of immune, inflammatory and lipid metabolism related changes in the plasma of GW agent exposed animals. Lipidomic studies conducted using plasma samples of mouse models of GW agent exposure showed that although ePC, diacyl PC containing PUFA and SM containing VLCFA were affected in both mouse models of GW agent exposure, the profiles were distinct for each mouse model with respect to the direction of changes in PC and SM and specific molecular species that were altered. These studies highlight a potential usefulness of lipidomics in classification of different sub-syndromes

of GWI. Major efforts are now underway at the Roskamp Institute geared towards translating biomarker discovery work from preclinical to clinical stage, where a direct examination of blood samples from veterans with GWI will be undertaken in the near future. This work, aimed at using Omics technology for the discovery and validation of biomarkers of GWI, is proposed as part of a collaborative multi-center application (PI: Fiona Crawford) and involves collection of samples from GWI patients at the James J Peters VA Medical center in Bronx, NY and the Boston VA Medical Center, Boston MA.

Chapter 4 also included pilot lipidomic work aimed at determining if the biological pathways that metabolize PC to LPC may be involved in the neurobehavioral and neuropathological abnormalities observed in mouse models of GW agent exposure. For mouse model A of GW agent exposure, examination of the brain PC and SM suggested dysfunction of the peroxisomal pathways and examination of the degree of unsaturation of PC suggested an abnormal increase in SCD activity in response to this GW agent exposure. For mouse model B, data from the brain and blood samples suggested that perhaps PLA_2 activity (or enzymes that have similar action to PLA_2) might be affected in response to GW agents. Recently, neuropathy target esterase (NTE), a major target of OP pesticide AChE inhibitors, was shown to have similar activity for hydrolyzing brain PC and LPC (Casida et al 2008). A number of studies show that inhibition of NTE by OP pesticides can lead to an abnormal accumulation of PC in the brain (Read et al 2009). It is therefore reasonable to propose that phospholipases involved in PC metabolism might be affected in response to GW agents. Since studies suggested that DHP-CCB can mitigate the adverse effects of LPC, nilvadipine was chosen for pilot treatment studies, since extensive preclinical safety and pharmacokinetics profiling of this drug has already been conducted at the Roskamp Institute. Pilot studies using nilvadipine showed that PC and LPC levels in plasma are amenable to targeting and that nilvadipine can "normalize" the GW agent induced lipid changes. Future studies in this area may be of value in discovering

treatments for GWI. Another interesting aspect of OP pesticide exposure that appears similar to GW agent exposure is the observation that levels of 2AG appear to increase after exposure to OP (Casida et al 2008) and after GW agent exposure (as observed here). Studies show that OP could directly inhibit activities of MAGL, leading to an increase in 2AG levels (Casida et al 2008). These findings suggest that perhaps examination of MAGL might also be an avenue worth exploring in future studies aimed at identifying GWI treatments.

Conclusion and future direction

The work described in this thesis has made significant advances towards developing well-characterized mouse models of GW agent exposure, in which the complexity of biological responses to exposures was captured using global proteomic approaches. Lipidomic approaches were used to fully characterize phosphocholine containing lipids in order to perform comprehensive evaluation of the brain and blood changes to identify biomolecular pathways that might be affected in response to GW agent exposure. These studies will help identify potential targets for therapeutic interventions in work that is already underway at the Roskamp Institute as well as future work aimed at identifying diagnostic biomarkers of GWI. As described above, the findings reported here have opened several novel avenues of investigation which are now part of planned projects that are now funded by the department of defense or the Veteran's Administration. It is anticipated that the future work based on these findings will provide tangible treatment targets and possibly lead to the discovery and validation of objective biomarkers of GWI.

References:

Abdel-Rahman, A., Abou-Donia, S., El-Masry, E., Shetty, A. & Abou-Donia, M., 2004, Stress and combined exposure to low doses of pyridostigmine bromide, DEET, and permethrin produce neurochemical and neuropathological alterations in cerebral cortex, hippocampus, and cerebellum, *Journal of toxicology and environmental health. Part A*, 67(2), pp. 163-92.

Abdel-Rahman, A., Shetty, A.K. & Abou-Donia, M.B., 2002, Disruption of the blood-brain barrier and neuronal cell death in cingulate cortex, dentate gyrus, thalamus, and hypothalamus in a rat model of Gulf-War syndrome, *Neurobiology of Disease*, 10(3), pp. 306-26.

Abdullah, L., Crynen, G., Reed, J., Bishop, A., Phillips, J., Ferguson, S., Mouzon, B., Mullan, M., Mathura, V., Mullan, M., Ait-Ghezala, G. & Crawford, F., 2011, Proteomic CNS profile of delayed cognitive impairment in mice exposed to Gulf War agents, *Neuromolecular medicine*, 13(4), pp. 275-88.

Abdullah L, Evans JE, Bishop A, Reed JM, Crynen G, Phillips J, Pelot R, Mullan MA, Ferro A, Mullan CM, Mullan MJ, Ait-Ghezala G, Crawford FC. Lipidomic Profiling of Phosphocholine Containing Brain Lipids in Mice with Sensorimotor Deficits and Anxiety-Like Features After Exposure to Gulf War Agents. *Neuromolecular Med.* 2012 Jul 14 [epub ahead of print].

Abou-Donia, M.B., Dechkovskaia, A.M., Goldstein, L.B., Abdel-Rahman, A., Bullman, S.L. & Khan, W.A., 2004, Co-exposure to pyridostigmine bromide, DEET, and/or permethrin causes sensorimotor deficit and alterations in brain acetylcholinesterase activity, *Pharmacology Biochemistry and Behavior*, 77(2), pp. 253-62.

Abou-Donia, M.B., Goldstein, L.B., Jones, K.H., Abdel-Rahman, A.A., Damodaran, T.V., Dechkovskaia, A.M., Bullman, S.L., Amir, B.E. & Khan, W.A., 2001, Locomotor and

sensorimotor performance deficit in rats following exposure to pyridostigmine bromide, DEET, and permethrin, alone and in combination, *Toxicological sciences : an official journal of the Society of Toxicology*, 60(2), pp. 305-14.

Adibhatla, R.M. & Hatcher, J.F., 2008, Altered lipid metabolism in brain injury and disorders, *Sub-cellular biochemistry*, 49, pp. 241-68.

Aguilar, R., Gil, L., Flint, J., Gray, J.A., Dawson, G.R., Driscoll, P., Giménez-Llort, L., Escorihuela, R.M., Fernández-Teruel, A. & Tobeña, A., 2002, Learned fear, emotional reactivity and fear of heights: a factor analytic map from a large F2 intercross of Roman rat strains, *Brain Research Bulletin*, 57(1), pp. 17-26.

Amenta, F. & Tayebati, S.K., 2008, Pathways of acetylcholine synthesis, transport and release as targets for treatment of adult-onset cognitive dysfunction, *Current medicinal chemistry*, 15(5), pp. 488-98.

Amourette, C., Lamproglou, I., Barbier, L., Fauquette, W., Zoppe, A., Viret, R. & Diserbo, M., 2009, Gulf War illness: Effects of repeated stress and pyridostigmine treatment on blood-brain barrier permeability and cholinesterase activity in rat brain, *Behavioural brain research*, 203(2), pp. 207-14.

Aquilonius, S.M., Eckernäs, S.A., Hartvig, P., Lindström, B., Osterman, P.O. & Stålberg, E., 1983, Clinical pharmacology of pyridostigmine and neostigmine in patients with myasthenia gravis, *Journal of neurology, neurosurgery, and psychiatry*, 46(10), pp. 929-35.

Bach, G., Perrin-Cocon, L., Gerossier, E., Guironnet-Paquet, A., Lotteau, V., Inchauspé, G. & Fournillier, A., 2010, Single lysophosphatidylcholine components exhibit adjuvant activities in vitro and in vivo, *Clin Vaccine Immunol*, 17(3), pp. 429-38.

Baker, P.R., Calvey, T.N., Chan, K., Macnee, C.M. & Taylor, K., 1978, Plasma clearance of neostigmine and pyridostigmine in the dog, *British journal of pharmacology*, 63(3), pp. 509-12.

Baldi, I., Gruber, A., Rondeau, V., Lebailly, P., Brochard, P. & Fabrigoule, C., 2011, Neurobehavioral effects of long-term exposure to pesticides: results from the 4-year follow-up of the PHYTONER study, *Occupational and environmental medicine*, 68(2), pp. 108-15.

Bansal, I., Waghmare, C.K., Anand, T., Gupta, A.K. & Bhattacharya, B.K., 2009, Differential mRNA expression of acetylcholinesterase in the central nervous system of rats with acute and chronic exposure of sarin & physostigmine, *J Appl Toxicol*, 29(5), pp. 386-94.

Bantscheff, M., Boesche, M., Eberhard, D., Matthieson, T., Sweetman, G. & Kuster, B., 2008, Robust and Sensitive iTRAQ Quantification on an LTQ Orbitrap Mass Spectrometer, *Molecular & Cellular Proteomics*, 7(9), pp. 1702-13.

Barbier, L., Diserbo, M., Lamproglou, I., Amourette, C., Peinnequin, A. & Fauquette, W., 2009, Repeated stress in combination with pyridostigmine Part II: changes in cerebral gene expression, *Behavioural brain research*, 197(2), pp. 292-300.

Bayes, A. & Grant, S.G.N., 2009, Neuroproteomics: understanding the molecular organization and complexity of the brain, *Nature reviews. Neuroscience*, 10(9), pp. 635-46.

Berta, S., Gert, L., Harald, H. & Sudarshan, P., 2007, Barnes maze, a useful task to assess spatial reference memory in the mice. Nature protocols.

Binns, Barlow, Clauw, Golomb, Graves, Hardie, Knox, Meggs, Nettleman, O'Callaghan, Smithson, Steele & White, 2008, Gulf War Illness and the Health of Gulf War Veterans, *Report from Research Advisory Committee on Gulf War Veterans' Illness*.

Blanchard, D.C., Griebel, G. & Blanchard, R.J., 2001, Mouse defensive behaviors: pharmacological and behavioral assays for anxiety and panic, *Neuroscience; Biobehavioral Reviews*, 25(3), pp. 205-18.

Bondolfi, L., Calhoun, M., Ermini, F., Kuhn, H.G., Wiederhold, K.-H., Walker, L., Staufenbiel, M. & Jucker, M., 2002, Amyloid-Associated Neuron Loss and Gliogenesis in

the Neocortex of Amyloid Precursor Protein Transgenic Mice, *The Journal of Neuroscience*, 22(2), pp. 515-22.

Boomsma & Parthasarthy, 1990, Huan use and exposure to insect repellents containing DEET., *EPA report.*

Broderick, G., Kreitz, A., Fuite, J., Fletcher, M.A., Vernon, S.D. & Klimas, N., 2011, A pilot study of immune network remodeling under challenge in Gulf War Illness, *Brain, behavior, and immunity*, 25(2), pp. 302-13.

Broglio, F., Gottero, C., Van Koetsveld, P., Prodam, F., Destefanis, S., Benso, A., Gauna, C., Hofland, L., Arvat, E. & van der Lely, A.J., 2004, Acetylcholine regulates ghrelin secretion in humans, *Journal of Clinical Endocrinology & Metabolism*, 89(5), pp. 2429-33.

Brouwers, J.F., 2011, Liquid chromatographic-mass spectrometric analysis of phospholipids. Chromatography, ionization and quantification, *Biochimica et biophysica acta*, 1811(11), pp. 763-75.

Carter, S.F., Schöll, M., Almkvist, O., Wall, A., Engler, H., Långström, B. & Nordberg, A., 2012, Evidence for Astrocytosis in Prodromal Alzheimer Disease Provided by 11C-Deuterium-L-Deprenyl: A Multitracer PET Paradigm Combining 11C-Pittsburgh Compound B and 18F-FDG, *Journal of Nuclear Medicine*, 53(1), pp. 37-46.

Casida, J.E., Nomura, D.K., Vose, S.C. & Fujioka, K., 2008, Organophosphate-sensitive lipases modulate brain lysophospholipids, ether lipids and endocannabinoids, *Chemico-biological interactions*, 175(1-3), pp. 355-64.

Chaney, L.A., Rockhold, R.W. & Hume, A.S., 2002, Cardiorespiratory Effects Following Acute Exposure to Pyridostigmine Bromide and/or N,N-Diethyl-m-toluamide (DEET) in Rats, *International journal of toxicology*, 21(4), pp. 287-300.

Chaney, L.A., Wineman, R.W., Rockhold, R.W. & Hume, A.S., 2000, Acute effects of an insect repellent, N,N-diethyl-m-toluamide, on cholinesterase inhibition induced by

pyridostigmine bromide in rats, *Toxicology and applied pharmacology*, 165(2), pp. 107-14.

Chiasserini, D., Parnetti, L., Andreasson, U., Zetterberg, H., Giannandrea, D., Calabresi, P. & Blennow, K., 2010, CSF Levels of Heart Fatty Acid Binding Protein are Altered During Early Phases of Alzheimer's Disease, *Journal of Alzheimer's Disease*, 22(4), pp. 1281-8.

Corbel, V., Stankiewicz, M., Bonnet, J., Grolleau, F., Hougard, J.M. & Lapied, B., 2006, Synergism between insecticides permethrin and propoxur occurs through activation of presynaptic muscarinic negative feedback of acetylcholine release in the insect central nervous system, *Neurotoxicology*, 27(4), pp. 508-19.

Corbel, V., Stankiewicz, M., Pennetier, C., Fournier, D., Stojan, J., Girard, E., Dimitrov, M., Molgó, J., Hougard, J.M. & Lapied, B., 2009, Evidence for inhibition of cholinesterases in insect and mammalian nervous systems by the insect repellent deet, *BMC Biol*, 7, p. 47.

Cowan, D.N., Lange, J.L., Heller, J., Kirkpatrick, J. & DeBakey, S., 2002, A case-control study of asthma among U.S. Army Gulf War veterans and modeled exposure to oil well fire smoke, *Military medicine*, 167(9), pp. 777-82.

Cox, Permethrin, *Journal of Pesticide Reform*, 18(2), pp. 14-20.

Crawford, F., Crynen, G., Reed, J., Mouzon, B., Bishop, A., Katz, B., Ferguson, S., Phillips, J., Ganapathi, V., Mathura, V., Roses, A. & Mullan, M., 2012, Identification of plasma biomarkers of TBI outcome using proteomic approaches in an APOE mouse model, *J Neurotrauma*, 29(2), pp. 246-60.

Crynen, Wood, Mouzon, Ferguson, Mullan & Crawford, 2012, Human Neuronal Genomic Response to Combinations of Gulf War Agents, *TBA (in preparation)*.

David, A.S., Farrin, L., Hull, L., Unwin, C., Wessely, S. & Wykes, T., 2002, Cognitive functioning and disturbances of mood in UK veterans of the Persian Gulf War: a comparative study, *Psychological medicine*, 32(8), pp. 1357-70.

Dodd, C.A. & Klein, B.G., 2009, Pyrethroid and organophosphate insecticide exposure in the 1-methyl-4-phenyl-1,2,3,6-tetrahydropyridine mouse model of Parkinson's disease: an immunohistochemical analysis of tyrosine hydroxylase and glial fibrillary acidic protein in dorsolateral striatum, *Toxicology and Industrial Health*, 25(1), pp. 25-39.

Donta, S.T., Clauw, D.J., Engel, C.C., Guarino, P., Peduzzi, P., Williams, D.A., Skinner, J.S., Barkhuizen, A., Taylor, T., Kazis, L.E., Sogg, S., Hunt, S.C., Dougherty, C.M., Richardson, R.D., Kunkel, C., Rodriguez, W., Alicea, E., Chiliade, P., Ryan, M., Gray, G.C., Lutwick, L., Norwood, D., Smith, S., Everson, M., Blackburn, W., Martin, W., Griffiss, J.M., Cooper, R., Renner, E., Schmitt, J., McMurtry, C., Thakore, M., Mori, D., Kerns, R., Park, M., Pullman-Mooar, S., Bernstein, J., Hershberger, P., Salisbury, D.C., Feussner, J.R. & VA Cooperative Study #470 Study Group, 2003, Cognitive behavioral therapy and aerobic exercise for Gulf War veterans' illnesses: a randomized controlled trial, *JAMA: the journal of the American Medical Association*, 289(11), pp. 1396-404.

Donta, S.T., Engel, C.C., Collins, J.F., Baseman, J.B., Dever, L.L., Taylor, T., Boardman, K.D., Kazis, L.E., Martin, S.E., Horney, R.A., Wiseman, A.L., Kernodle, D.S., Smith, R.P., Baltch, A.L., Handanos, C., Catto, B., Montalvo, L., Everson, M., Blackburn, W., Thakore, M., Brown, S.T., Lutwick, L., Norwood, D., Bernstein, J., Bacheller, C., Ribner, B., Church, L.W., Wilson, K.H., Guduru, P., Cooper, R., Lentino, J., Hamill, R.J., Gorin, A.B., Gordan, V., Wagner, D., Robinson, C., DeJace, P., Greenfield, R., Beck, L., Bittner, M., Schumacher, H.R., Silverblatt, F., Schmitt, J., Wong, E., Ryan, M.A., Figueroa, J., Nice, C., Feussner, J.R. & VA Cooperative #475 Group, 2004, Benefits and harms of doxycycline treatment for Gulf War veterans' illnesses: a randomized, double-blind, placebo-controlled trial, *Annals of internal medicine*, 141(2), pp. 85-94.

Farooqui, A.A., Horrocks, L.A. & Farooqui, T., 2007, Interactions between neural membrane glycerophospholipid and sphingolipid mediators: a recipe for neural cell survival or suicide, *Journal of neuroscience research*, 85(9), pp. 1834-50.

Faul & Erdfelder, 2007, G*Power 3: a flexible statistical power analysis program for the social, behavioral, and biomedical sciences, *Behav Res Methods*, 39(2), pp. 175-91.

Filiou, M.D., Martins-de-Souza, D., Guest, P.C., Bahn, S. & Turck, C.W., 2012, To label or not to label: applications of quantitative proteomics in neuroscience research, *Proteomics*, 12(4-5), pp. 736-47.

Fisher, A., 2012, Cholinergic modulation of amyloid precursor protein processing with emphasis on M1 muscarinic receptor: perspectives and challenges in treatment of Alzheimer's disease, *Journal of neurochemistry*, 120 Suppl 1, pp. 22-33.

Folch, Lees & Slone Stanely, 1957, A simple method for the isolation and purification of total lipides from animal tissues, *J Biol. Chem.*, 226, pp. 497-509.

Fox, L.M., Cox, D.G., Lockridge, J.L., Wang, X., Chen, X., Scharf, L., Trott, D.L., Ndonye, R.M., Veerapen, N., Besra, G.S., Howell, A.R., Cook, M.E., Adams, E.J., Hildebrand, W.H. & Gumperz, J.E., 2009, Recognition of lyso-phospholipids by human natural killer T lymphocytes, *PLoS Biol*, 7(10), p. e1000228.

Fredman, G. & Serhan, C.N., 2011, Specialized proresolving mediator targets for RvE1 and RvD1 in peripheral blood and mechanisms of resolution, *The Biochemical journal*, 437(2), pp. 185-97.

Friedman, A., Kaufer, D., Shemer, J., Hendler, I., Soreq, H. & Tur-Kaspa, I., 1996, Pyridostigmine brain penetration under stress enhances neuronal excitability and induces early immediate transcriptional response, *Nat Med*, 2(12), pp. 1382-5.

Fu, Q., Garnham, C.P., Elliott, S.T., Bovenkamp, D.E. & Van Eyk, J.E., 2005, A robust, streamlined, and reproducible method for proteomic analysis of serum by delipidation, albumin and IgG depletion, and two-dimensional gel electrophoresis, *Proteomics*, 5(10), pp. 2656-64.

Gallegos, C.E., Pediconi, M.F. & Barrantes, F.J., 2008, Ceramides modulate cell-surface acetylcholine receptor levels, *Biochimica et Biophysica Acta (BBA)* -

Biomembranes, 1778(4), pp. 917-30.

Ghigo, E., Goffi, S., Arvat, E., Nicolosi, M., Procopio, M., Bellone, J., Imperiale, E., Mazza, E., Baracchi, G. & Camanni, F., 1990, Pyridostigmine partially restores the GH responsiveness to GHRH in normal aging, *Acta Endocrinologica*, 123(2), pp. 169-73.

Golfman, Haughey, Wong, Jiang, Lee, Geiger & Choy, 1999, Lysophosphatidylcholine induces arachidonic acid release

and calcium overload in cardiac myoblastic H9c2 cells , *Journal of lipid research*, 40, pp. 1818-26.

Golier, J.A., Schmeidler, J. & Yehuda, R., 2009, Pituitary response to metyrapone in Gulf War veterans: relationship to deployment, PTSD and unexplained health symptoms, *Psychoneuroendocrinology*, 34(9), pp. 1338-45.

Golomb, B.A., 2008, Acetylcholinesterase inhibitors and Gulf War illnesses, *Proceedings of the National Academy of Sciences of the United States of America*, 105(11), pp. 4295-300.

Goodyer, L. & Behrens, R.H., 1998, Short report: The safety and toxicity of insect repellents, *The American journal of tropical medicine and hygiene*, 59(2), pp. 323-4.

Gorgas, K., Teigler, A., Komljenovic, D. & Just, W.W., 2006, The ether lipid-deficient mouse: tracking down plasmalogen functions, *Biochimica et biophysica acta*, 1763(12), pp. 1511-26.

Graessler, J., Schwudke, D., Schwarz, P.E., Herzog, R., Shevchenko, A. & Bornstein, S.R., 2009, Top-down lipidomics reveals ether lipid deficiency in blood plasma of hypertensive patients, *PloS one*, 4(7), p. e6261.

Grauer, E., Nathan, D.B., Lustig, S., Kobiler, D., Kapon, J. & Danenberg, H.D., 2001, Viral neuroinvasion as a marker for BBB integrity following exposure to cholinesterase inhibitors, *Life sciences*, 68(9), pp. 985-90.

Gray, G.C., Kaiser, K.S., Hawksworth, A.W., Hall, F.W. & Barrett-Connor, E., 1999, Increased postwar symptoms and psychological morbidity among U.S. Navy Gulf War veterans, *The American journal of tropical medicine and hygiene*, 60(5), pp. 758-66.

Rook, G.A., Zumla, A. 1997 Gulf War syndrome: is it due to a systemic shift in cytokine balance towards a Th2 profile? *Lancet* 349(9068):1831-3.

Haley, R.W., 1997, Is Gulf War syndrome due to stress? The evidence reexamined, *American journal of epidemiology*, 146(9), pp. 695-703.

Haley, R.W., Kurt, T.L. & Hom, J., 1997, Is there a Gulf War Syndrome? Searching for syndromes by factor analysis of symptoms, *JAMA : the journal of the American Medical Association*, 277(3), pp. 215-22.

Haley, R.W., Spence, J.S., Carmack, P.S., Gunst, R.F., Schucany, W.R., Petty, F., Devous, M.D., Bonte, F.J. & Trivedi, M.H., 2009, Abnormal brain response to cholinergic challenge in chronic encephalopathy from the 1991 Gulf War, *Psychiatry research*, 171(3), pp. 207-20.

Haley, R.W., Vongpatanasin, W., Wolfe, G.I., Bryan, W.W., Armitage, R., Hoffmann, R.F., Petty, F., Callahan, T.S., Charuvastra, E., Shell, W.E., Marshall, W.W. & Victor, R.G., 2004, Blunted circadian variation in autonomic regulation of sinus node function in veterans with Gulf War syndrome, *The American journal of medicine*, 117(7), pp. 469-78.

Hasegawa, H., Lei, J., Matsumoto, T., Onishi, S., Suemori, K. & Yasukawa, M., 2011, Lysophosphatidylcholine enhances the suppressive function of human naturally occurring regulatory T cells through TGF-β production, *Biochemical and biophysical research communications*, 415(3), pp. 526-31.

Hayden, K.M., Norton, M.C., Darcey, D., Ostbye, T., Zandi, P.P., Breitner, J.C., Welsh-Bohmer, K.A. & Cache County Study Investigators, 2010, Occupational exposure to pesticides increases the risk of incident AD: the Cache County study, *Neurology*, 74(19), pp. 1524-30.

Hilborne, Golomb, Marshall, Davis & Sherbourne, 2005, Examining possible causes of Gulf War Illness: RAND Policy Investigation and Reviews of the Scientific Literature, *RAND Survey*, RB-7544-OSD.

Hill, E.G., Schwacke, J.H., Comte-Walters, S., Slate, E.H., Oberg, A.L., Eckel-Passow, J.E., Therneau, T.M. & Schey, K.L., 2008, A statistical model for iTRAQ data analysis, *Journal of proteome research*, 7(8), pp. 3091-101.

Hoy, Cornell, Karlix, Tebbett & Van Haaren, 2000, Repeated coadministrations of pyridostigmine bromide, DEET, and permethrin alter locomotor behavior of rats, *Veterinary and human toxicology*, 42(2), pp. 72-6

Hoy, J.B., Cody, B.A., Karlix, J.L., Schmidt, C.J., Tebbett, I.R., Toffollo, S., Van Haaren, F. & Wielbo, D., 1999, Pyridostigmine bromide alters locomotion and thigmotaxis of rats: gender effects, *Pharmacology, biochemistry, and behavior*, 63(3), pp. 401-6.

Isacson, O., Seo, H., Lin, L., Albeck, D. & Granholm, A.-C., 2002, Alzheimer's disease and Down's syndrome: roles of APP, trophic factors and ACh, *Trends in Neurosciences*, 25(2), pp. 79-84.

Jackson & Woods, 2009, Direct profiling of tissue lipids by MALDI-TOFMS, *Journal of chromatography. B, Analytical technologies in the biomedical and life sciences*, 877(26), pp. 2822-9.

Jones, C.K., Brady, A.E., Davis, A.A., Xiang, Z., Bubser, M., Tantawy, M.N., Kane, A.S., Bridges, T.M., Kennedy, J.P., Bradley, S.R., Peterson, T.E., Ansari, M.S., Baldwin, R.M., Kessler, R.M., Deutch, A.Y., Lah, J.J., Levey, A.I., Lindsley, C.W. & Conn, P.J., 2008, Novel selective allosteric activator of the M1 muscarinic acetylcholine receptor regulates amyloid processing and produces antipsychotic-like activity in rats, *The Journal of neuroscience: the official journal of the Society for Neuroscience*, 28(41), pp. 10422-33.

Jortner, B.S., 2006, The return of the dark neuron. A histological artifact complicating contemporary neurotoxicologic evaluation, *Neurotoxicology*, 27(4), pp. 628-34.

Kabarowski, J.H., 2009, G2A and LPC: Regulatory functions in immunity, *Prostaglandins & other lipid mediators*, 89(3–4), pp. 73-81.

Katz, M.H., 2011, *Multivariable analysis: a practical guide for clinicians and public health researchers,* Cambridge University Press, Cambridge; New York.

Kayihan, G.C., Wood, M., Mouzon, B., Ferguson, S., Margenthaler, E., Mathura, V., Mullan, M. & Crawford, F., 2010, Gulf War agents trigger discrete transcriptional changes in human neuronal cells, *Toxicological & Environ Chemistry*, 92(9), pp. 1783-99.

Kroenke, K., Koslowe, P. & Roy, M., 1998, Symptoms in 18,495 Persian Gulf War Veterans: Latency of Onset and Lack of Association with Self-Reported Exposures, *Journal of occupational and environmental medicine / American College of Occupational and Environmental Medicine*, 40(6), pp. 520-8.

Kumar-Singh, McGowan, Serbeeks, Dickson, Hardy & Van Broekhaven, 2005, Dense-Core Plaques in Tg2576 and PSAPP Mouse Models of Alzheimer's Disease Are Centered on Vessel Walls , *Neurobiology*, 167(2).

Kurt, T.L., 1998, Epidemiological association in US veterans between Gulf War illness and exposures to anticholinesterases, *Toxicology letters*, 102-103, pp. 523-6.

Lamproglou, I., Barbier, L., Diserbo, M., Fauvelle, F., Fauquette, W. & Amourette, C., 2009, Repeated stress in combination with pyridostigmine Part I: long-term behavioural consequences, *Behavioural brain research*, 197(2), pp. 301-10.

Lange, G., Tiersky, L.A., Scharer, J.B., Policastro, T., Fiedler, N., Morgan, T.E. & Natelson, B.H., 2001, Cognitive functioning in Gulf War Illness, *Journal of clinical and experimental neuropsychology*, 23(2), pp. 240-9.

Lange, J.L., Schwartz, D.A., Doebbeling, B.N., Heller, J.M. & Thorne, P.S., 2002, Exposures to the Kuwait oil fires and their association with asthma and bronchitis among gulf war veterans, *Environmental health perspectives*, 110(11), pp. 1141-6.

Li, B., Mahan, C.M., Kang, H.K., Eisen, S.A. & Engel, C.C., 2011a, Longitudinal

health study of US 1991 Gulf War veterans: changes in health status at 10-year follow-up, *American journal of epidemiology*, 174(7), pp. 761-8.

Li, X., Spence, J.S., Buhner, D.M., Hart, J., Cullum, C.M., Biggs, M.M., Hester, A.L., Odegard, T.N., Carmack, P.S., Briggs, R.W. & Haley, R.W., 2011b, Hippocampal dysfunction in Gulf War veterans: investigation with ASL perfusion MR imaging and physostigmine challenge, *Radiology*, 261(1), pp. 218-25.

Liu, P., Aslan, S., Li, X., Buhner, D.M., Spence, J.S., Briggs, R.W., Haley, R.W. & Lu, H., 2011, Perfusion deficit to cholinergic challenge in veterans with Gulf War Illness, *Neurotoxicology*, 32(2), pp. 242-6.

Lue, L.F., Kuo, Y.M., Beach, T. & Walker, D.G., 2010, Microglia activation and anti-inflammatory regulation in Alzheimer's disease, *Molecular neurobiology*, 41(2-3), pp. 115-28.

MAclennan KM, Smith & Darlington, 1996, Platelet-Activating Factors in the CNS, *Progress in Neurobiology*, 50, pp. 585-96.

Mankidy, R., Ahiahonu, P.W., Ma, H., Jayasinghe, D., Ritchie, S.A., Khan, M.A., Su-Myat, K.K., Wood, P.L. & Goodenowe, D.B., 2010, Membrane plasmalogen composition and cellular cholesterol regulation: a structure activity study, *Lipids in health and disease*, 9, p. 62.

Maruff, P. & Falleti, M., 2005, Cognitive Function in Growth Hormone Deficiency and Growth Hormone Replacement, *Hormone Research in Paediatrics*, 64(Suppl. 3), pp. 100-8.

Masuda, T., Tomita, M. & Ishihama, Y., 2008, Phase Transfer Surfactant-Aided Trypsin Digestion for Membrane Proteome Analysis, *J Proteome Res*, 7(2), pp. 731-40.

Matsubara, M., Yao, K. & Hasegawa, K., 2006, Benidipine, a dihydropyridine-calcium channel blocker, inhibits lysophosphatidylcholine-induced endothelial injury via stimulation of nitric oxide release, *Pharmacological Research*, 53(1), pp. 35-43.

Matsuura, E., Shen, L., Matsunami, Y., Quan, N., Makarova, M., Geske, F.J., Boisen, M., Yasuda, S., Kobayashi, K. & Lopez, L.R., 2010, Pathophysiology of beta2-glycoprotein I in antiphospholipid syndrome, *Lupus*, 19(4), pp. 379-84.

Mauck, B., Lucot, J.B., Paton, S. & Grubbs, R.D., 2010, Cholinesterase inhibitors and stress: effects on brain muscarinic receptor density in mice, *Neurotoxicology*, 31(5), pp. 461-7.

McGowan, E., Sanders, S., Iwatsubo, T., Takeuchi, A., Saido, T., Zehr, C., Yu, X., Uljon, S., Wang, R., Mann, D., Dickson, D. & Duff, K., 1999, Amyloid Phenotype Characterization of Transgenic Mice Overexpressing both Mutant Amyloid Precursor Protein and Mutant Presenilin 1 Transgenes, *Neurobiology of Disease*, 6(4), pp. 231-44.

Medeiros, R., Kitazawa, M., Caccamo, A., Baglietto-Vargas, D., Estrada-Hernandez, T., Cribbs, D.H., Fisher, A. & LaFerla, F.M., 2011, Loss of Muscarinic M1 Receptor Exacerbates Alzheimer's Disease–Like Pathology and Cognitive Decline, *The American Journal of Pathology*, 179(2), pp. 980-91.

Menon, P.M., Nasrallah, H.A., Reeves, R.R. & Ali, J.A., 2004, Hippocampal dysfunction in Gulf War Syndrome. A proton MR spectroscopy study, *Brain Res*, 1009(1-2), pp. 189-94.

Motohashi, K., Yamamoto, Y., Shioda, N, Kondo, H., Owada, Y., Fukunaga, K., 2009, Role of Heart-type Fatty Acid Binding Protein in the Brain Function, *Yakugaku Zasshi,* 129(2), pp. 191-5.

Mouzon, Chaytow, Crynen, Bachmeier, Stewart, Stewart, Mullan & Crawford, 2012, Repetitive mild traumatic brain injury in a mouse model produces learning and memory deficits accompanied by histological changes, *J Neurotrauma (accepted).*

Murphy, E.J., Owada, Y., Kitanaka, N., Kondo, H. & Glatz, J.F., 2005, Brain arachidonic acid incorporation is decreased in heart fatty acid binding protein gene-ablated mice, *Biochemistry*, 44(16), pp. 6350-60.

Ong, S.E., 2012, The expanding field of SILAC, *Analytical and bioanalytical chemistry*.

Patil, S.S., Sunyer, B., Höger, H. & Lubec, G., 2009, Evaluation of spatial memory of C57BL/6J and CD1 mice in the Barnes maze, the Multiple T-maze and in the Morris water maze, *Behavioural brain research*, 198(1), pp. 58-68.

Peden-Adams, M.M., Dudley, A.C., EuDaly, J.G., Allen, C.T., Gilkeson, G.S. & Keil, D.E., 2004, Pyridostigmine bromide (PYR) alters immune function in B6C3F1 mice, *Immunopharmacology and immunotoxicology*, 26(1), pp. 1-15.

Pellegrino, M., Steinbach, N., Stensmyr, M.C., Hansson, B.S. & Vosshall, L.B., 2011, A natural polymorphism alters odour and DEET sensitivity in an insect odorant receptor, *Nature*, 478(7370), pp. 511-4.

Phillips, M.C., Gillotte, K.L., Haynes, M.P., Johnson, W.J., Lund-Katz, S. & Rothblat, G.H., 1998, Mechanisms of high density lipoprotein-mediated efflux of cholesterol from cell plasma membranes, *Atherosclerosis*, 137, pp. S13-7.

Pittman, J.T., Dodd, C.A. & Klein, B.G., 2003, Immunohistochemical Changes in the Mouse Striatum Induced by the Pyrethroid Insecticide Permethrin, *International journal of toxicology*, 22(5), pp. 359-70.

Pope, C., Karanth, S. & Liu, J., 2005, Pharmacology and toxicology of cholinesterase inhibitors: uses and misuses of a common mechanism of action, *Environmental toxicology and pharmacology*, 19(3), pp. 433-46.

Power, L.E. & Sudakin, D.L., 2007, Pyrethrin and pyrethroid exposures in the United States: a longitudinal analysis of incidents reported to poison centers, *J Med Toxicol*, 3(3), pp. 94-9.

Prater, M.R., Blaylock, B.L. & Holladay, S.D., 2005, Combined dermal exposure to permethrin and cis-urocanic acid suppresses the contact hypersensitivity response in C57BL/6N mice in an additive manner, *Journal of photochemistry and photobiology. B,*

Biology, 78(1), pp. 29-34.

Prater, M.R., Gogal, R.M., Blaylock, B.L. & Holladay, S.D., 2003, *International journal of toxicology*, 22(1), pp. 35-42.

Prater, M.R., Gogal Jr, R.M., Blaylock, B.L., Longstreth, J. & Holladay, S.D., 2002, Single-dose topical exposure to the pyrethroid insecticide, permethrin in C57BL/6N mice: effects on thymus and spleen, *Food and chemical toxicology : an international journal published for the British Industrial Biological Research Association*, 40(12), pp. 1863-73.

Punareewattana, Smith, Blaylock , Longstreth, Snodgrass, Gogal & Prater , function in C57Bl/6N mice. Food Chem Toxicol. 2001

Feb;39(2):133-9

Qiu, H., Jun, H.W. & Tao, J., 1997, Pharmacokinetics of insect repellent N,N-diethyl-m-toluamide in beagle dogs following intravenous and topical routes of administration, *Journal of pharmaceutical sciences*, 86(4), pp. 514-516

Ray, D.E. & Fry, J.R., 2006, A reassessment of the neurotoxicity of pyrethroid insecticides, *Pharmacology & therapeutics*, 111(1), pp. 174-93.

Read, D.J., Li, Y., Chao, M.V., Cavanagh, J.B. & Glynn, P., 2009, Neuropathy Target Esterase Is Required for Adult Vertebrate Axon Maintenance, *The Journal of Neuroscience*, 29(37), pp. 11594-600.

Rona, R.J., Fear, N.T., Hull, L. & Wessely, S., 2007, Women in novel occupational roles: mental health trends in the UK Armed Forces, *International journal of epidemiology*, 36(2), pp. 319-26.

Serhan, C.N., Yacoubian, S. & Yang, R., 2008, Anti-inflammatory and proresolving lipid mediators, *Annu Rev Pathol*, 3, pp. 279-312.

Singh, I., Singh, A.K. & Contreras, M.A., 2009, Peroxisomal dysfunction in inflammatory childhood white matter disorders: an unexpected contributor to neuropathology, *J Child Neurol*, 24(9), pp. 1147-57.

Skowera, A., Hotopf, M., Sawicka, E., Varela-Calvino, R., Unwin, C., Nikolaou, V., Hull, L., Ismail, K., David, A.S., Wessely, S.C. & Peakman, M., 2004, Cellular immune activation in Gulf War veterans, *Journal of clinical immunology*, 24(1), pp. 66-73.

Slack, B.E., Breu, J., Petryniak, M.A., Srivastava, K. & Wurtman, R.J., 1995, Tyrosine Phosphorylation-dependent Stimulation of Amyloid Precursor Protein Secretion by the m3 Muscarinic Acetylcholine Receptor, *Journal of Biological Chemistry*, 270(14), pp. 8337-44.

Smith, T.C., Heller, J.M., Hooper, T.I., Gackstetter, G.D. & Gray, G.C., 2002, Are Gulf War veterans experiencing illness due to exposure to smoke from Kuwaiti oil well fires? Examination of Department of Defense hospitalization data, *American journal of epidemiology*, 155(10), pp. 908-17.

Stanford, S.C., 2007, The Open Field Test: reinventing the wheel, *Journal of Psychopharmacology*, 21(2), pp. 134-5.

Steele, L., 2000, Prevalence and patterns of Gulf War illness in Kansas veterans: association of symptoms with characteristics of person, place, and time of military service, *American journal of epidemiology*, 152(10), pp. 992-1002.

Steele, L., Sastre, A., Gerkovich, M.M. & Cook, M.R., 2012, Complex factors in the etiology of Gulf War illness: wartime exposures and risk factors in veteran subgroups, *Environmental health perspectives*, 120(1), pp. 112-8.

Takayama, M., Yao, K. & Wada, M., 2009, The dihydropyridine calcium channel blocker benidipine prevents lysophosphatidylcholine-induced endothelial dysfunction in rat aorta, *J Biomed Sci*, 16, p. 57.

Tandon, A., Rogaeva, E., Mullan, M. & St George-Hyslop, P.H., 2000, Molecular genetics of Alzheimer's disease: the role of β-amyloid and the presenilins, *Current Opinion in Neurology*, 13(4), pp. 377-84.

Terry, A.V., Buccafusco, J.J., Gearhart, D.A., Beck, W.D., Middlemore-Risher, M.L.,

Truan, J.N., Schwarz, G.M., Xu, M., Bartlett, M.G., Kutiyanawala, A. & Pillai, A., 2011, Repeated, intermittent exposures to diisopropylfluorophosphate in rats: protracted effects on cholinergic markers, nerve growth factor-related proteins, and cognitive function, *Neuroscience*, 176, pp. 237-53.

Toomey, R., Alpern, R., Vasterling, J.J., Baker, D.G., Reda, D.J., Lyons, M.J., Henderson, W.G., Kang, H.K., Eisen, S.A. & Murphy, F.M., 2009, Neuropsychological functioning of U.S. Gulf War veterans 10 years after the war, *J Int Neuropsychol Soc*, 15(5), pp. 717-29.

Tracey, K.J., 2007, Physiology and immunology of the cholinergic antiinflammatory pathway, *The Journal of clinical investigation*, 117(2), pp. 289-96.

Tymoczko, J.L., Berg, J.M. & Stryker, L., 2012, *Biochemistry: a short course,* W.H. Freeman and company, Basingstoke.

2002, U.S. Environmental ProtectionAgency (EPA) [webpage on the Internet]. Interim Reregistration Eligibility Decision for Chlorpyrifos, *EPA*, pp. 738-R-01-007.

Ueda, H., Morishita, R., Itoh, H., Narumiya, S., Mikoshiba, K., Kato, K. & Asano, T., 2001, Galpha11 induces caspase-mediated proteolytic activation of Rho-associated kinase, ROCK-I, in HeLa cells, *The Journal of biological chemistry*, 276(45), pp. 42527-33.

Vadhana, M.S., Carloni, M., Nasuti, C., Fedeli, D. & Gabbianelli, R., 2011, Early life permethrin insecticide treatment leads to heart damage in adult rats, *Exp Gerontol*, 46(9), pp. 731-8.

Vance, D.E. & Vance, J.E., 2008, *Biochemistry of lipids, lipoproteins and membranes,* Elsevier, Amsterdam; Boston.

Vogel, J.S., Keating, G.A. & Buchholz, B.A., 2002, Protein binding of isofluorophate in vivo after coexposure to multiple chemicals, *Environmental health perspectives*, 110 Suppl 6, pp. 1031-6.

Vythilingam, M., Luckenbaugh, D.A., Lam, T., Morgan, C.A., Lipschitz, D., Charney, D.S., Bremner, J.D. & Southwick, S.M., 2005, Smaller head of the hippocampus in Gulf War-related posttraumatic stress disorder, *Psychiatry research*, 139(2), pp. 89-99.

Wada-Isoe, K., Imamura, K., Kitamaya, M., Kowa, H. & Nakashima, K., 2008, Serum heart-fatty acid binding protein levels in patients with Lewy body disease, *Journal of the neurological sciences*, 266(1), pp. 20-4.

Wenk, M.R., 2005, The emerging field of lipidomics, *Nature reviews. Drug discovery*, 4(7), pp. 594-610.

Whistler, T., Fletcher, M.A., Lonergan, W., Zeng, X.R., Lin, J.M., Laperriere, A., Vernon, S.D. & Klimas, N.G., 2009, Impaired immune function in Gulf War Illness, *BMC medical genomics*, 2, p. 12.

White, R.F., Proctor, S.P., Heeren, T., Wolfe, J., Krengel, M., Vasterling, J., Lindem, K., Heaton, K.J., Sutker, P. & Ozonoff, D.M., 2001, Neuropsychological function in Gulf War veterans: relationships to self-reported toxicant exposures, *American journal of industrial medicine*, 40(1), pp. 42-54.

Wong, C.G. & Ladisch, S., 1983, Retention of gangliosides in serum delipidated by diisopropyl ether-1-butanol extraction, *Journal of lipid research*, 24(5), pp. 666-9.

Xie, F., Liu, T., Qian, W.J., Petyuk, V.A. & Smith, R.D., 2011, Liquid chromatography-mass spectrometry-based quantitative proteomics, *The Journal of biological chemistry*, 286(29), pp. 25443-9.

Yasuda, S., Tsutsumi, A., Chiba, H., Yanai, H., Miyoshi, Y., Takeuchi, R., Horita, T., Atsumi, T., Ichikawa, K., Matsuura, E. & Koike, T., 2000, β2-glycoprotein I deficiency: prevalence, genetic background and effects on plasma lipoprotein metabolism and hemostasis, *Atherosclerosis*, 152(2), pp. 337-46.

Zhang, D., Hu, X., Qian, L., O'Callaghan, J.P. & Hong, J.S., 2010, Astrogliosis in CNS pathologies: is there a role for microglia? *Molecular neurobiology*, 41(2-3), pp. 232-41.

Zhang, Q., Zhou, X.-D., Denny, T., Ottenweller, J.E., Lange, G., LaManca, J.J., Lavietes, M.H., Pollet, C., Gause, W.C. & Natelson, B.H., 1999, Changes in Immune Parameters Seen in Gulf War Veterans but Not in Civilians with Chronic Fatigue Syndrome, *Clinical and diagnostic laboratory immunology*, 6(1), pp. 6-13.

Zhang, W., Yamada, M., Gomeza, J., Basile, A.S. & Wess, J., 2002, Multiple muscarinic acetylcholine receptor subtypes modulate striatal dopamine release, as studied with M1-M5 muscarinic receptor knock-out mice, *The Journal of neuroscience: the official journal of the Society for Neuroscience*, 22(15), pp. 6347-52.

Zhou, Z., Marepally, S.R., Nune, D.S., Pallakollu, P., Ragan, G., Roth, M.R., Wang, L., Lushington, G.H., Visvanathan, M. & Welti, R., 2011, LipidomeDB data calculation environment: online processing of direct-infusion mass spectral data for lipid profiles, *Lipids*, 46(9), pp. 879-84.

Zieske, L.R., 2006, A perspective on the use of iTRAQ reagent technology for protein complex and profiling studies, *J Exp Bot*, 57(7), pp. 1501-8.

Züchner, T., Perez-Polo, J.R. & Schliebs, R., 2004, Beta-secretase BACE1 is differentially controlled through muscarinic acetylcholine receptor signaling, *Journal of Neuroscience Research*, 77(2), pp. 250-7.